Yuan, S., Williams-Jones, A.E., Romer, R.L., Zhao, P., Mao, J., 2019.
Protolith-Related Thermal Controls on the Decoupling of Sn and W in Sn-W Metallogenic Provinces:
Insights from the Nanling Region, China. Economic Geology, 114(5): 1005-1012.

Protolith-related thermal controls on the decoupling of Sn and W in Sn-W metallogenic provinces: insights from the Nanling region, China

Shunda Yuan[1*], A.E. Williams-Jones[2], Rolf L. Romer[3], Panlao Zhao[1], Jingwen Mao[1]

1. *MLR Key Laboratory of Metallogeny and Mineral Assessment, Institute of Mineral Resources, Chinese Academy of Geological Sciences, Beijing 100037, China*
2. *Department of Earth and Planetary Sciences, McGill University, 3450 University Street, Montreal H3A 0E8, Canada*
3. *Deutsches GeoForschungsZentrum GFZ, Telegrafenberg, D-14473 Potsdam, Germany*

ABSTRACT

The Nanling region of South China hosts the largest W-Sn metallogenic province in the world, accounting for more than 54% of global tungsten resources as well as important resources of tin and rare metals. An important feature of this province, which is shared by a number of other W-Sn metallogenic provinces, is that W deposits occur separately from Sn and Sn-W deposits, with the latter being concentrated in the west of the region (especially along the deep, NE-trending Chenzhou-Linwu fault) and the W deposits to the east of them. All the deposits are associated with S-type, ilmenite series granites. However, the granites associated with the Sn and Sn-W deposits can be distinguished from the W granites by their higher bulk rock εNd values and their higher zircon εHf values. Most importantly, the Sn and Sn-W granites are characterized by higher zircon saturation temperatures (800 ± 20°C) than the W granites (650 ~ 750°C). The Sn and Sn-W granites

[*]Corresponding author. E-mail address: shundayuan@cags.ac.cn

also contain abundant mantle-derived mafic microgranular enclaves, whereas such enclaves are rare in the W granites. A model is proposed in which the protolith to the W granites released W to the melt as a result of the breakdown of muscovite. The temperature of melting, however, was too low for biotite to melt. Upwelling of mantle material, particularly along the Chenzhou-Linwu fault, however, led to higher temperatures in the west (the location of the Sn and Sn-W deposits), thereby enabling the breakdown of both muscovite and biotite and the consequent release of both W and Sn to form Sn and Sn-W granites. This model, which is based on differences in the protolith melting temperature and thus mobilization temperatures for Sn and W, is potentially applicable to any Sn-W metallogenic province in which the Sn and Sn-W deposits occur separately from the W deposits.

Keywords: tin; tungsten; decoupling; anhydrous melting; metallogenic province

Introduction

Magmatic tin-tungsten mineralization is commonly associated with highly evolved reduced granites that have undergone extensive magmatic fractionation, followed by the partitioning of tin and tungsten into late-magmatic hydrothermal fluids (Ishihara, 1977; Lehmann, 1990). The spatial distribution of magmatic Sn and W mineralization in discontinuous belts along the margins of cratons reflects the distribution of (i) sedimentary protoliths, which have experienced intense chemical alteration (loss of Na, Ca) on the continent before they were redistributed to the continent margin, and (ii) heat sources leading to the partial melting of these protoliths (Romer and Kroner, 2015, 2016). The nature of the sedimentary protoliths determines both the melting behavior of the source rocks and the nature of the metal-sequestering phases in the protolith, which in turn control the partitioning of Sn and W between melt and restite phases (e.g., Simons et al., 2017; Wolf et al., 2018).

Tin and tungsten are concentrated in the same type of granite, and develop deposits that occur within the same metallogenic province and have similar tectonic settings. Nonetheless, the two metals typically form separate deposits or one metal predominates strongly over the other metal. At the scale of individual intrusions, possible explanations for this separation of tin and tungsten include differences in fractionation and oxidation state (Blevin and Chappell, 1992), contrasting magmatic histories (Cheng et al., 2018), or different paths of metal redistribution during late stage magmatic and hydrothermal processes (Schmidt, 2018). At the scale of metallogenic provinces, however, such a regional predominance of Sn over W mineralization and *vice versa* has to be linked to features that operate over the entire province.

In South China, there are two age groups of Sn-W mineralization that define separate belts, which formed above subduction zones during periods of back-arc extension and extension associated with the changing relative movement direction of the Paleo-Pacific plate, which change from subduction oblique to the continental margin to subduction parallelism with the continental margin (Mao et al., 2013). The more important of these belts developed mainly between 160 and 150 Ma (Yuan et al., 2008, 2011; Hu et al., 2012, 2017; Hu and Zhou, 2012), and is located in the Nanling region (Fig. 1A). This belt constitutes the largest W-Sn metallogenic province in the world, accounting for more than 54% of global tungsten resources and appreciable resources of tin and rare metals (Yuan et al., 2018). The spatial distribution of these Sn-W deposits is heterogeneous with W deposits occurring throughout the region (although mainly in the east) and Sn deposits being largely restricted to the western part, especially along the deep, NE-trending Chenzhou-Linwu fault (Fig.

1B). Although many of the deposits contain economic concentrations of both Sn and W, they are typically dominated by one of the metals. Among the deposits in which Sn and W were decoupled, the giant Yaogangxian W deposit and the giant Furong Sn deposit are the most prominent examples (Fig. 1B). The Nanling Sn-W metallogenic province, therefore, provides an ideal setting in which to investigate the reasons for the separation or decoupling between Sn-W, Sn and W deposits at a regional scale.

The partitioning of W and Sn during partial melting of sedimentary rocks is thought to be controlled largely by the restite mineralogy and melting temperature (e.g., Wolf et al., 2018). Thus, the contrasting distribution of Sn and W mineralization within Sn-W metallogenic provinces may reflect variations in protolith composition and/or the conditions at which it melted. Using available whole-rock geochemical and zircon Hf isotopic data for Sn-, Sn-W-, and W-related granites in the Nanling W-Sn metallogenic province, we demonstrate that the protoliths of the granites related to Sn and Sn-W mineralization melted at higher temperatures than those with related W-Sn and W mineralization. In so doing, we are able to make the case that the difference in the source temperature was the key control on the spatial decoupling of Sn and W mineralization in the Nanling metallogenic province.

Geological setting

The Nanling region is located in the northwestern part of the Cathaysia block of South China (Fig. 1A，B). After assembly of the Yangtze Craton and Cathaysia Block along the Qinhang tectonic belt, at ~1.1- 0.83 Ga to form the South China Block (Chen and Jahn, 1998; Zhao et al., 2011), South China was extensively reworked by Early Paleozoic and Early Mesozoic orogenies as well as the

Late Mesozoic subduction of the Paleo-Pacific plate. This produced large volumes of granitic rocks. Only the Late Mesozoic granites, however, are enriched in Sn and W (Fig. 1A, Mao et al., 2013). These granites formed during two separate tectono-magmatic events, the first of which occurred in the Late Jurassic (160-150 Ma) and is mainly represented in the Nanling region. This event took place in response to the opening of a large slab window or the development of an intra-arc rift during the subduction of the Palaeo-Pacific plate (Jiang et al., 2009; Mao et al., 2013), and is the focus of this paper (Fig. 1B). The second event occurred in the Early-Mid Cretaceous (120-80 Ma) and was a response to the development of pull-apart basins along the South China continental margin (Fig. 1A, Mao et al., 2013).

Multiple tectono-thermal events in Nanling region created a regional basement consisting of Sinian-Silurian metamorphic rocks, which are unconformably overlain by a cover sequence of Devonian to Triassic marine and continental strata, including clastic and carbonate facies (Li and Zhong, 1991). These strata, especially the Upper Devonian and Carboniferous carbonate facies, are widely exposed in the western part of the region, where they were intruded by Late Jurassic Sn-W-bearing granites. In the east, the exposed strata are mainly Sinian to Cambrian clastic rocks and were intruded by Late Jurassic W-bearing granites (Fig. 1B).

The W-Sn Mineralization

The type of tungsten and tin mineralization in the Nanling region varies considerably due in large part to the variable nature of the rocks that host the intrusions. Tungsten mineralization occurs throughout the region. In the east, it occurs dominantly as quartz-vein-type wolframite deposits hosted by siliciclastic rocks, whereas in the west, it mainly takes the form of skarn-type scheelite deposits hosted by carbonate rocks. In contrast to W, the Sn and Sn-W mineralization is restricted to the western part of the region (especially along the deep, NE-trending Chenzhou-Linwu fault), where it occurs mainly in skarns hosted by carbonate rocks and to a much lesser extent in cassiterite-sulfide veins hosted by siliciclastic rocks (Fig. 1B).

The quartz-vein-type wolframite deposits mainly occur along the contacts between the Late Jurassic granite plutons and their siliciclastic sedimentary host rocks, especially near the intersection of NNE and EW trending faults. In addition to wolframite, the veins contain minor proportions of bismuthinite, molybdenite, arsenopyrite, cassiterite, pyrite, scheelite, galena, chalcopyrite and sphalerite (Hu et al., 2012). The quartz gangue is accompanied by minor K-feldspar, mica, topaz, tourmaline, chlorite and calcite (Hu et al., 2012; Ni et al., 2015). On the basis of mineral textures and crosscutting vein relationships, an early oxide-sulfide stage is interpreted to have been followed by a silicate stage and finally by a carbonate stage (Hu et al., 2012). Vein emplacement was associated with silicification of the wall rocks and, locally, minor greisenization and sericitization (Wu et al., 1987).

The skarn type deposits (W, Sn and Sn-W) are found invariably at the interface between Late Jurassic granitic plutons and Late Paleozoic carbonate rocks and appear to have been controlled structurally by NE-trending faults. They mainly belong to the oxidized calcic skarn class, which is characterized by prograde stage characterized by a high garnet/pyroxene ratio, andradite-rich garnet and diopside-rich pyroxene and a retrograde stage comprising epidote, actinolite, and chlorite. In some cases, e.g., the giant Shizhuyuan W-Sn-Mo-Bi deposit in southern Hunan Province, both the adjacent granite and the skarn was subjected to greisenization and overprinted by a quartz stockwork (Lu et al., 2003). The mineralization of the skarn-type deposits takes the form of scheelite and/or cassiterite and is mainly restricted to the retrograde skarns (Lu et al., 2003; Yuan et al., 2011). In addition to the main ore minerals there are minor proportions of molybdenite, bismuthinite, arsenopyrite, pyrrhotite, galena and sphalerite.

The geochemistry of the Sn and W granites

Late Jurassic granites of the Nanling belt with associated Sn and W mineralization are interpreted to have originated from highly fractionated crustal melts (high SiO_2 and Rb/Sr ratios, Fig. 2 A and B, Supplementary Table 1). Only the granite related to the giant Furong Sn deposit provides evidence of being less evolved (lower SiO_2 concentration and a low Rb/Sr ratio; Figure 2). Although some of the W-specialized granites have Fe_2O_3/FeO ratios indicative of a slightly higher oxygen fugacity (Fig. 2), most of the Sn- and W-mineralized granites are ilmenite series, peraluminous granites ($Fe_2O_3/FeO<0.5$, Fig. 2) (Ishihara, 1981). Furthermore, there is no correlation between the Fe_2O_3/FeO and Rb/Sr ratios (Fig. 2), indicating that the oxygen fugacity reflects the magma source and not the fractionation (Burnham and Ohmoto, 1980; Blevin and Chappell, 1992; Sato, 2012). Even though some of the W and Sn granites are geochemically distinct, most of the Late Jurassic granites with associated Sn and W deposits have broadly overlapping chemical compositions (Fig. 2), indicating that they experienced a similar degree of fractionation and have the same reduced redox state (Ishihara, 1981). Thus, magma evolution and redox state alone cannot account for the regional W-Sn decoupling of Late Jurassic W-Sn mineralization in the Nanling belt. Instead, the decoupling reflects contrasting sources and/or conditions of metal mobilization from the source rocks.

The temperature of melting and sources of heat and protolith

Two key factors controlling the regional distribution of Sn mineralization are (i) the distribution of intensely altered sedimentary protoliths in the melting volume and (ii) the availability of a heat source to facilitate biotite-controlled anhydrous melting (Romer and Kroner, 2015, 2016). The exogenic chemical alteration of the protolith results in a residual enrichment of Sn and W, but more importantly the loss of Na and Ca results in a protolith that during prograde metamorphism stabilizes large amounts of muscovite and biotite. This, in turn, allows for the generation of large amounts of melt and multiple stages of melt extraction (Wolf et al., 2018). Tin and tungsten may behave differently during parting melting, depending largely on the restite mineralogy. During muscovite-controlled anhydrous melting, Sn partitions preferentially into the restite, whereas W may remain in the melt. Thus, the loss of these low-temperature melts (c. 720-740 °C, Viruete et al., 2000) results in the enrichment of Sn in the restite and may deplete W in the restite. Biotite-controlled anhydrous melting of the restite at higher temperature (c. >800 °C, Barbero, 1995) results in melts that may be strongly enriched in Sn (Wolf et al., 2018).

We estimated the temperature of melting of Sn-, Sn-W-, and W-related granites using the temperature of zircon-saturation (Watson and Harrison, 1983). The various granites in the region show systematically lower zircon-saturation temperatures for more evolved samples that have experienced fractional crystallization (Supplementary Fig. 1). Thus, the least evolved samples of individual granite suites provide the best estimates of the melting temperature. The Sn and Sn-W granites along the Chenzhou-Linwu fault in the western part of the Nanling region yield significant higher melting temperatures (>800 ºC) than the W-related granites in the eastern part (<750 ºC; Fig. 3; Supplementary Fig. 1), which implies that the region along the Chenzhou-Linwu fault reached higher temperature. This suggests that the spatial separation of Sn and W mineralization may be related to the source rock mineralogy and temperature of melting. Some Sn (W)-bearing granites in the western part of the Nanling region have higher Nb/Ta ratios than those of the W-bearing granites (Fig. 2), which may also reflect differences in the extent of melting or different mineral assemblages in the restite (Ballouard et al., 2016).

Internal heating of orogenically thickened crust may possibly generate minimum-temperature melts by muscovite decomposition. Higher temperatures, however, are needed for biotite-controlled anhydrous melting and this requires input of heat from the mantle (e.g., Clark et al., 2011), which may be accomplished by the input of mantle melts in subduction and extensional zones or the tectonic emplacement of UHT metamorphic rocks in collisional orogens (e.g., Romer and Kroner, 2015, 2016). In the Nanling region, Late Jurassic granitic magmatism took place in response to the opening of a large slab window or the development of an intra-arc rift during the subduction of the Palaeo-Pacific plate.

The Late Jurassic granites with associated Sn and W mineralization show a broad range of whole-rock Nd and zircon Hf isotopic compositions. Consistent with the spatial separation of the Sn and W mineralization, granites with associated Sn (W) mineralization along the Chenzhou-Linwu fault in the western part of the Nanling region have significantly higher whole-rock εNd and zircon εHf values than those associated with W mineralization in the eastern part (Fig. 4; Supplementary Tables 1 and 2). The strongly negative εNd (-15.5~-9.8, Fig. 4; Supplementary Table 1) values of granites with associated W deposits reflect the melting of old continental crust. The regionally contrasting Nd and Hf isotopic composition of granites could indicate differences in the "average" age of the crustal blocks on both sides of the Chenzhou-Linwu fault or variable input of mantle-derived melts in the source region of the granites with associated Sn mineralization.

Based on previous studies, the Mesozoic W-Sn-related granites in the Nanling region were mainly derived from the regional metamorphic basement that was previously considered to have formed in the Paleo-Mesoproterozoic (Xu et al., 2005). Recent detrital zircon dating and geochemical studies of the basement metamorphic rocks from the western, central and eastern parts of the Nanling region have shown that the protoliths to the granites are mainly late Neoproterozoic metasedimentary rocks with major contributions from Grenvillian (1000 – 900 Ma) and Mesoproterozoic sources and a minor contribution from an Archaean source. The geochemical studies have also shown that these metasedimentary rocks do not vary significantly in composition across the Nanling region, and are characterized by high La/Yb, a negative Eu anomaly, high K_2O/Na_2O, La/Co and Th/Sc ratios and low Cr/Zr ratios. This suggests a high degree of maturity of the supracrustal source, which was probably located along the northern margin of East Gondwanaland (Yu et al., 2005, 2006a, b; Wei et al., 2009).

From the above observations, the metamorphic basement in the Nanling region is interpreted to have formed after the assembly of the Yangtze Craton and Cathaysia Block and, thus, its composition and distribution were not controlled by the Chenzhou-Linwu fault. This is also supported by the observation that most of the Sn (W) deposits are located relatively the Chenzhou-Linwu fault. Therefore, the contrasting Nd and Hf isotopic compositions of the ore-related granites in the western and eastern parts of the Nanling region likely reflect variable inputs of mantle-derived melts in the source region of the granites with associated Sn mineralization rather than differences in the “average” age of the crustal blocks on opposite sides of the Chenzhou-Linwu fault.

It is notable that mantle-derived mafic microgranular enclaves (MMEs) are ubiquitous in the

Yuan, S., Williams-Jones, A.E., Romer, R.L., Zhao, P., Mao, J., 2019.
Protolith-Related Thermal Controls on the Decoupling of Sn and W in Sn-W Metallogenic Provinces:
Insights from the Nanling Region, China. Economic Geology, 114(5): 1005-1012.

western part of the Nanling region, most prominently in the Furong Sn granite and Lisong granite whereas they are absent in granitic rocks in the eastern part of the Nanling region (Li et al., 2009; Zhao et al., 2012). It is also of note that zircon collected from MMEs in the Lisong granite have high $\varepsilon_{Hf}(t)$ (3.1~8.0) and low $\delta^{18}O$ (5.1‰~6.5‰) values, suggesting that they crystallized in equilibrium with mantle-derived melts (Li et al., 2009). Moreover, He-Ar isotopic studies of pyrite from Sn- and Sn-W deposits in the western part of the Nanling region provide evidence for a significant mantle input, whereas corresponding studies of W deposits in the eastern part of the regions indicate that the mantle input was insignificant (Li Z.L., et al., 2007; Li G.L., et al., 2011). Because of the low Sn content of the mantle (0.6 ppm; Lehmann, 1990), the role of the mantle was not to provide a source for Sn, but rather to supply the heat needed to generate high-temperature granitic melts.

A Model for the spatial decoupling of W and Sn deposits

Anhydrous melting is controlled by the breakdown of hydrous minerals such as muscovite, biotite and amphibole (Clemens and Viezeuf, 1987). The amount of melt formed by muscovite breakdown in pelitic rocks depends on the proportion of muscovite (Clemens and Viezeuf, 1987; Breton and Thompson, 1988), which may be high in intensely altered metamorphosed sedimentary rocks that have low contents of Ca and Na (cf. Wolf et al., 2018). Melting by biotite-breakdown requires higher temperature (Clemens and Viezeuf, 1987; Schmidt et al. 2004) and is only possible with heat input from the mantle (Clark et al. 2011).

The behavior of Sn and W during partial melting is controlled by the stability of their host and whether the released Sn and W remain in the melt or partition back into restite minerals, which depends on the P-T conditions of melting and the mineral assemblage of the restite. The available evidence suggests that biotite incorporates Sn more easily than does muscovite and consequently low-temperature melts lose Sn as long as biotite is stable in the restite (Chappell et al., 1987; Simons et al., 2017). Thus, during low-temperature melting Sn remains preferentially in the restite (Wolf et al., 2018) and may be repartitioned from the melt into restite biotite to a much higher extent than W. Tin is released mostly during biotite melting. These observations suggest that the regional separation of Sn and W deposits may result from differences in the temperature at which the protoliths for the corresponding granites melt.

The separation of the mineralization in the Nanling region into a western Sn, Sn-W domain and an eastern W domain is consistent with the higher melting temperature of the protoliths forming the Sn and Sn-W granites compared to that of the protoliths for the W granites in the east (Fig. 1, 3). It is also consistent with the higher whole rock εNd and zircon εHf values of the Sn granites relative to the W granites (Figs. 4), and the abundance of mantle-derived MMEs in the Sn and Sn-W granites but not in the W granites. We therefore propose that the spatial decoupling of Sn and W mineralization in the Nanling Region was a direct response to the difference in the temperature of melting of the protoliths for the corresponding granites. This also satisfactorily explains why the Sn-W deposits are associated with the Sn(W) deposits in the west but not the W-only deposits in the east (Fig. 1); melting temperatures in the west were high enough to melt both muscovite (the source of W) and biotite (the main source of Sn).

The Late Jurassic granitic rocks and associated W-Sn mineralization in the region are interpreted to have resulted from extension above the subducting Palaeo-Pacific plate that led to the creation of a large slab window or intra-arc rift (Jiang et al., 2009; Mao et al., 2013). The deep

Chenzhou-Linwu fault in the western part of the belt, which represents a major tectonic boundary separating the Yangtze and Cathaysia blocks (Wang et al., 2003), may have localized the upwelling of mantle material, thereby accounting for both the higher melting temperature and the addition of mantle melts to the Late Jurassic granites that are associated with Sn and Sn-W mineralization in the western part of the Nanling belt.

The model proposed above, which involves differences in the protolith melting temperature and thus mobilization temperature for Sn and W, is potentially applicable to any Sn-W metallogenic province in which the Sn deposits occur separately from the W deposits. Simply put, granites with associated W mineralization reflect muscovite-dehydration melting, whereas granites with associated Sn mineralization reflect biotite-dehydration melting, possibly with an earlier loss of low-temperature melts. At a low temperature of melting (muscovite-dehydration melting), W is partitioned preferentially into the melt, whereas Sn remains in the restite.

Acknowledgements

This research was supported financially by the National Natural Science Foundation of China (Nos. 41822304, 41672095, 41373047) and the National Nonprofit Institute Research Grant of CAGS (YYWF201711).

References:

Ballouard, C., Poujol, M., Boulvais, P., Branquet, Y., Tartèse, R., and Vigneresse, J.L., 2016, Nb-Ta fractionation in peraluminous granites: A marker of the magmatic-hydrothermal transition:

Geology, v. 44, p. 231-234.

Barbero, L., 1995, Granulite-facies metamorphism in the Anatectic Complex of Toledo, Spain: late Hercynian tectonic evolution by crustal extension: Journal of the Geological Society, v. 152, p. 365-382.

Blevin, P.L., and Chappell, B.W., 1992, The role magma sources, oxidation states and fractionation in determining the granite metallogeny of eastern Australia: Earth and Environmental Science Transactions of the Royal Society of Edinburgh, v. 83, p. 305-316.

Breton, N.L., and Thompson, A.B., 1988, Fluid-absent (dehydration) melting of biotite in metapelites in the early stages of crustal anataxis: Contrib. Mineral Petrol, v. 99, p. 226-237.

Burnham, C.W., and Ohmoto, H., 1980, Late-stage processes of felsic magmatism, *in* Ishihara, S., and Takenouchi, S. eds., Granitic Magmatism and Related Mineralization: Mining Geology Special Issue, v. 8, p. 1-11.

Chappell, B.W., White, A.J.R., and Wyborn, D., 1987, The importance of residual source material (restite) in granite petrogenesis: Journal of Petrology, v. 28, p. 1111-1138.

Chen, J.F., and Jahn, B.M., 1998, Crustl evolution of southeastern China: Nd and Sr isotopic evidence: Tectonophysics, v. 284, p. 101-133.

Cheng, Y., Spandler, C., Chang, Z., and Clarke, G., 2018, Volcanic–plutonic connections and metal fertility of highly evolved magma systems. A case study from the Herberton Sn–W–Mo Mineral Field, Queensland, Australia: Earth and Planetary Science Letters, v. 486, p. 84-93.

Clark, C., Fitzsimmons, I.C.W., and Healy, D., 2011, How does the continental crust get really hot?: Elements, v. 7, p. 235-240.

Clemens, J.D., and Vielzeuf, D., 1987, Constraints on melting and magma production in the crust:

Earth and Planetary Science Letters, v. 86, p. 287-306.

Hu, R.Z., and Zhou, M.F., 2012, Multiple Mesozoic mineralization events in South China—an introduction to the thematic issue: Mineralium Deposita, v. 47, P. 579-588.

Hu, R.Z., Chen, W.T., Xu, D.R., and Zhou, M.F., 2017, Reviews and new metallogenic models of mineral deposits in South China: An introduction: Journal of Asian Earth Sciences, v.137, p. 1-8.

Hu, R.Z., Wei, W.F., Bi, X.W., Peng, J.T., Qi, Y.Q., Wu, L.Y., and Chen, Y.W., 2012, Molybdenite Re-Os and muscovite ^{40}Ar/^{39}Ar dating of the Xihuashan tungsten deposit, central Nanling district, South China: Lithos, v. 150, p. 111-118.

Ishihara, S., 1977, The magmetite-series and ilmenite-series granitic rocks: Mining Geology, v.27, p. 293-305.

_____1981, The granitoid series and mineralization: Economic Geology, v. 75, p. 458-484.

Jiang, Y.H., Jiang, S.Y., Dai, B.Z., Liao, S.Y., Zhao, K.D., and Ling, H.F., 2009, Middle to late Jurassic felsic and mafic magmatism in southern Hunan Province, southeast China: Implications for a continental arc to rifting: Lithos, v. 107, p. 185-204.

Lehmann, B., 1990, Metallogeny of tin: Berlin, Springer, 211 p.

Li, G.L., Hua, R.M., Zhang, W.L., Hu, D.Q., Wei, X.L., Huang, X.E., Xie, L., Yao, J.M., and Wang, X.D., 2011, He-Ar isotope composition of pyrite and wolframite in the Tieshanlong tungsten deposit, Jiangxi, China: Implications for fluid evolution: Resource Geology, v. 61, p. 356-366.

Li, X.H., Li, W.X., Wang, X.C., Li, Q.L., Liu, Y., and Tang, G.Q., 2009, Role of mantle-derived magma in genesis of early Yanshanian granites in the Nanling Range, South China: in situ zircon Hf-O isotopic constraints: Science in China series D: Erth Sciences, v. 52, p. 1262-1278.

Li, Y.Q., and Zhong, X.Y., 1991, Mineralogy of tungsten deposits in Nanling and neighboring area, China: China University of Geosciences Press, Wuhan, p, 1-455(in Chinese with English abstract.

Li, Z.L., Hu, R.Z., Yang, J.S., Peng, J.T., Li, X.M., Bi, and X.W., 2007, He, Pb and S isotopic constraints on the relationship between the A-type Qitianling granite and the Furong tin deposit, Hunan Province, China: Lithos, v. 97, p. 161-173.

Liu, X.C., Xing, H.L., and Zhang, D.H., 2014, Fluid focusing and its link to vertical morphological zonation at the Dajishan vein-typr tungsten deposit, South China: Ore Geology Reviews, v. 62, p. 245-258.

Lu, H.Z., Liu, Y.M., Wang, C.L., Xu, Y.Z., and Li, H.Q., 2003, Mineralization and fluid inclusion study of the Shizhuyuan W-Sn-Bi-Mo-F skarn deposit, Hunan Province, China: Economic Geology, v. 98, p. 955-974.

Mao, J.W., Cheng, Y.B., Chen, M.H., and Pirajno, F., 2013, Major types and time-space distribution of Mesozoic ore deposits in South China and their geodynamic setting: Mineralium Deposita, v. 48, p. 267-294.

Mao, J.W., Xie, G.Q., Guo, C.L., and Chen, Y.C., 2007, Large-scale tungsten-tin mineralization in the Nanling region, South China: Metallogenic ages and corresponding geodynamic processes: Acta Petrologica Sinica, v. 23, p. 2329-2338 (in Chinese with English Abstract).

Meinert, L.D., Dipple, G.M., and Nicolescu S., 2005, World skarn deposits: Economic Geology, v. 100th Anniversary, p. 299-336.

Ni, P., Wang, X.D., Wang, G.G., Huang, J.B., Pan, J.Y., and Wang, T.G., 2015, An infrared microthermometric study of fluid inclusions in coexisting quartz and molframite from Late

Mesozoic tungsten deposits in the Gannan metallogenic belt, South China: Ore Geology Reviews, v. 65, p. 1062-1077.

No. 932 Team, Guangdong Metallurgical Geological Exploration Corp., 1966, How to apply the "five-floor mineral model" to assessment, prospecting and exploration for the wolframite-quartz vein type of tungsten deposits: Geol. Explor., v.5, p. 15-19 (in Chinese).

Romer, R.L., and Kroner, U., 2015, Sediment and weathering control on the distribution of Paleozoic magmatic tin-tungsten mineralization: Mineralium Deposita, v. 50, p. 327-338.

_____2016, Phanerozoic tin and tungsten mineralization—tectonic controls on the distribution of enriched protoliths and heat sources for crustal melting: Gondwana Research, v. 31, p.60-95.

Sato, K., 2012, Sedimentary crust and metallogeny of granitoid affinity: implications from the geotectonic histories of the Circum-Japan Sea Region, Central Andes and southeastern Australia: Resource Geology, v. 62, p. 329–351.

Schmidt, C., 2018, Formation of hydrothermal tin deposits: Raman spectroscopic evidence for an important role of aqueous Sn(IV) species: Geochimica et Cosmochimica Acta, v. 220, p. 499–511.

Schmidt, M.W., Vielzeuf, D., and Auzanneau, E., 2004. Melting and dissolution of subducting crust at high pressures: the key role of white mica: Earth and Planetary Science Letters, v. 228, p. 65-84.

Simons, B., Andersen, J.C., Shail, R.K., and Jenner, F.E., 2017, Fractionation of Li, Be, Ga, Nb, Ta, In, Sn, Sb, W and Bi in the peraluminous Early Permian Variscan granites of the Cornubian Batholith: precursor processes to magmatic-hydrothermal mineralization: Lithos, v. 278, p. 491-512.

Viruete, J.E., Indares, A., and Arenas, R., 2000, P-T paths derived from garnet growth zoning in an extensional setting: an example from the Tormes gneiss dome (Iberian massif, Spain): Journal of Petrology, v. 41, p. 1489-1515.

Wang, Y.J., Fan, W.M., Guo, F., Peng, T.P., and Li, C.W., 2003, Geochemistry of Mesozoic mafic rocks adjacent to the Chenzhou-Linwu fault, South China: implications for the lithospheric boundary between the Yangtze and Cathaysia blocks: International Geology Review, v. 45, p. 263-286.

Watson, E.B., and Harrison, T. M., 1983, Zircon saturation revisited: temperature and composition effects in a variety of crustal magma types: Earth and Planetary Science Letters, v. 64, p. 295-304.

Wei, Z.Y., Yu, J.H., Wang, L.J., and Shu, L.S., 2009, Geochemical features and tectonic significances of Neoproterozoic metasedimentary rocks from Nanling Range: Geochimica, v. 38, p. 1-19. (in Chinese with English abstract)

Wolf, M., Romer, R.L., Franz, L., and López-Moro, F.J., 2018, Tin in granitic melts: The role of melting temperature and protolith composition: Lithos, v. 310-311, p. 20-30.

Wu, Y.L., Mei, Y.W., Liu, P.C., Cai, C.L., and Lu, T.Y., 1987, Geology of Xihuashan tungsten deposit: Geol. Publ. House, Beijing, China, p. 320 (in Chinese).

Xu, X.S., O'Reilly, S.Y., Griffin, W.L., Deng, P., and Pearson, N.J., 2005, Relict Proterozoic basement in the Nanling Mountains (SE China) and its tectonothermal overprinting. Tectonic, v. 24, TC2003.

Yao, Y., Chen, J., Lu, J.J., Wang, R.C., and Zhang, R.Q., 2014, Geology and genesis of the Hehuaping magnesian skarn-type cassiterite-sulfide deposit, Hunan Province, southern China:

Ore Geology Reviews, v. 58, p. 163-184.

Yu, J.H., Wang, L.J., Zhou, X.M., Jiang, S.Y., Wang, R.C., Xu, X.S., and Qiu, J.S., 2006a, Compositions and formation history of the basement metamorphic rocks in Northeastern Guangdong Province: Earth Sci. v. 31, p. 38-48. (in Chinese with English abstract)

Yu J.H., Wei Z.Y., Wang L.J., Wang R.C., Jiang S.Y., Shu L.S., and Sun T., 2006b, Cathaysia Block: A young continent composed of ancient materials: Geol. J. China Univ. v. 12, p. 440-447. (in Chinese with English abstract)

Yu J.H., Zhou X.M., O'Reilly S.Y., Zhao L., Griffin W.L., Wang R.C., Wang L.J., and Chen X.M., 2005, Formation history and protolith characteristics of granulites facies metamorphic rock in Central Cathaysia deduced from U-Pb and Lu-Hf isotopic studies of single zircon grains: Chinese Sci. Bull, v. 50, p. 2080-2089.

Yuan, S.D., Peng, J.T., Hao, S., Li, H.M., Geng, J.Z., and Zhang, D.L., 2011, In situ LA-MC-ICP-MS and ID-TIMS U-Pb geochronology of cassiterite in the giant Furong tin deposit, Hunan Province, South China: New constraints on the timing of tin-polymetallic mineralization: Ore Geology Reviews, v. 43, p. 235-242.

Yuan, S.D., Peng, J.T., Hu, R.Z., Li, H.M., Shen, N.P., and Zhang, D.L., 2008, A precise U-Pb age on cassiterite from the Xianghualing tin-polymetallic deposit (Hunan, South China): Mineralium Deposita, v. 43, p. 375-382.

Yuan, S.D., Williams-Jones, A.E., Mao, J.W., Zhao, P.L., Yan, C., and Zhang, D.L., 2018, The origin of the Zhangjialong tungsten deposit, South China: implications for W-Sn mineralization in large granite batholiths: Economic Geology, v.113, p. 1193-1208.

Zhao, J.H., Zhou, M.F., Yan, D.P., Zheng, J.P., and Li, J.W., 2011, Reappraisal of the ages of

Neoproterozoic strata in South China: No connection with the Grenvillian orogeny: Geology, v. 39, p. 299-302.

Zhao, K.D., Jiang, S.Y., Yang, S.Y., Dai, B.Z., and Lu, J.J., 2012, Mineral chemistry, trace elements and Sr-Nd-Hf isotope geochemistry and petrogenesis of Cailing and Furong granites and mafic enclaves from the Qitianling batholith in the Shi-Hang zone, South China: Gondwana Research, v. 22, p. 310-324.

Zhao, P.L., Yuan, S.D., Mao, J.W., Yuan, Y.B., Zhao, H.J., Zhang, D.L., and Shuang, Y., 2018, Constraints on the timing and genetic link of the large-scale accumulation of proximal W-Sn-Mo-Bi and distal Pb-Zn-Ag mineralization of the world-class Dongpo orefield, Nanling Range, South China: Ore Geology Reviews, v. 95, p. 1140-1160.

Figure captions

Figure 1. A: The location of Jurassic to Cretaceous W/Sn deposits and associated granites in South China (adapted from Mao et al., 2013). B: The distribution of Late Jurassic (160-150 Ma) W, Sn, and Sn-W deposits and associated granites in the Nanling region, South China (modified from Zhao et al., 2018).

Figure 2. Plot of Fe_2O_3/FeO *versus* (A) SiO_2, (B) Rb/Sr, (C) Nb/Ta, and (D) Zr/Hf, (C) A/NK versus A/CNK, and (D) A/CNK versus ε_{Nd}(t) values for Late Jurassic (160-150 Ma) W-, Sn-, and Sn-W-related granites in the Nanling region. Symbols as in Fig. 1B. Data are from Supplementary Table

1.

Figure 3. A plot of average zircon saturation temperature (T_{Zr}) versus vertical distance to the Chenzhou-Linwu (CL) Fault. The maximum temperature for individual intrusions was used to represent the initial magmatic temperature (see Supplementary Figure 1). Symbols as in Fig. 1B.

Figure 4. Probability distributions of (A) ε_{Nd}(t) values and (B) zircon ε_{Hf}(t) values for Late Jurassic (160-150 Ma) W-, Sn-, and Sn-W-related granites in the Nanling region. The color of the lines is as in Fig. 1B.

Supplementary Figure 1. Plots of zircon saturation temperature (T_{Zr} °C) versus Nb/Ta and Zr/Hf ratios for the W-, Sn- and Sn-W-related granites in the Nanling region. The maximum zircon saturation temperature was taken to approximate the initial magma temperature (see Watson and Harrison, 1983). The Nb/Ta and Zr/Hf ratios are assumed to represent the degree of fractional crystallization, except in the case of deposits hosting Nb-Ta mineralization (e.g., Xianghualing), for which the Nb/Ta ratio may be an unreliable index of fractional crystallization. Symbols as in Fig. 1B.

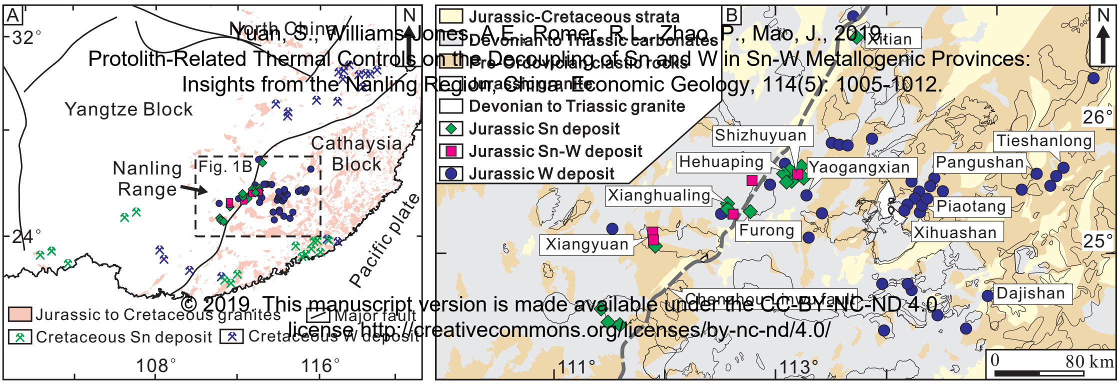
A
N
32°
North China
Yangtze Block
Cathaysia
Block
Nanling
Range
Fig. 1B
24°
Pacific plate
Jurassic to Cretaceous granites
Major fault
Cretaceous Sn deposit
Cretaceous W deposit
108°
116°
B
N
Jurassic-Cretaceous strata
Devonian to Triassic carbonates
Pre-Ordovician clastic rocks
Jurassic granite
Devonian to Triassic granite
Jurassic Sn deposit
Jurassic Sn-W deposit
Jurassic W deposit
Xitian
26°
Shizhuyuan
Tieshanlong
Hehuaping
Yaogangxian
Pangushan
Xianghualing
Piaotang
Furong
Xihuashan
Xiangyuan
25°
Chenzhou-Linwu fault
Dajishan
111°
113°
0
80 km

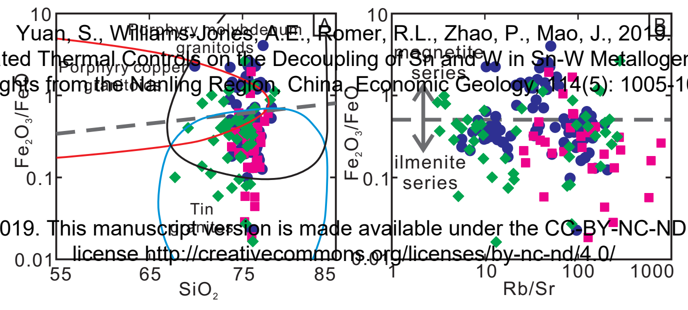
A
Porphyry molybdenum granitoids
Porphyry copper granitoids
Tin granites
Fe_2O_3/FeO
SiO_2
10
1
0.1
0.01
55
65
75
85
B
magnetite series
ilmenite series
Rb/Sr
1
10
100
1000

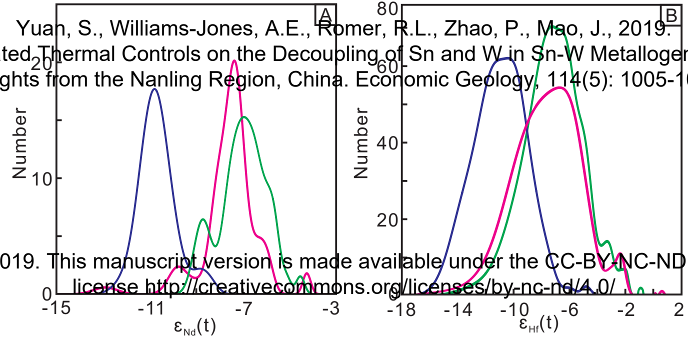
A
B
Number
Number
20
10
0
80
60
40
20
0
-15
-11
-7
-3
-18
-14
-10
-6
-2
2
$\varepsilon_{Nd}(t)$
$\varepsilon_{Hf}(t)$

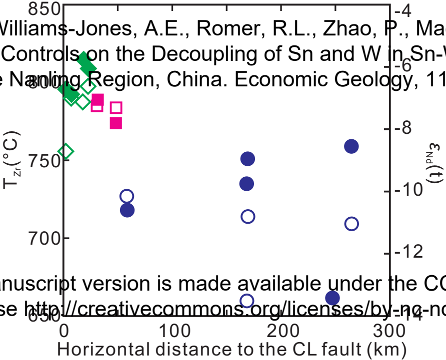
850
800
750
700
650
T_zr (°C)
0
100
200
300
Horizontal distance to the CL fault (km)
-4
-6
-8
-10
-12
-14
ε_Nd(t)

Yuan, S., Williams-Jones, A.E., Romer, R.L., Zhao, P., Mao, J., 2019.
Protolith-Related Thermal Controls on the Decoupling of Sn and W in Sn-W Metallogenic Provinces:
Insights from the Nanling Region, China. Economic Geology, 114(5): 1005-1012.

Table DR1 Whole-rock geochemical and Sm-Nd isotopic data of the representative Late Jurassic (160-150 Ma) W-Sn-related granite in the Nanling region, South China

Deposit	Sample Number	Rock type	SiO_2	TiO_2	Al_2O_3	TFe_2O_3	FeO	Fe_2O_3	MnO	MgO	CaO	Na_2O	K_2O	P_2O_5	La	Ce	Pr	Nd	Sm	Eu
Xihuashan W deposit	XHS-3	The first medium-grained porphyritic biotite granite	75.95	0.13	12.82	1.4	0.8	0.51	0.07	0.22	0.64	3.03	4.95	0.05	33.4	63.7	8.02	29.5	7.75	0.39
	XHS-4		75.39	0.12	12.95	1.57	0.94	0.52	0.07	0.2	0.47	2.85	5.27	0.04	21.6	41.5	5.86	23.4	8.72	0.29
	XHS-7		75.84	0.08	12.83	1.23	0.87	0.26	0.07	0.16	1	3.39	4.56	0.02	15.9	35.7	4.48	18	6.52	0.29
	XHS-8		76.47	0.07	12.73	1.17	0.78	0.3	0.07	0.16	0.9	3.35	4.66	0.03	14.8	31.7	4.22	16.9	6.22	0.23
	XHS-9		74.53	0.09	13.25	1.28	0.88	0.31	0.07	0.17	0.96	3.42	4.86	0.04	16.7	35.5	4.71	19.1	7	0.35
	XHS-10		74.71	0.1	13.31	1.24	0.94	0.2	0.07	0.19	1.09	3.36	4.95	0.03	16.9	36.4	4.83	19.7	6.84	0.41
	XHS-11		77.01	0.1	12.1	1.45	1.02	0.32	0.08	0.2	0.98	3.18	4.5	0.03	19	44.7	5.67	23.3	8.29	0.28
	XHS-25		74.61	0.14	13.42	1.59	1.13	0.33	0.06	0.29	1.35	2.86	5.15	0.04	17.9	37.3	4.92	19.8	6.37	0.5
	XHS-30		75.51	0.09	12.69	1.35	0.88	0.37	0.07	0.15	1.03	3.23	4.81	0.03	26.5	55	6.61	24.4	6.54	0.3
	XHS-31		76.05	0.08	12.62	1.18	0.77	0.33	0.07	0.13	0.92	3.22	4.88	0.02	27.3	55.9	6.51	23.8	6.47	0.28
	XHS-32		76.45	0.09	12.41	1.38	0.91	0.36	0.08	0.16	0.95	3.12	4.84	0.03	23.4	50.7	6.24	23.9	7.29	0.3
	XHS-33		75.15	0.09	13.06	1.31	0.89	0.32	0.07	0.15	1.01	3.19	5.19	0.03	26.9	57.6	6.89	25.9	6.89	0.32
	XHS-34		76.78	0.09	11.99	1.38	0.94	0.34	0.08	0.15	0.88	3.09	4.69	0.03	18.6	39.3	4.95	19.2	5.66	0.26
	XHS-35		74.77	0.09	13.26	1.17	0.78	0.3	0.07	0.14	1.04	3.43	5.07	0.03	22	47.1	5.8	22.2	6.86	0.41
	X09-3	The second garnet-bearing fine-grained biotite granite	75.79	0.02	13.07	0.86	0.54	0.26	0.12	0.05	0.46	3.99	4.4	0.01	5.9	15.2	2.49	11.8	7.06	0.071
	X09-4		76.31	0.01	13.02	0.75	0.56	0.13	0.12	0.06	0.51	4.14	4.48	0.01	4.98	12.6	2.06	9.84	6.25	0.054
	X09-5		76.01	0.02	12.94	0.78	0.56	0.15	0.11	0.07	0.54	3.92	4.63	0.01	6.99	16.7	2.52	11.1	6.05	0.095
	XHS-1		76.8	0.01	12.66	0.79	0.62	0.1	0.11	0.04	0.6	3.8	4.69	0.01	4.49	12.9	2.41	12.7	8.73	0.06
	XHS-2		76.03	0.01	13.06	0.86	0.61	0.18	0.11	0.04	0.55	4.02	4.66	0.01	4.68	11.3	1.85	8.89	5.64	0.061
	XHS-12		75.67	0.01	13.26	0.65	0.42	0.19	0.06	0.04	0.54	3.99	4.71	0.01	6.33	16.2	2.68	12.9	7.84	0.067
	XHS-13		75.52	0.02	13.01	0.77	0.51	0.21	0.08	0.05	0.6	4.11	4.58	0.01	8.1	21.5	3.4	15.6	9.5	0.069

XHS-14		75.69	0.02	12.93	0.75	0.55	0.14	0.1	0.05	0.64	4.13	4.36	0.01	5.38	13.7	2.27	11	6.96	0.063
XHS-21		76.09	0.02	12.95	0.85	0.56	0.23	0.09	0.06	0.65	4.14	4.35	0.01	7.24	19.3	3.3	16	10.7	0.057
XHS-22		76.2	0.02	12.91	0.82	0.54	0.22	0.08	0.06	0.71	4.04	4.35	0.01	6.67	16.4	2.62	12.1	6.98	0.1
XHS-23		75.81	0.01	13.02	0.83	0.56	0.21	0.08	0.04	0.59	4.02	4.66	0.01	5.02	12.9	2.1	10.3	6.45	0.065
XHS-24		76.19	0.02	13.11	0.82	0.49	0.28	0.07	0.04	0.58	4.13	4.41	0.01	6.26	16.5	2.86	14.2	9.22	0.066
XHS-15	The third garnet-bearing fine-grained porphyritic biotite granite	75.33	0.08	12.96	1.61	1.09	0.4	0.1	0.12	0.7	3.49	4.51	0.03	27.7	63.5	7.84	30.5	10.6	0.26
XHS-16		75.59	0.07	12.74	1.34	0.5	0.78	0.1	0.13	0.59	3.45	4.52	0.03	27.1	60.4	7.37	28.9	10	0.23
XHS-17		74.97	0.09	13.43	1.58	1.5	-	0.1	0.13	0.75	3.58	4.64	0.03	37.6	84.7	10.5	41.3	13.8	0.29
XHS-18		75.82	0.08	13.06	1.2	0.81	0.3	0.1	0.13	0.57	3.51	4.78	0.03	28.7	64	7.71	29.8	10.2	0.24
XHS-19		75.88	0.06	13.09	1	0.65	0.28	0.1	0.11	0.7	3.73	4.54	0.02	25.5	59.5	7.34	29.4	10.7	0.18
XHS-20		75.1	0.08	12.94	1.34	0.93	0.3	0.09	0.15	0.69	3.6	4.55	0.03	31	67.6	8.45	33.2	11.5	0.25
XHS-26		78.07	0.04	12.08	0.78	0.48	0.25	0.09	0.08	0.44	3.71	4.23	0.02	13.5	32.9	4.19	17	7.16	0.093
XHS-27		76.03	0.07	13	1.09	0.71	0.3	0.07	0.13	0.6	3.54	4.87	0.03	25.8	57.9	7.24	28.7	10	0.22
XHS-28		76.26	0.03	12.66	0.79	0.54	0.19	0.09	0.06	0.52	3.88	4.7	0.01	11.3	25.8	3.44	13.4	5.74	0.077
XHS-29		76.29	0.03	12.84	0.82	0.6	0.15	0.09	0.05	0.55	4.03	4.48	0.01	10.9	24.4	3.42	13.6	6.25	0.064
X-1	Medium-grained porphyritic biotite granite	73.85	0.06	12.66		0.84	0.15	0.06	0.46	1.29	3.63	4.46	0.02	12.9	27.9	3.62	16.1	6.64	0.23
X-2		74.51	0.09	13.73		1.04	0.3	0.07	0.15	0.96	3.68	4.76	0.03	16.3	34.5	4.36	18.3	7.03	0.28
X-4		75.6	0.08	13.33		1.1	0.25	0.07	0.14	0.93	4.55	4.27	0.03	10.4	22	2.88	12.5	5.6	0.25
X-5		75.55	0.09	13.45		1.15	0.31	0.07	0.16	0.98	4.07	4.43	0.03	13.2	27.9	3.63	15.6	6.65	0.28
X-6		75.1	0.1	12.82		1.19	0.32	0.08	0.18	0.89	5.23	4.21	0.03	18.4	39.3	4.97	20.6	7.72	0.29
X-18		74.38	0.09	13.09		0.88	0.37	0.07	0.13	0.99	3.8	4.74	0.02	15.4	32.7	4.12	17.3	6.24	0.3
X-19		74.77	0.09	12.67		0.85	0.34	0.07	0.12	1.03	4.11	4.33	0.02	17	36.3	4.58	19.4	7.27	0.29
X-21		75.39	0.07	13.01		0.75	0.24	0.06	0.08	0.89	3.79	4.65	0.01	11.3	26.6	3.53	16.1	7.21	0.23
X-8	Medium-grained biotite granite	76.26	0.02	13.05		0.45	0.16	0.11	0.03	0.49	4.69	4.41	0.003	5.8	15.6	2.34	11.8	7.81	0.05
X-9		75.58	0.02	12.99		0.62	0.23	0.09	0.03	0.59	4.24	4.24	0.003	4.8	11.4	1.73	8.1	4.9	0.06

	X-11		75.7	0.02	12.93		0.71	0.25	0.1	0.02	0.61	4.26	4.42	0.002	4.08	10.4	1.49	7.25	4.56	0.06
	X-12		76.1	0.02	13.49		0.48	0.22	0.1	0.04	0.57	4.93	4.23	0.003	4.51	11.5	1.62	7.68	4.53	0.06
	X-13		75.7	0.03	12.96		0.52	0.23	0.09	0.03	0.64	4.61	4.23	0.005	8.71	20.6	2.79	12.6	6.21	0.1
	X-14		75.85	0.02	12.87		0.5	0.19	0.08	0	0.55	4	4.64	0.002	4.58	11.6	1.67	7.84	4.4	0.06
	X-16		75.4	0.02	12.96		0.59	0.24	0.07	0.01	0.57	4.19	4.47	0.001	4.59	13.1	1.96	9.22	5.5	0.06
	X-17		75.71	0.02	12.95		0.56	0.17	0.1	0	0.56	4.18	4.36	0.001	4.52	13.1	2.16	11.2	8.17	0.05
	X-20		76.1	0.02	12.87		0.44	0.28	0.08	0.03	0.62	4.65	4.16	0.003	5.53	14.2	2.04	9.54	5.65	0.06
	X-22		76.49	0.02	12.51		0.53	0.29	0.09	0.06	0.66	4.18	4.36	0.003	5.12	13.1	1.96	9.33	6.04	0.08
	X-23		75.43	0.02	12.93		0.48	0.27	0.11	0.01	0.59	4.28	4.14	0.001	4.8	14	2.36	12.7	8.96	0.06
	X-10	Fine-grained	76.42	0.02	13.08		0.6	0.27	0.15	0.03	0.51	4.6	4.23	0.001	3.97	11.3	2.05	11.3	8.7	0.05
	X-7	two-mica granite	75.7	0.02	13.06		0.75	0.24	0.07	0.02	0.6	4.59	4.25	0.004	10.5	25.6	3.8	16.8	8.99	0.06
	PT03	K-feldspar	73.97	0.08	13.87			1.09	0.14	0.01	0.72	4.19	4.9	0.02	7.72	21	3.41	17.6	11.6	0.14
	PT06	granite	72.78	0.09	14.49			2.67	0.56	0.04	1.13	2.05	4.1	0.03	14.8	35.8	4.7	19.9	7.58	0.14
	PT11		74.57	0.08	13.4			1.24	0.16	0.06	0.87	3.29	4.9	0.03	10.4	25.6	3.61	15.6	8.1	0.16
Piaotang W	PT-01		76.61	0.11	12.36		0.8	1.05	0.17	0	0.65	3.15	4.88	0.02	8.35	22.5	3.14	13.8	7.19	0.08
deposit	PT-03	Biotite	76.63	0.12	12.38		0.93	1.28	0.08	0.07	0.72	3.43	4.26	0.02	13.1	31.6	3.99	15.7	6.22	0.13
	PT-04	monzogranite	76.96	0.12	12.37		0.77	1.09	0.07	0.05	0.75	3.33	4.64	0.02	12.9	30.9	4.37	19.4	9.46	0.15
	PT-06		76.55	0.1	12.6		0.79	0.93	0.1	0.02	0.63	3.57	4.59	0.02	10.3	25.8	3.42	14.4	6.53	0.09
	PT-07		75.38	0.09	12.87		0.44	0.74	0.1	0.07	0.61	3.81	4.46	0.02	6.79	17.4	2.54	12.5	7.55	0.04
	TS-5	The main-phase	75.3	0.03	13.7		0.47	0.09	0.12	0.47	1.42	0.13	5.17	0.04	12.1	28.3	3.57	13.8	5.65	0.1
	TS9-1	coarse-medium	76	0.04	13.3		0.88	0.02	0.11	0.07	0.55	3.32	4.86	0.05	17.9	42.6	5.23	20	7.19	0.1
Tieshanlong	TS9-3	grained	75.9	0.04	13.5		0.75	0.15	0.09	0.07	0.61	3.69	4.43	0.05	15.8	43.3	4.92	18.2	5.63	0.04
W deposit	TS9-4	porphyritic	76	0.04	13.5		0.75	0.27	0.12	0.12	0.5	3.14	4.48	0.08	11.4	25.4	3.32	12.5	4.62	0.1
	TS9-24	biotite granite	73.4	0.13	14.4		1.03	0.39	0.11	0.22	0.88	3.16	5.16	0.19	23.2	54.1	5.47	18.5	4.09	0.32
	TS9-5		76.1	0.06	13.8		1.23	0.16	0.17	0.17	0.43	0.13	5.82	0.05	26.8	64.2	7.54	29	9.38	0.11

	TS-7	Two-mica granite and muscovite granite	75.5	0.04	13.7		0.61	0.06	0.09	0.33	0.6	3.08	4.6	0.05	10.9	26	3.21	12.1	4.73	0.07
	TS-26		77.1	0.03	13.7		1.21	0.15	0.18	0.09	0.29	3.11	3.73	0.07	3	8.4	0.83	2.9	0.96	0.02
	TSY-1		76.7	0.02	13.4		0.69	0.12	0.16	0.17	0.48	3.57	3.75	0.06	9.3	24.5	3.29	12.8	5.21	0.03
	TSY-7		76.5	0.01	13.5		0.63	0.14	0.17	0.16	0.57	2.81	3.99	0.06	7.1	18.2	2.47	9.1	4.25	0.03
Yaogangxian W deposit	YGX-21-7	Coarse-grained two-mica granite	75.62	0.03	12.75			0.86	0.14	0.01	0.56	3.62	4.57	0.01	5.99	16.4	2.48	11.3	6.65	0.06
	YGX-23-8		75	0.04	12.85			1.13	0.11	0.02	0.63	3.39	4.76	0.02	13.6	32.6	4.43	18.7	8.35	0.13
	YGX-23-12		74.68	0.05	12.98			1.08	0.1	0.04	0.77	3.58	4.64	0.01	10.8	24.7	3.26	13.4	5.62	0.16
	YGX-23-14		74.34	0.07	13.15			1.23	0.07	0.1	0.9	3.56	4.57	0.02	18.2	38.6	4.95	19.3	6.39	0.32
	YGX-23-15		74.4	0.05	12.94			1.11	0.1	0.03	0.73	3.57	4.61	0.02	12.9	29.1	3.84	16.1	6.77	0.16
	YGX-23-17		74.99	0.04	12.88			1.06	0.09	0.04	0.66	3.76	4.53	0.02	7.6	18.5	2.68	12.4	6.37	0.11
	YGX-23-24		75.31	0.04	12.83			0.87	0.11	0.01	0.6	3.85	4.42	0.01						
	YGX-19-2	Coarse- to medium-grained two-mica granite	75.66	0.03	12.53			1.09	0.14	0	0.52	3.6	4.39	0.01	4.67	12.9	1.83	8.91	5.58	0.05
	YGX-19-3		74.49	0.02	12.92			0.88	0.13	0.03	0.52	3.67	4.88	0.01	2.6	9.78	1.13	5.16	3.05	0.02
	YGX-19-12		75.77	0.03	12.92			0.86	0.14	0.02	0.61	4.09	4.36	0.01	3.95	13.4	1.52	6.83	4.02	0.04
	YGX-19-18		75.69	0.03	12.92			0.98	0.11	0.01	0.58	3.97	4.41	0.01	2.55	10.2	0.99	4.32	2.28	0.02
	YGX-21-10		75.57	0.02	12.79			0.95	0.16	0.02	0.6	3.33	4.68	0.01						
	YGX-21-12		75.86	0.03	12.58			1	0.15	0.01	0.53	3.72	4.34	0.01	2.65	10.3	1.04	4.89	2.75	0.03
	YGX-23-13		74.75	0.03	13.24			0.89	0.11	0.04	0.63	3.93	4.55	0.01	5.07	14.7	1.66	7.51	3.39	0.06
	YGX-23-21		74.74	0.03	13.01			0.98	0.13	0.04	0.53	4.13	4.43	0.01	4.41	15.1	1.56	6.8	3.44	0.03
	YGX-23-29		76.65	0.03	12.65			0.91	0.13	0.03	0.6	3.93	4.39	0.01	5.3	14	1.63	6.95	3.54	0.05
	YGX-16-7	Fine-grained muscovite granite	76.67	0.03	13.09			0.96	0.16	0.01	0.53	3.38	5.07	0.01	8.57	21.4	3.13	13.7	8.33	0.07
	YGX-16-13		75.11	0.03	13.05			0.87	0.08	0.02	0.51	4.35	4.73	0.01	2.6	10.9	1.11	4.85	2.95	0.02
	YGX-23-4		75.72	0.03	12.62			0.96	0.1	0	0.55	4.03	4.28	0.01	3.38	12.4	1.11	4.8	2.49	0.02
	YGX-23-25		75.32	0.03	12.72			0.92	0.12	0	0.56	4.1	4.3	0.01	5.94	15	2.04	9.24	5.15	0.06
	YGX-1-1		76.55	0.02	12.99			0.82	0.12	0.08	0.51	4.21	4.18	0.01	1.51	5.98	0.68	3.13	1.69	0.01

	YGX-1-2		77.04	0.02	12.91			0.83	0.11	0	0.49	4.16	4.03	0.01	1.99	7.39	0.96	3.95	1.7	0.01
	YGX-1-3		75.89	0.02	12.9			0.68	0.14	0	0.48	4	4.22	0.01	2.37	8.64	1.11	4.57	2.65	0.01
	YGX-1-7		76.8	0.02	12.71			0.82	0.14	0	0.45	3.72	4.27	0.01	2.21	10.8	0.97	4.68	3.18	0.01
Pangushan W deposit	NLSD2-1348	K-feldspar granite	76.57	0.11	12.31		1.06	0.25	0.08	0.1	0.83	3.21	5.04	0.02	11.1	22.1	2.85	11.1	2.87	0.48
	NLSD2-1522		73.72	0.16	12.85		1.35	0.67	0.09	0.22	1.14	3.31	4.77	0.03	25.2	55.6	7.37	28.8	8.34	0.5
	NLSD2-1880		76.14	0.09	12.8		0.95	0.34	0.12	0.17	1.03	3.49	4.54	0.03	10.6	25.1	3.33	14.3	5.08	0.32
	NLSD2-1882		75.56	0.1	12.95		0.92	0.27	0.1	0.2	1.17	3.45	4.53	0.03	9.95	21.8	2.96	12.3	4.34	0.39
Dajishan W deposit	DJS-01	Muscovite albite-rich garnite	73.67	0.08	14.77		0.24	0.52	0.07	0.13	0.44	4.59	4.09	0.03	2.345	7.0752	1.075	4.171	4.507	0.042
	DJS-05		69.88	0.08	16.66		0.25	0.56	0.17	0.04	0.53	4.28	6.28	0.03	2.896	10.646	1.62	6.944	7.846	0.046
	DJS-07		75.34	0.07	14.3		0.15	0.38	0.03	0	0.24	5.06	3.72	0.03	2.007	6.688	1	3.922	4.616	0.037
	DJS-10		74.35	0.09	14.63		0.5	0.38	0.17	0.15	0.42	4.67	3.22	0.03	2.604	8.4536	1.322	5.22	5.117	0.037
	DJS-2	Muscovite albite-rich garnite	75.6	0.01	13.62		0.13	0.29	0.06	0.16	0.74	4.27	4.17	0.02	0.99	2.75	0.41	1.79	1.15	0.04
	DJS-20		78.09	0.01	12.49		0.17	0.12	0.07	0.06	0.44	4.4	3.5	0.02	2.46	7.04	1.07	4.15	3.24	0.09
	DJS-7		73.62	0.02	14.8		0.17	0.15	0.05	0.09	0.59	4.42	5.2	0.02	4.26	13.1	2.03	8.23	7.79	0.1
	DJS-14	Muscovite K-feldspar granite	75.83	0.01	14.58		0.08	0.2	0.13	0.13	0.33	5.05	3.64	0.02	2.74	7.82	1.45	5.62	6.75	0.09
	DJS-13		77.21	0.01	14.09		0.11	0.44	0.03	0.15	0.42	4.22	3.25	0.01	2.23	6.69	1.22	4.97	4.69	0.05
	DJS-12		76.87	0.01	13.83		0.18	0.24	0.11	0.14	0.66	4.11	3.8	0.02	3.05	7.98	1.34	4.95	3.4	0.07
	DJS-11		77.45	0.01	14.02		0.21	0.26	0.16	0.06	0.71	3.56	3.95	0.01	4.95	12.4	1.93	8.14	5.42	0.09
	DJS-8		76.38	0	13.76		0.13	0.29	0.06	0.13	0.75	4.25	4.21	0.02	1.99	5.68	1.32	5.79	3.15	0.08
	DJS-6		76.34	0.01	13.91		0.17	0.12	0.07	0.06	0.45	4.17	4.58	0.02	2.46	7.24	1.27	4.15	3.24	0.09
	DJS-5		75.31	0.01	13.99		0.42	0.59	0.24	0.08	0.32	4.66	4.43	0.02	2.13	0.7	1.14	5.1	4.19	0.12
	DJS-4		73.9	0.02	13.55		0.68	0.97	0.35	0.15	0.23	3.99	4.69	0.02	3.26	13.1	2.03	8.23	7.79	0.1
	DJS-3		74.42	0.01	14.18		0.78	0.96	0.55	0.18	0.32	4.47	4.29	0.02	3.66	13	2.12	9.6	7.21	0.04
	DJS-1		75.08	0.01	13.32		0.57	0.83	0.58	0.12	0.28	4.51	4.19	0.02	2.07	6.5	1.72	4.79	4.22	0.04
Shizhuyuan	SZY-23	The first-phase	74.28	0.2	12.85	0.51	0.4	0.07	0.02	0.27	2.43	2.66	4.98	0.06	39.2	75.4	9.09	33.9	7.97	0.49

Yuan, S., Williams-Jones, A.E., Romer, R.L., Zhao, P., Mao, J., 2019.
Protolith-Related Thermal Controls on the Decoupling of Sn and W in Sn-W Metallogenic Provinces:
Insights from the Nanling Region, China. Economic Geology, 114(5): 1005-1012.

Sn-W	SZY-24	microfine-grained	73.65	0.22	13.09	1.29	0.76	0.45	0.03	0.35	1.77	2.59	5.5	0.07	44.8	84.3	10.4	38.8	8.73	0.59
deposit	SZY-25	porphyritic	73.98	0.2	12.99	0.93	0.65	0.21	0.02	0.31	1.76	2.85	5.38	0.06	41.4	82.3	9.62	37	8.3	0.6
	SZY-26	biotite granite	73.7	0.23	13.17	1.33	0.87	0.36	0.02	0.36	1.6	2.81	5.5	0.07	40	77.2	9.43	35.4	7.91	0.57
	SZY-27		74.44	0.21	12.91	1.21	0.73	0.4	0.02	0.31	1.56	2.84	5.41	0.06	43.4	87	10.5	38.9	9.14	0.58
	SZY-28		74.24	0.24	12.99	1.33	0.91	0.32	0.02	0.33	1.5	2.87	5.29	0.07	42.8	84.8	9.98	37.7	8.2	0.72
	SZY-13	The second-phase	73.31	0.27	13.47	0.39	0.34	0.01	0.03	0.39	1.74	2.54	6.79	0.11	37.8	66.6	10.5	40.8	8.64	0.69
	SZY-14	fine-grained	73.21	0.28	13.5	0.41	0.32	0.05	0.04	0.41	1.77	2.45	6.91	0.12	53.5	111	12.9	49	10.2	0.75
	SZY-29	porphyritic	74.07	0.22	12.88	1.91	1.29	0.48	0.07	0.29	1.16	3.45	4.58	0.06	52.3	112	12.9	49.8	12.1	0.55
	SZY-30	biotite granite	74.73	0.19	12.74	1.57	1.24	0.19	0.05	0.24	1.11	3.5	4.53	0.05	47.3	98.6	11.2	41.8	10	0.5
	SZY-31		74.67	0.22	12.71	1.84	1.21	0.5	0.06	0.27	1.13	3.45	4.52	0.06	52.5	113	12.8	47.8	11.6	0.48
	SZY-1		75.19	0.01	13.55	1.22	0.94	0.18	0.06	0.06	0.54	4.19	4.03	0.01	30.1	66.7	10.1	41.8	16.3	<0.05
	SZY-2		75.31	0.01	13.63	0.17	0.18	0	0.01	0.03	0.45	4.73	4.55	0.01	25.5	59.1	8.8	37.1	15.5	<0.05
	SZY-3		76	0.01	13.33	0.61	0.54	0.01	0.03	0.03	0.5	3.91	4.53	0.01	18.5	57.9	6.75	27.4	10.9	<0.05
	SZY-4	The third-phase	75.65	0.01	13.22	0.88	0.58	0.24	0.02	0.02	0.64	3.66	4.58	0.01	24.3	58.2	9.09	40.4	18	<0.05
	SZY-5	medium-grained	73.85	0.01	14.65	1.33	0.99	0.23	0.04	0.02	0.73	3.35	4.36	0.01	26.5	69.3	11	45.7	20.1	<0.05
	SZY-6	equigranular	75.55	0.01	13.51	0.76	0.61	0.08	0.02	0.03	0.6	4.42	3.8	0.01	26	63.3	9.81	42.6	19.3	<0.05
	SZY-7	zinnwaldite	74.25	0.01	14.15	1.58	1.08	0.38	0.05	0.03	0.78	3.29	4.2	0.01	19.4	57.3	7.74	32.4	13.7	<0.05
	SZY-12	granite	77.38	0.03	11.77	1.27	0.8	0.38	0.03	0.15	0.65	3.23	4.04	0.01	28.7	68.7	8.85	37.3	13.8	<0.05
	SZY-19		76.63	0.01	12.72	0.79	0.52	0.21	0.02	0.04	0.47	4.08	4.27	0.01	21.1	40.5	7.32	34.2	16.5	<0.05
	SZY-20		75.87	0.04	12.73	1.08	0.76	0.24	0.03	0.06	0.6	3.55	4.82	0.02	25.2	45.8	7.29	30.1	10.1	0.06
	SZY-21		77.74	0.04	11.44	1.12	0.66	0.39	0.04	0.06	0.6	3.21	4.34	0.01	22.1	45.6	6.47	26.6	9.3	0.06
	SZY-22		76.34	0.01	12.91	0.27	0.23	0.01	0.01	0.06	0.46	3.89	5.04	0.01	24.1	53	9.35	40.8	18.5	<0.05
	JCT-29	Porphyritic	74.49	0.12	12.81		1.02	0.45	0.04	0.14	1.11	2.65	5.39	0.03	74	138	12.4	51.5	10.3	0.31
	SZY-19	biotite granite	74.87	0.11	12.6		1.03	0.5	0.04	0.17	1.16	2.82	5.23	0.03	122	261	23.5	74.8	11.4	0.27
	SZY-1	Equigranular	75.86	0.05	12.67		0.5	0.52	0.03	0.12	0.9	3.49	4.8	0.01	29	62	9.3	33.4	11.7	0.11

	SZY-20	biotite granite	75.92	0.05	12.41		0.44	0.84	0.03	0.15	0.85	3.24	4.57	0.01	70	131	18.5	68.3	15.7	0.12
	SZY-9		74.62	0.01	13.55		0.09	0.15	0.01	0.09	0.88	4.02	5.12	0.01	38	108	12.1	49	15.4	0.01
	QLS-1		72.4	0.34	12.98	2.45			0.03	0.52	1.45	3.18	5.23	0.09	72.9	148	15.3	52.9	9.88	0.84
	QLS-2		71.66	0.3	13.26	2.21			0.03	0.46	1.47	3.04	5.92	0.08	62.8	128	13.3	45.8	9	0.98
	QLS-73		72.34	0.34	13.13	2.42			0.04	0.52	1.46	3.26	5.32	0.09	73.4	148	15.4	53.5	10.5	0.89
	QLS-74	Porphyritic	71.87	0.32	13.42	2.25			0.03	0.48	1.46	3.24	5.67	0.09	71.6	145	15	51.1	9.76	1.01
	QLS-76	biotite granite	72.48	0.32	13.12	2.31			0.03	0.51	1.44	3.25	5.26	0.09	62.2	126	13.3	46.4	9.34	0.77
	QLS-156		72.53	0.33	12.81	2.33			0.03	0.51	1.4	3.13	5.24	0.09	73.3	150	15.7	54.3	10.9	0.93
	QLS-157		71.71	0.33	13.34	2.34			0.04	0.51	1.41	3.25	5.4	0.09	66.6	134	13.9	47.2	9.25	0.9
	QLS-158		72.59	0.32	12.96	2.43			0.03	0.51	1.46	3.27	5.18	0.09	74.1	149	15.4	51.7	9.32	0.85
	QLS-115		74.43	0.02	14.01	0.62			0.03	0.42	0.62	5.24	4.37	0	21.4	58.6	8.07	32.2	13.5	0.03
	QLS-116		76.04	0.01	13.34	0.68			0.03	0.14	0.5	4.4	4.32	0	24.1	59.7	9.17	38.8	16.9	0.03
	QLS-117		74.78	0.02	13.52	0.72			0.03	0.17	0.61	3.53	5.19	0	22.5	60.2	8.73	36.4	17	0.03
	QLS-119		75.07	0.02	13.46	0.69			0.03	0.16	1.07	3.72	4.58	0.01	15.4	41.7	5.87	24.4	10.2	0.03
	QLS-152		76.35	0.02	12.75	0.52			0.03	0.13	0.46	4.68	3.89	0	20.8	50.8	7.59	31.3	13.6	0.03
	QLS-154		75.11	0.02	13.53	0.81			0.05	0.15	0.45	4.21	4.53	0.01	20.5	50.7	7.57	30.8	14.1	0.03
	QLS-155		75.82	0.02	13.06	0.78			0.04	0.19	0.54	3.99	4.43	0.02	24.1	66.2	9.01	37.3	17.1	0.03
	QLS-46	Equigranular	75.47	0.04	12.59	0.72			0.03	0.18	0.66	3.98	4.76	0.03	21.2	54	6.44	26.2	9.85	0.05
	QLS-48	granite	76.33	0.05	12.26	1.13			0.04	0.18	0.73	3.47	4.82	0.01	33	82.7	10.3	42.4	14.9	0.08
	QLS-81		74.62	0.02	14.06	1.22			0.08	0.17	0.4	4.73	3.53	0.04	21.4	79	8.29	33.6	13.3	0.02
	QLS-83		74.53	0.02	14.06	0.81			0.04	0.45	0.57	5	3.83	0	30.6	82.9	11.5	47	20.2	0.02
	QLS-147		74.22	0.02	14.01	0.78			0.05	0.14	0.46	4.74	4.04	0.01	24.1	73.7	9.34	39.3	16.4	0.02
	QLS-150		74.61	0.02	13.93	0.81			0.05	0.15	0.56	4.61	3.88	0.01	26.5	70.7	10.6	44.4	19.7	0.02
	QLS-151		74.95	0.02	13.79	0.54			0.04	0.13	0.5	5.05	3.57	0.01	26.8	70.5	10.3	42.9	18.1	0.02
	QLS-29		75.05	0.03	13.36	0.79			0.03	0.14	1.02	3.88	4.74	0	17.8	45.1	6.29	26.3	11.3	0.02

	Q1		75.2	0.14	12.61		1.5	0.05	0.14	0.08	2.29	4.87	0.03						
	Q2		76.01	0.15	13.5		1.37	0.06	0.17	0.74	2.62	5.03	0.03						
	Q3	Porphyritic	74.2	0.15	13		1.83	0.08	0.19	0.94	1.99	5.29	0.03	56.1	80.1	12.9	50.6	12.2	0.86
	Q4	biotite granite	77.2	0.14	12.4		1.09	0.05	0.12	0.73	2.81	4.97	0.03	30.4	76.1	7.83	31.1	8	0.53
	Q5		76.95	0.14	11.88		1.49	0.06	0.12	0.64	2.64	4.35	0.03	32.6	76.9	8.46	33.4	8.68	0.64
	490-46		75.12	0.16	13.03		1.72	0.09	0.18	1.03	2.89	4.95	0.04	42.6	91.8	11.6	44.9	11.1	0.7
	490-18		74.81	0.01	13.96		0.18	0.06	0.03	0.72	2.85	4.12	0.02	52.4	149	21.5	95.7	35.3	0.7
	490-19		75.03	0.02	13.64		0.89	0.06	0.02	0.75	3.59	4.14	0.01	19.3	51.3	7.44	32.7	13.4	0.24
	490-20		77.95	0.02	12.13		0.57	0.05	0.02	0.49	3.34	4.02	0	23.7	62.4	8.77	38.4	15	0.27
	490-21		75.79	0.02	13.84		0.96	0.06	0.03	0.65	3.62	4.89	0	19.6	62.4	7.33	38.4	14.7	0.24
	490-22	Equigranular	74.82	0.02	13.4		2.26	0.11	0.03	0.63	2.81	3.89	0.01	34.2	95.1	13.4	60.8	22.8	0.42
	490-28	granite	75.71	0.04	13.44		0.73	0.05	0.02	0.79	3.15	4.94	0.02	29	75.8	9.92	43.1	15.4	0.33
	490-29		74.84	0.02	13.84		0.86	0.05	0.02	0.72	3.54	4.09	0	25.8	67.5	9.41	40.4	14.3	0.32
	490-31		77.84	0.04	11.95		0.48	0.05	0.05	1.67	2.13	5.07	0.02	26.7	69.3	8.84	37.2	13.5	0.3
	490-32		78.68	0.03	10.92		0.49	0.05	0.02	1.79	2.11	4.43	0.01	15.9	32.7	3.89	14.2	4.03	0.24
	490-33		77.85	0.04	11.62		0.64	0.06	0.05	1.36	2.29	4.75	0.01						
	SZY-21-02		71.9	0.31	13.6	2.31		0.04	0.38	1.5	2.93	5.76	0.1	79.2	148	16.4	52.8	9.54	0.89
	SZY-22	Phase-1	73.4	0.32	12.8	2.37		0.04	0.38	1.55	2.95	5.16	0.09	83.6	162	16.9	56.8	10.4	0.86
	SZY-23-01	porphyritic	72.9	0.27	13	2.1		0.03	0.35	1.27	2.83	5.57	0.08	78.4	152	16	50.6	9.24	0.94
	SZY-34-01	biotite granite	73	0.32	12.5	2.43		0.04	0.38	1.39	3.03	4.74	0.09	82.5	164	17.2	54.9	10.3	0.69
	SZY-38		71.8	0.29	13.4	2.21		0.04	0.35	1.35	2.86	5.98	0.08	82.1	156	17.7	55.9	10.1	0.88
	SZY-39		73.7	0.32	12.3	2.43		0.04	0.39	1.27	2.92	4.98	0.09	84.6	162	18.4	58.6	11.1	0.66
	SZY-05	Phase-2	73.9	0.01	14.1	0.9		0.03	0.02	1.01	3.66	4.39	0.01	26.9	80.4	11.9	47.7	21.7	<0.03
	SZY-06	equigranular	75.3	0.01	13.8	0.16		<0.01	0.14	0.66	3.94	4.59	0	31.1	91	12.9	50.2	21.3	<0.03
	SZY-07	biotite granite	73.8	0.01	14.9	0.84		0.05	0.01	0.39	4.62	4.14	0	39.8	115.5	16.8	66.7	30.2	<0.03

	SZY-11-01		75.8	0.01	13.3	0.32			0.02	0.03	0.52	4.41	4.63	0.01	22.7	61.4	8.76	36.4	16.8	<0.03
	SZY-11-02		75.3	0.01	13.4	0.39			0.02	0.02	0.52	4.11	4.83	0.01	25.2	70.1	9.98	41.6	19.8	<0.03
	SZY-12		75.6	0.01	13.5	0.26			0.01	0.03	0.33	3.62	5.14	0.01	27.9	73.2	10.4	42.9	19.1	<0.03
	SZY-13		75.7	0.01	13.6	0.22			0.01	0.02	0.47	4.59	4.56	0.01	25.9	68	9.64	39.2	17.4	<0.03
	SZY-15		76.5	0.01	12.9	0.73			0.03	0.09	0.57	3.71	4.42	0.01	26.4	70.2	10.1	41	19.1	<0.03
	SZY-16		73.5	0.01	14.4	1.27			0.08	0.12	0.88	3.71	3.79	0.01	47.1	150.5	22.4	88.2	40.3	<0.03
	SZY-26-03		75.3	0.01	13.1	1.4			0.06	0.06	0.95	2.87	4.63	0.01	24.4	64.1	9.18	35.7	18.2	<0.03
	SZY-36		75.1	0.01	13.2	0.9			0.04	0.02	0.59	3.46	4.96	0.01	24.7	63.5	8.95	37.2	15.9	0.03
	SZY-37		76.3	0.01	13	1.25			0.05	0.02	0.53	3.73	4.54	0.01	22.1	55.6	7.69	29.8	11.7	0.03
Xiangyuan Sn-W deposit	JJL-01	Biotite granite	76.18	0.11	12.68		1.02	0.21	0.03	0.09	0.69	3.55	4.92	0.03	40.14	91.92	11.92	46.72	12.71	0.15
	JJL-04		75.49	0.11	12.5		1.02	0.29	0.02	0.09	0.79	3.55	4.44	0.02	33.86	78.19	10.3	40.16	10.78	0.17
	JJL-10		76.51	0.1	12.63		1.26	0.19	0.03	0.08	0.7	3.29	4.98	0.03	46.32	104.6	13.41	52.54	13.54	0.3
	JJL-18		75.88	0.1	12.12		1.19	0.32	0.03	0.08	0.65	3.03	5.1	0.02	16.69	34	4.77	20.11	5.28	0.15
	JJL-11	Two-mica granite	74.62	0.11	13.16		1.17	0.23	0.03	0.07	0.68	3.43	5.51	0.02	31.23	73.08	8.76	35.14	8.61	0.18
	JJL-12		74.73	0.13	13.33		1.13	0.36	0.03	0.07	0.77	3.49	5.15	0.03	46.19	112.68	13.51	52.57	13.21	0.29
	JJL-17		76.27	0.14	11.85		1.51	0.32	0.04	0.08	0.59	2.97	4.94	0.03	57.69	131.31	16.72	69.98	15.32	0.31
	JJL-09		75.28	0.1	12.68		1.38	0.08	0.03	0.08	0.75	3.42	4.48	0.03	37.79	92.45	11.08	43	10.93	0.21
	PXM-01	Two-mica granite	76.94	0.05	12.5		0.81	0.25	0.03	0.02	0.21	3.41	4.86	0.01	19.1	48.1	5.9	23.29	6.17	0.07
	PXM-02		76.23	0.05	12.67		0.88	0.19	0.03	0.02	0.63	3.85	4.65	0.01	20.33	46.46	6.88	28.7	8.28	0.07
	PXM-03		76.1	0.05	12.68		0.95	0.12	0.03	0.06	0.7	3.41	4.7	0.01	23.68	56.2	7.64	31.95	9.45	0.08
	PXM-04		75.23	0.05	12.91		1.06	0.03	0.03	0.01	0.64	3.9	4.64	0.01	23.58	63.74	7.89	33.24	11.02	0.07
	PXM-05		76.88	0.03	12.2		0.84	0.11	0.06	0.22	0.67	2.53	4.57	0.01	32.36	66.81	11.02	49.43	15.42	0.09
	PXM-06		76.97	0.01	12.42		0.61	0.16	0.05	0	0.38	4.51	3.57	0.01	7.35	20.68	2.89	12.62	4.21	0.02
	PXM-07		76.33	0.01	12.93		0.88	0.05	0.06	0	0.49	3.92	3.9	0.01	10.67	30.89	4.45	19.75	7.53	0.03
	PXM-08		76.62	0.02	12.44		0.75	0.12	0.06	0	0.44	3.48	4.86	0.01	9.13	29.98	4.32	20.18	8.82	0.03

	JJL-07																			
	JJL-19																			
	JJL-20																			
	HGY-4		70.7	0.34	14.5	2.45	1.43	1.13	0.09	0.61	1.57	3.02	5.16	0.15	69.5	132	14.7	50	7.49	1.55
	HGY-7		72.7	0.32	13.4	2.88	2.12	0.84	0.06	0.4	1.13	3.08	4.86	0.15	62.5	123	14.1	50.7	10.4	1.17
	HGY-9		75.3	0.03	13.2	1.28	0.92	0.4	0.04	0.01	0.46	4.5	4.28	0.01	21.9	46.1	7.48	32.1	14.4	0.13
	D0017		71.7	0.3	15.2	2.23	1.18	1.17	0.09	0.54	0.54	3.79	4.03	0.12	45.3	80	8.58	29.3	4.41	0.9
	D0094	Phophyritic	76.1	0.1	12.6	1.86	1.83	0.03	0.05	0.17	0.37	3.25	4.55	0.04	30.3	54.8	7.27	27.3	6.62	0.39
	D5136	biotite monzonite	76.2	0.07	12.9	1.11	0.7	0.46	0.03	0.08	0.33	3.71	4.61	0.02	12.9	22.7	3.17	12.4	3.71	0.28
	D0041		75.5	0.04	13.2	1.38	1	0.42	0.09	0.04	0.35	4.33	4.37	0.02	11.8	41.3	3.64	14.4	5.56	0.13
	H13		73.58	0.2	13.36		1.75	0.78	0.04	0.16	0.95	2.87	5.63	0.05	89.2	172	19.5	67.6	12.3	1.06
	H4		70.67	0.34	14.46		1.43	1.13	0.09	0.61	1.57	3.02	5.16	0.15	69.5	132	14.7	50	7.5	1.55
Xitian Sn	H7		72.67	0.32	13.43		2.12	0.84	0.06	0.4	1.13	3.08	4.86	0.15	62.5	123	14.1	50.7	10.4	1.17
deposit	XT-60	Medium- to	74.64	0.12	12.72	1.41	1.17	0.11	0.05	0.34	1.33	1.92	4.28	0.03	50.33	112.12	13.1	45.7	11.81	0.3
	Xt0416	fine-grained	73.07	0.26	13.44	2.5			0.08	0.31	0.87	3.29	4.79	0.13	37.44	81.61	9.79	36.52	7.6	0.044
	Dahu	two-mica	75.82	0.05	12.03	2.92	2.45	0.2	0.06	0.12	0.7	3.18	4.7	0.02	30.82	70.92	9.89	37.05	11.92	0.12
	Shanyangkeng	monzonite	75.52	0.07	12.06	3.07	2.28	0.54	0.08	0.2	0.62	3.23	4.45	0.01	20.63	45.86	6.16	25.64	8.57	0.13
	Bamuzhai		75.51	0.11	12.68	2.19	1.52	0.5	0.05	0.22	0.46	3.1	5.12	0.03	22.13	42.37	5.84	22.96	5.74	0.34
	Xt0413	Granite	73.92	0.03	15.28	1.19			0.04	0	0.4	3.97	4.67	0.01	19.66	50.96	6.79	26.34	9.78	0.05
	X0406	Medium- to	69.36	0.39	13.4			3.01	0.07	0.93	1.71	3.32	4.39	0.13	58.89	121.1	13.65	47.65	7.603	0.935
	X0417	fine-grained	73.07	0.26	13.44			2.5	0.08	0.31	0.87	3.29	4.79	0.13	37.44	81.61	9.792	36.52	7.603	0.436
	X01	porphyritic	71.9	0.325	13.7		2.23	0.62	0.071	0.635	1.82	3.08	5	0.134	73.78	141.1	16.2	56.13	9.89	0.62
	X02	biotite monzonite	73.43	0.222	13.05		2.01	0.34	0.068	0.56	1.23	2.98	4.6	0.138	22.13	42.37	5.84	22.96	5.74	0.34

	X03	Medium-grained biotite monzonite	74.8	0.12	12.97		1.12	0.2	0.047	0.235	0.68	3.21	5	0.049	20.63	45.6	6.16	25.64	8.57	0.13
	ZK10C02-01	Fine-grained	74.39	0.03	13.72			0.69	0.04	0.42	1.93	0.27	3.54	0.01	14.1	42.9	7.1	32	14.2	0.02
	ZK10C02-17	granite	74.64	0.12	13.08			1.63	0.05	0.07	0.75	2.93	5.25	0.02	47.2	126	14.01	51.4	12.3	0.18
	ZK10C02-19	Porphyritic	75.31	0.12	12.78			1.58	0.05	0.09	0.8	2.85	4.84	0.02	44.8	122	13.61	50.8	12.6	0.16
	ZK10C02-20	quartz granite	75.22	0.13	12.52			1.81	0.06	0.14	0.86	2.42	4.92	0.02	51	134	14.84	54.1	12.4	0.18
	ZK10C02-36		76.68	0.09	12.35			1.44	0.04	0.06	0.82	2.04	4.95	0.02	12.5	35.3	5.64	25.6	11.2	0.07
	ZK10C02-30		73.54	0.06	12.84			1.39	0.08	0.2	2.22	0.1	5.85	0.01	18.8	52.5	7.87	33.2	12.1	0.08
	ZK10C02-22	Medium- to	75.76	0.15	13.09			1.48	0.05	0.28	0.86	0.16	5.04	0.02	57.2	148	16.11	58.3	12.6	0.24
	ZK10C02-25	fine-grained	76.95	0.19	13.57			1.23	0.03	0.14	0.25	0.07	3.88	0.02	61.2	154	16.38	58.9	12.1	0.28
	ZK10C02-12	porphyritic	74.9	0.13	12.7			1.87	0.08	0.13	0.81	2.34	5.12	0.02	49.2	128	14.09	51.5	11.7	0.17
	ZK10C02-03	granite	74.27	0.1	12.81			2.07	0.1	0.11	1.45	0.14	5.87	0.02	34.9	98.2	11.22	41.8	10.8	0.1
	ZK10C02-15		74.29	0.12	12.49			1.66	0.05	0.09	0.81	3.93	4.91	0.02	49.4	128	14.06	51.8	11.8	0.2
	ZK10C02-27		74.54	0.06	13.48			1.57	0.05	0.18	0.91	0.15	5.07	0.02	11.7	33.5	5.58	26.5	12.1	0.08
	ZK10C02-07	Fine-grained porphyritic biotite granite	75.84	0.1	12.88			1.52	0.07	0.17	0.94	0.1	5.55	0.02	36.4	98.4	11.02	40.5	9.7	0.14
	ZK10C02-33	Fine-grained porphyritic biotite monzonite	76.12	0.05	12.56			1.35	0.05	0.38	0.7	2.97	4.71	0.02	13.2	37.5	5.78	25.1	9.9	0.07
Hehuaping Sn deposit	WXL-15	Biotite monzonite	75.95	0.04	12.73	1.46	1.07		0.06	0.05	0.63	3.29	4.75	0.01	29.7	60.7	8.5	32.6	10	0.07
	WXL-16		77.24	0.04	12.26	1.03	7.18		0.02	0.11	0.72	3.24	4.5	0.01	34.3	71.7	10.6	43.3	14.9	0.12
	WXL-17		76.09	0.03	12.82	1.16	0.81		0.04	0.04	0.61	3.57	4.6	0.02	34.5	74.7	11.1	44.6	16	0.09

	WXL-18		77.98	0.03	11.76	0.97	0.49		0.04	0.08	0.47	3.07	4.64	0.01	32.7	71.4	9.65	38.2	13.2	0.07
	ZK16003-3		75.94	0.12	12.35	1.59	0.99	0.5	0.02	0.1	0.83	2.57	4.73	0.03	74.8	154	17.8	64.7	12.4	0.36
	ZK16003-4		74.91	0.12	13.11	1.54	1	0.44	0.02	0.1	0.91	2.7	5.01	0.03	72.3	149	17.1	62.3	12.5	0.45
	ZK12802-4		73.19	0.1	14.3	1.2	0.77	0.35	0.02	0.15	0.99	2.95	5.28	0.02	59.9	120	13.6	51.5	10.2	0.71
	ZK12802-8		73.28	0.28	12.94	2.49	1.68	0.62	0.03	0.24	1.69	2.78	4.22	0.09	94.7	201	23.2	87.6	17.2	0.66
	ZK14401-4		73	0.18	13.65	2.02	1.04	0.86	0.03	0.21	1.07	2.44	5.37	0.01	73.4	147	17	62.9	11.3	0.75
	ZK11202-27		73.57	0.22	13.31	2.04	1.43	0.46	0.03	0.16	1.47	3	4.63	0.06	70.6	147	16.8	63.7	12.4	0.66
	ZK11202-24		74.41	0.21	13.03	1.95	1.39	0.4	0.03	0.16	1.22	2.79	5.09	0.06	62.3	130	14.8	58.1	12.1	0.74
	ZK0004-6		76.34	0.06	12.39	1.17	0.65	0.45	0.03	0.05	0.78	3.18	4.57	0.04	26.7	60.4	7	28.6	6.9	0.1
	HHPD-42	Biotite granite	75.87	0.09	12.66	1.52	1.03	0.38	0.04	0.08	0.83	3.2	4.86	0.05	71.1	159.4	18.2	71	18	0.36
	HHPD-45		74.81	0.09	13.23	1.5	1.17	0.2	0.05	0.08	1.49	3.67	3.59	0.05	61.5	131.7	15.3	58.5	14.8	0.46
	HHPD38																			
	HHPD41																			
	HHPD43																			
	ZK45201-04																			
	ZK20001-03																			
	ZK20001-07																			
	ZK16002-2																			
	ZK11202-10																			
	ZK11202-20																			
	ZK11202-28																			
	ZK004-01																			
Furong Sn deposit	FR-63	Granite (Furong phase)	67.36	0.74	14.34		3.23	1.49	0.08	0.78	2.68	3.39	5.07	0.23	61.40	119.57	14.56	53.40	9.63	1.63
	FR-33		67.05	0.7	14.36		3.03	1.28	0.08	0.84	2.64	3.37	5.39	0.21	58.22	116.96	13.35	47.43	8.82	1.55
	FR-12		67.32	0.74	14.41		2.87	1.29	0.06	1.00	2.43	3.12	5.44	0.21	99.30	168.00	17.98	58.88	9.29	1.55

FR-19		70.28	0.28	13.77		2.04	0.88	0.09	0.46	1.8	3.36	6.21	0.09	83.97	154.11	17.59	62.01	13.19	0.60
GT-2-1		70.14	0.49	14.1		1.13	3.35	0.06	0.57	1.99	3.22	4.99	0.14	68.32	115.74	13.39	44.81	7.63	1.20
FR-43		68.90	0.53	14.29		2.36	0.88	0.06	0.65	2.15	3.21	5.42	0.16	59.63	117.51	12.46	42.56	7.65	1.33
GT-4-4		67.14	0.56	15.12		2.29	0.92	0.06	0.98	1.44	3.09	5.78	0.18	88.57	155.73	16.63	53.52	8.59	1.44
QTL-6		67.28	0.92	13.93		3.29	2.17	0.1	1.01	3.11	3.31	4.11	0.25	64.61	150.47	16.96	62.45	11.33	1.58
QTL-14		67.26	0.71	14.03		2.88	1.71	0.09	0.91	3.26	3.8	4.97	0.23	60.91	141.97	15.08	55.47	9.98	1.71
QT-27	Granite (Cailing	67.64	0.86	12.6		4.32	1.8	0.15	1.1	2.5	2.92	4.46	0.3	78.29	184.10	16.16	73.64	14.39	0.90
QT-29	phase)	67.01	0.88	13.06		4.17	1.69	0.16	1.22	2.58	3.22	4.37	0.33	45.47	121.40	12.05	59.12	12.22	1.19
QT-30		66.5	0.72	14.01		3.41	1.45	0.11	1.1	2.2	3.07	4.94	0.3	100.30	177.90	18.80	69.17	12.29	1.81
QT-38		66.67	0.89	13.7		3.83	1.55	0.13	1.15	3.07	2.99	4.42	0.25	166.12	290.10	23.58	94.00	13.98	1.73
2ksc-10a		67.03	0.58	14.27	4.73		0.06	0.72	1.85	3.14	5.35	0.19		77.03	143.98	16.2	54.91	9.87	1.58
2ksc-10b		67.67	0.6	14.51	3.43		0.07	0.76	1.88	3	6.18	0.23		57.65	114.99	14.01	50.46	9.83	1.68
2ksc-10d		69.59	0.48	12.96	3.54		0.06	0.58	1.6	2.77	5.63	0.16		84.23	149.44	15.95	51.18	8.3	1.3
2ksc-10e		67.97	0.78	14.19	5.12		0.08	0.9	2.84	3.3	4.28	0.26		74.21	147.95	17.62	62.07	11.64	1.49
2ksc-12		66.48	0.72	14.33	4.95		0.07	0.85	2.5	3.42	4.77	0.24		80.66	153.55	17.55	59.91	10.88	1.49
2ksc-13		64.84	1.12	13.36	7.08		0.11	1.34	3.15	3	4.48	0.36		78.83	190.1	22.97	85.82	17.74	1.54
2ksc-14		74.57	0.24	12	2.06		0.03	0.25	1.31	2.84	5.37	0.09		50.92	90.23	9.48	30.08	4.47	0.88
2ksc-15	Granite	69.08	0.58	13.57	4.23		0.05	0.72	2.46	3.31	4.98	0.21		64.18	122.72	14.16	49.18	9.3	1.37
2ksc-16		69.19	0.64	13.85	4.32		0.07	0.75	2.35	3.12	5.52	0.21		89.77	178.85	18.08	60.02	10.12	1.47
2ksc-17		69.59	0.66	13.15	4.56		0.08	0.79	2.75	3.21	4.43	0.22		84.14	151.05	16.52	54.57	9.5	1.36
2ksc-18		67.63	0.58	13.47	4.41		0.07	0.56	2.26	2.99	5.56	0.21		53.86	108.92	13.77	52.45	10.61	1.87
2ksc-22a		70.55	0.45	13.88	3.39		0.05	0.52	2.02	3.15	5.08	0.12		70.47	128.68	14.21	47	8.16	1.23
2ksc-23		75.32	0.1	12.5	1.55		0.02	0.05	0.67	3.17	5.74	0		79.58	144.99	15.02	45.32	7.91	0.26
2ksc-24		76.59	0.13	11.78	1.4		0.02	0.09	0.66	2.82	5.7	0.01		88.54	148.47	14.38	40.42	5.16	0.59
2ksc-25		75.44	0.21	12.33	1.92		0.02	0.18	1.33	3.06	4.64	0.04		75.07	129.47	13.28	40.45	6.51	0.8

	2ksc-26		72.41	0.15	13.36	3.39		0.05	0.43	1.83	3.22	4.99	0.11	79.04	141.73	15.64	50.67	8.94	1.01
	2ksc-27a		66.14	0.29	14.81	4.39		0.07	0.86	2.34	3.21	5.83	0.21	35.43	79.42	10.76	43.31	9.39	1.72
	2ksc-27b		65.95	0.94	13.77	6.03		0.09	1.21	2.81	3.07	4.84	0.28	52.95	112.04	14.61	55.89	11.38	1.65
	2ksc-27c		67.25	0.81	14.03	5.06		0.08	0.95	2.81	2.99	4.17	0.26	40.79	92.93	12.47	48.69	10.15	1.51
	D202_1		68.42	0.68	13.43	0.27	4.82	0	0.8	2	2.98	5.12	0.21	73.38	146.81	15.57	57.22	10.52	1.37
	D202_2		65.84	0.88	14.36	0.32	5.14	0	1.29	2.57	3.46	4.22	0.25	63.93	127.54	13.66	50.9	10.08	1.28
	D203_1		71.28	0.37	13.59	0.06	2.98	0	0.4	1.53	3.5	5	0.1	63.7	119.93	11.69	39.41	7.89	0.92
	D208_1		68.88	0.56	13.88	0.16	4.02	0	0.68	2.02	3.31	5.24	0.17	69.13	136.34	15.24	54.49	11.02	1.27
	D208_2		73.84	0.19	12.54	0.05	2.41	0	0.19	1.01	3.12	5.46	0.05	70.94	113.28	12.75	40.88	6.6	0.57
	XN09-1		70.14	0.49	13.41	0.26	4.35	0	0.57	2	3.37	4.59	0.16	64.34	125.28	13.33	48.06	8.99	1.15
	D210-1		70.94	0.42	13.19	0.14	3.86	0	0.45	1.67	3.09	4.9	0.13	75.93	123.59	14.73	49.33	8.74	1
	D213-1	Granite	72.08	0.27	13.77	0.19	2.75	0	0.3	1.4	3.28	5.62	0.07	66.25	119.36	11.95	39.22	7.02	0.97
	D219-1		67.28	0.72	14.17	0.6	4.36	0	1.02	2.55	3.09	4.95	0.23	96.59	159.86	16.5	54.66	8.97	1.57
	D220-1		67.64	0.86	12.6	1.8	4.32	0.15	1.1	2.5	2.92	4.46	0.3	78.29	184.1	16.16	73.64	14.39	0.9
	QT-27		66.67	0.89	13.7	1.55	3.83	0.13	1.15	3.07	2.99	4.42	0.25	166.1	290.1	23.58	94	13.98	1.73
	QT-38		68.56	0.51	14.23	0.51	3.94	0	0.62	1.83	3.34	5.13	0.22	51.04	102.26	10.56	36.91	7.02	0.95
	D215-1		75.72	0.1	12.27	0.11	2.17	0	0.08	0.55	3.4	5.09	0.02	67.03	124.45	12.1	38.43	7.19	0.24
	D218-1		75.22	0.12	12.25	0	2.69	0	0.13	0.5	3.04	5.21	0.02	83.48	147.01	14.43	45.09	8.05	0.27
	D218-2		72.37	0.24	13.11	0.21	2.9	0.05	0.35	1.46	3.25	4.8	0.15	64.54	117.33	11.31	36.12	6.12	0.54
	XN04-1		72.71	0.19	13.14	0.35	2.61	0.05	0.29	1.51	2.55	5.18	0.17	48.95	96.7	9.67	32.03	5.6	0.54
	C22		75.63	0.24	11.78	0.46	2.1	0.04	0.34	0.89	2.72	4.98	0.06	97.2	165.4	16.13	47.71	7.29	0.65
	C41		75.38	0.15	11.8	0.55	2.6	0.04	0.15	0.61	3.07	4.99	0.02	87.24	161.8	17.43	55.11	9.48	0.29
	C40	Granite	75.68	0.16	11.99	0.32	2.47	0.05	0.18	0.76	3.06	4.59	0.03	91.08	159	16.97	51.76	8.92	0.46
	C43		73.75	0.21	12.36	0.32	2.97	0.05	0.24	1.13	2.97	5.27	0.04	71.54	126.8	13.32	43.98	7.76	0.6
	C55		71.13	0.41	13.26	0.73	3.27	0.06	0.49	2.21	3.34	4.1	0.11	104.97	175.5	17.56	59.83	9.78	1.09

	C24		71.57	0.48	12.9	0.58	3.02	0.06	0.6	1.77	2.82	2.29	0.13		91.74	158.6	16.51	53.6	8.72	1.08
	C42		72.17	0.3	13.21	0.88	2.75	0.05	0.36	1.3	3.12	5.11	0.07		104.6	119.2	18.8	63.32	10.42	1.1
	C21		67.89	0.61	13.74	1.49	3.65	0.08	0.66	2.45	3.14	5.09	0.21		89.4	161	17.8	58.08	11.24	1.73
	C23		69.49	0.59	13.03	0.82	4.08	0.07	0.86	2.31	2.93	4.8	0.18		74.37	133.1	14.66	49.39	8.67	1.41
	C48-1		67.96	0.75	13.47	1.24	3.9	0.08	0.95	2.52	2.87	4.84	0.24		79.04	143.2	16.86	59.45	10.99	1.59
	C60		70.49	0.47	13.61	0.59	2.97	0.05	0.59	2.19	3	4.68	0.14		78.95	135.6	15.43	53.2	9.38	1.33
	C47		68.38	0.73	13.17	0.78	4.5	0.09	1.07	2.81	2.86	4.26	0.23		57.37	119.8	15.22	61.26	12.8	1.39
	C48-2		66.1	0.86	14.07	1.06	4.5	0.09	1.1	2.84	2.98	5.06	0.27		63.64	121.9	14.72	53.61	10.19	1.88
	C54		65.92	0.82	14.32	1.23	3.98	0.09	1.08	3.01	3.02	4.97	0.25		67.83	126.9	14.63	55.1	9.9	2.01
	FR-1		67.68	0.47	14.94			4.09	0.09	0.64	2.23	3.58	4.87	0.18	43.66	93.02	10.54	39.12	8.09	1.42
	FR-10-1		57.35	0.61	18.25			4.698	0.15	0.71	2.77	7.5	0.99	0.28	26.17	57.94	7.11	29.9	8.04	0.64
	FR-10-4		65.2	0.6	13.63			4.68	0.12	0.86	2.88	3.15	4.36	0.21	116.75	186.34	21.82	73.01	11.19	1.34
	FR-19-12		71.62	0.41	12.83			3.47	0.11	0.57	1.78	2.86	4.99	0.13	82.2	134.92	14.4	45.81	7.49	0.91
	FR-19-13		68.62	0.44	13.35			3.71	0.1	0.73	1.73	2.77	5.37	0.15	55	109.03	11.41	40.05	7.46	1.13
	FR-19-31		66.48	0.64	14.07			4.7	0.11	0.787	2.61	3.52	4.81	0.22	52.41	106.85	11.9	43.66	8.14	1.55
	FR-19-34		71.16	0.45	13.04			3.77	0.08	0.72	1.76	3.27	4.54	0.15	99.19	172.42	18.32	57.98	9.08	0.95
	FR-19-41	Granite	65.17	0.83	14.47			5.33	0.13	1.12	3.05	3.26	4.85	0.3	58.94	127.49	14.84	56.07	11.07	1.66
	FR-3		69.03	0.49	14.08			3.93	0.1	0.65	2.24	3.37	4.87	0.18	51.22	103.66	11.28	42.04	8.13	1.15
	FR-32-1		68.5	0.52	13.76			4.32	0.12	0.7	2.3	3.26	4.91	0.19	52.65	106.92	11.5	41.68	7.84	1.28
	FR-43-4		70.23	0.52	13.5			4.16	0.1	0.72	2.14	3.17	4.83	0.18	56.55	110.59	11.8	41.5	7.5	1.17
	GTL-55-1		75.1	0.13	12.53			2.12	0.11	0.23	0.93	3.5	4.62	0.03	45.49	97.08	10.24	35.26	7.64	0.37
	GTL-3-2		71.04	0.13	11.45			3.49	0.13	0.72	1.09	1.45	4.58	0.03	46.78	99.69	10.71	36.73	7.96	0.22
	GTL-55-7		75.15	0.1	12.21			2.27	0.11	0.24	0.79	3.29	4.86	0.02	23.74	51.57	5.62	19.7	4.51	0.34
	SMK-54-1		72.13	0.26	13.19			2.82	0.1	0.46	1.25	2.92	5.41	0.08	48.41	96.23	9.97	34.3	7.37	0.71
	TXW-3-3		70.69	0.33	13.67			3.08	0.09	0.6	1.43	3.09	5.32	0.1	46.45	90.08	9.32	33.06	7.1	1

TXW-3-4	71.84	0.24	13.12			2.29	0.07	0.67	0.99	2.65	5.78	0.08	42.67	84.27	8.66	28.7	5.1	0.77
FR-32-3													33.99	85.72	10	33.46	9.49	0.18

Gd	Tb	Dy	Ho	Er	Tm	Yb	Lu	Y	Rb	Sr	Zr	Nb	Hf	Ta	Rb/Sr	Nb/Ta	Zr/Hf	Fe_2O_3/FeO	T_{Zr}(℃)	εNd(t)	References
7.76	1.47	9.3	1.89	5.76	1.02	6.34	1.03	68.5	484	47.3	96.9	29.1	4.08	7.5	10.23	3.9	23.8	0.64	754		
12.7	2.95	21.7	4.75	15	2.59	15.9	2.6	179	475	36.5	152	29.6	6.95	9.64	13.04	3.1	21.9	0.55	795	-10.8	
9.29	2.08	15.1	3.18	10.2	1.68	11.6	1.83	106	487	47.2	99.8	23.5	4.8	7.99	10.32	2.9	20.8	0.30	750		
9.05	2.2	16.3	3.55	11.4	1.99	12.6	2.06	124	515	37.4	86.8	22.5	4.54	7.91	13.77	2.8	19.1	0.38	740		
8.33	1.85	13	2.83	8.58	1.48	9.49	1.54	95.6	588	55.6	85.3	21	4.13	8.8	10.58	2.4	20.7	0.35	737	-10.7	
7.88	1.73	11.8	2.4	7.53	1.35	8.61	1.43	83.4	461	66.6	84.6	17.1	4.19	7.23	6.92	2.4	20.2	0.21	735		
9.93	2.14	15.1	3.21	10.2	1.7	11.9	1.87	110	480	42	109	22.9	5.15	8.55	11.42	2.7	21.2	0.31	757		
7.42	1.57	11.4	2.44	7.73	1.33	8.85	1.38	82.6	461	81.8	118	22.7	5.46	6.6	5.63	3.4	21.6	0.29	764	-11.2	
6.91	1.35	9.13	1.84	5.97	0.98	6.87	1.06	66.3	467	41.3	91.7	28.8	4.11	7.08	11.32	4.1	22.3	0.42	742		
6.33	1.26	8.33	1.68	5.47	0.92	6.4	1.01	60.2	470	35.8	96.5	28.1	4.29	6.9	13.14	4.1	22.5	0.43	747	-10.5	
7.84	1.59	10.6	2.23	7.25	1.18	8.21	1.3	77.6	475	37.9	128	33.1	5.69	7.74	12.54	4.3	22.5	0.40	770		Guo et al., 2012
7.1	1.39	9.3	1.86	6.21	1.04	7.07	1.12	70	511	45.2	89.1	23.5	3.84	5.62	11.31	4.2	23.2	0.36	739		
6.46	1.31	8.96	1.83	5.93	0.98	6.92	1.1	67.9	463	34.2	95.3	23.2	4.36	7.02	13.55	3.3	21.9	0.36	746	-10.4	
7.49	1.49	9.79	1.95	6.6	1.1	7.56	1.2	74.3	492	54.8	98.5	23.5	4.69	6.43	8.97	3.7	21.0	0.38	746		
11.8	2.89	21.7	4.77	15.3	2.61	19.5	2.92	163	725	7.85	68.5	28.6	5.23	12.4	92.44	2.3	13.1	0.48	723	-10.6	
10.8	2.74	21.2	4.83	16.1	2.85	22	3.44	168	717	7.58	104	33.2	9.54	14.3	94.58	2.3	10.9	0.23	753		
10.4	2.59	20	4.63	15.3	2.65	20	3.05	173	707	10	73.5	31.1	5.47	14	70.57	2.2	13.4	0.27	726		
14.1	3.52	26	5.64	17.8	3.02	22.1	3.41	178	770	7.19	70.7	35.4	5.52	13.1	107.12	2.7	12.8	0.16	722	-10.9	
9.77	2.42	19.2	4.29	14.4	2.5	18.6	2.93	149	772	6.69	68.7	39	5.49	14.6	115.45	2.7	12.5	0.30	720		
12.1	2.97	22.4	4.91	16.4	2.85	20.3	3.24	173	826	7.3	59.6	29.3	4.9	15	113.14	2.0	12.2	0.45	710		
13.7	3.27	23.5	4.93	15.1	2.66	17.1	2.73	170	764	8.85	67.5	29.4	5.24	16.9	86.35	1.7	12.9	0.41	717		

11.4	2.83	21.5	4.72	15.7	2.78	19.7	3.19	169	742	7.62	62.2	29.6	4.96	13.7	97.33	2.2	12.5	0.25	711	-11.3	
16.9	4.03	29.4	6.05	19.2	3.22	22.2	3.45	208	783	6.71	84.3	33.4	6.86	17	116.69	2.0	12.3	0.41	735	-11	
10.8	2.59	19.2	4.09	13	2.24	15.5	2.41	142	748	13.2	76.2	28.7	5.3	12.5	56.73	2.3	14.4	0.41	727	-11.3	
10.1	2.54	19.4	4.27	13.6	2.43	16.7	2.63	160	803	7.67	70.4	25.5	5.46	12.5	104.76	2.0	12.9	0.38	721		
14.7	3.48	26.1	5.35	16.8	2.84	18.8	2.9	181	778	6.29	71.8	28.6	5.72	13.6	123.68	2.1	12.6	0.57	724		
12.4	2.6	17.7	3.6	11.3	1.99	14.2	2.28	129	888	25.4	109	36.5	5.78	14.1	34.99	2.6	18.9	0.37	762	-10.9	
11.7	2.42	16.8	3.44	10.5	1.92	13	2.13	127	781	21.4	105	30.9	5.46	14.7	36.53	2.1	19.2	1.56	759	-11	
14.6	2.95	19.2	3.72	11.4	2.13	14.7	2.48	146	929	29.4	109	25.5	5.73	11.7	31.6	2.2	19.0		761		
11.2	2.32	15.8	3.15	9.92	1.8	12.4	2.05	115	818	22.3	92.5	36.5	5.07	17.5	36.68	2.1	18.2	0.37	748	-11.2	
12.2	2.54	17.2	3.55	10.8	1.97	14.2	2.3	133	814	21.2	82.4	33.3	5.14	17.6	38.41	1.9	16.0	0.43	737	-10.4	
12.1	2.53	17.1	3.53	10.7	1.94	13.3	2.17	129	792	23.6	92.1	33.5	4.82	14.1	33.61	2.4	19.1	0.32	746		
9.99	2.35	18.4	4.03	13.9	2.64	19.7	3.31	140	703	9.96	76.7	46	5.4	15	70.62	3.1	14.2	0.52	733		
11	2.37	15.9	3.23	10.2	1.77	12.5	1.93	120	814	22.1	94.4	36.2	5.17	13.7	36.92	2.6	18.3	0.42	748		
7.86	1.89	14.1	3.15	10.7	1.89	13.4	2.13	119	727	9.11	87.7	39.3	5.82	18.1	79.81	2.2	15.1	0.35	738		
9.34	2.17	16.7	3.54	11.7	2.11	15.1	2.37	122	791	7.71	67.6	43.1	4.93	26.2	102.61	1.6	13.7	0.25	719		
9	1.97	16.3	3.75	10.5	1.76	12.5	1.75	115	625	35.5	87.8	22.6	5.04	10.8	17.7	2.09	17.4	0.18	732		
8.83	1.88	15.5	3.45	10.1	1.63	12.1	1.7	109	666	48.8	74	18.9	3.99	7.98	13.6	2.37	18.5	0.29	726		
9.24	2.08	18	4.14	12.1	2.02	14.1	2.03	142	662	37.8	79	13.5	4.34	5.46	17.5	2.48	18.2	0.23	723		
9.12	1.95	16.6	3.7	10.6	1.78	12.9	1.89	117	628	41	102	20.2	5.35	7.57	15.3	2.67	19	0.27	748	−11.46	
9.7	2.05	16.3	3.64	10.6	1.76	12.6	1.83	119	623	39.4	104	23.1	4.84	9.48	15.8	2.43	21.4	0.27	732	−10.88	Yang et al.,
8.17	1.66	13.3	2.97	8.51	1.42	9.68	1.39	96	561	48.1	87.3	16.6	4.27	5.65	11.7	2.94	20.4	0.42	734	−11.28	2012
8.81	1.88	15.3	3.41	9.76	1.57	11.6	1.62	111	610	46.6	103	20.4	5.01	6.8	13.1	2.99	20.5	0.40	743	−11.01	
8.03	1.66	12.9	2.97	7.78	1.28	9.27	1.35	83.8	655	34.6	78.1	23.9	4.48	8.73	18.9	2.73	17.4	0.32	728	−10.84	
11.49	2.58	21.7	4.72	13	2.25	15.6	2.18	151	948	10.4	63.2	25.7	5.65	13.8	90.8	1.87	11.2	0.36	708		
8.4	1.92	18	4.35	13.5	2.36	17.6	2.52	150	943	7.94	59.4	40.8	5.36	30.3	119	1.35	11.1	0.37	709	−9.78	

7.37	1.73	15.8	3.64	10.8	1.88	13.5	1.94	141	1001	7.44	58.7	36.6	5.06	29.1	134	1.26	11.6	0.35	705		
7.34	1.72	15.8	3.84	11.9	2.08	15.4	2.29	141	994	7.01	74.7	30.5	6.03	14.1	142	2.17	12.4	0.46	721	−10.39	
9.28	2.06	18.2	4.17	12.4	2.1	14.9	2.16	143	949	12.7	75.2	30.1	5.52	13.9	74.7	2.17	13.6	0.44	721		
6.63	1.52	13.7	3.33	10.1	1.82	13.2	1.96	116	1091	7.54	66.3	27	5.85	12.4	145	2.18	11.3	0.38	0		
8.44	1.95	17.2	3.87	12.1	2.08	15.5	2.27	140	1031	8.2	75.9	27.6	6.48	16.8	126	1.64	11.7	0.41	726	−10.73	
12.75	2.85	24.5	5.39	15.5	2.58	18.8	2.62	177	1011	7.08	72.2	28.5	6.39	14.1	143	2.03	11.3	0.30	0	−9.77	
8.15	1.9	16.9	3.98	11.7	2.01	14.5	2.06	141	991	8	63	28.4	5.39	14.5	124	1.97	11.7	0.64	708	−10.69	
9.69	2.28	20.8	4.95	15.1	2.68	19.7	2.88	168	949	8.11	71.6	28.3	6.22	13.6	117	2.09	11.5	0.55	719		
14.37	3.2	27.4	6.18	18	3.04	22.1	3.17	200	951	6.91	59.6	29.1	5.41	12.3	138	2.37	11	0.56	709		
13.65	3.18	28.2	6.53	20	3.65	28.4	4.25	207	983	5.1	55.9	26.2	5.07	11.4	193	2.3	11	0.45	702	−10.39	
13.25	2.78	23.1	4.94	13	1.95	12.6	1.7	203	971	8.41	65.9	34.6	5.72	17.4	115	1.99	11.5	0.32	712	−10.12	
18.4	3.5	22.8	4.77	13.4	2.09	13.5	1.99	149	602	14.2	64.4	36.5	4.68	9.77		3.7	13.8		713		
9.86	1.78	11.6	2.59	7.34	1.12	7.24	1.05	74.8	1010	7.46	82.7	18.8	4.99	4.01		4.7	16.6		763		He et al., 2010,
13.9	2.71	18.8	4.48	12.8	2.06	14.1	2.1	131	522	23	83	38.7	5.65	9.32		4.2	14.7		740		
8.51	1.89	14.2	3.08	9.87	1.71	12.72	2	109	691	11.2	89	31.6	6.27	11.5	61.7	2.7	14.2	1.31	745		
7.33	1.54	11.1	2.31	6.92	1.13	7.34	1.03	82.8	676	20.3	78.2	27.1	4.96	11.5	33.3	2.4	15.8	1.38	736		
10.76	2.29	16.4	3.33	10	1.71	11.2	1.59	104	559	23.2	85.8	33.3	4.57	8.58	24.1	3.9	18.8	1.42	741		Hua et al., 2003
7.7	1.71	12.8	2.76	8.54	1.45	10.1	1.5	91.1	595	12.9	69.8	36.4	4.73	12.6	46.1	2.9	14.8	1.18	725		
10.4	2.48	18.6	4.14	12.9	2.34	16.6	2.48	132	589	10	64	30	5.04	11.7	58.9	2.6	12.7	1.68	717		
8.01	1.7	13.2	2.78	8.95	1.58	12.15	1.96	80.9	908	17.3	56.6	62.5	4.16	20.5	52.5	3.0	13.6	0.19	740		
8.52	1.67	12.88	2.69	8.32	1.43	10.1	1.59	77.3	916	9.5	62.8	66.1	3.86	26.7	96.4	2.5	16.3	0.02	722		
6.15	1.07	7.9	1.69	5.29	0.87	5.88	0.88	47.5	813	6.2	64.4	58.8	4.44	17.5	131.1	3.4	14.5	0.20	723		
5.37	0.99	7.35	1.51	4.78	0.82	5.57	0.84	42.8	985	11.1	47.3	63.2	3.02	25.6	88.7	2.5	15.7	0.36	707		Li, 2011
3.92	0.6	4.44	0.93	2.87	0.41	2.75	0.4	23.5	643	44.1	100	41.4	3.49	14.1	14.6	2.9	28.7	0.38	758	-11.8	
10.1	1.78	12.96	2.75	8.22	1.35	9.01	1.39	79.5	1190	7.8	64.8	61.2	3.56	20.2	152.6	3.0	18.2	0.13	759	-12.2	

5.73	1.12	8.65	1.8	5.72	1.05	7.52	1.2	50.6	940	11.5	49.1	63.7	3.71	23.6	81.7	2.7	13.2	0.10	709	-15.5	
0.93	0.2	1.42	0.3	1.04	0.19	1.67	0.26	8.5	909	4.4	24.1	103.6	1.82	19.3	206.6	5.4	13.2	0.12	668	-10.7	
4.95	0.95	6.46	1.17	3.77	0.79	6.88	1.1	36.7	943	7.9	37.1	85.6	3.97	42.2	119.4	2.0	9.3	0.17	690	-10.5	
3.61	0.68	4.73	0.84	2.64	0.58	4.99	0.84	29	899	12.5	43.7	61.4	4.87	30.6	71.9	2.0	9.0	0.22	708	-9.9	
8.49	2.02	13.6	3.07	9	1.5	10.9	1.57	95.7	624	6.55	50.5	36.2	4.48	16.4	95.3	2.2	11.3		701	-8.8	
9.47	2.04	11.8	2.44	6.28	0.86	5.5	0.71	70.3	646	12.1	97.2	35.9	5.61	9.64	53.4	3.7	17.3		752	-11.2	
7.02	1.51	9.56	2.17	6.13	1	6.8	1.01	63.4	606	37.6	63.4	30.3	3.72	8.96	16.1	3.4	17.0		716	-9.0	
7.77	1.66	11.5	2.65	7.64	1.2	8.6	1.29	78.2	458	31.6	75.8	25.7	3.79	7.07	14.5	3.6	20.0		729	-10.5	
9.1	1.99	12.9	2.96	7.94	1.15	7.57	1.06	79.5	626	16.6	82.1	34.5	5.1	10.5	37.7	3.3	16.1		736		
9.28	2.18	15.2	3.59	10.7	1.76	12.5	1.86	110	617	7.19	68	32.9	4.97	12.4	85.8	2.7	13.7		721		
8.16	1.83	11.9	2.75	7.79	1.24	8.55	1.2	85.5	639	3.78	48	33.9	3.99	12.6	169.0	2.7	12.0		698		
4.24	0.93	6.49	1.53	4.56	0.74	5.27	0.77	42.3	648	3.69	70.3	33.2	5.56	14.4	175.6	2.3	12.6		724		
5.45	1.28	8.6	2.01	6.11	0.96	7.29	1.03	61.4	539	4.43	70.1	37.8	4.85	11.2	121.7	3.4	14.5		722		
2.99	0.69	4.58	1.09	3.21	0.52	3.49	0.51	27.8	516	5.92	57.1	37.2	4.17	10.7	87.2	3.5	13.7		708		Dong et al., 2014
4	0.92	6.01	1.34	4.02	0.68	4.73	0.66	41.2	576	4.3	53.5	34.1	3.97	13	134.0	2.6	13.5		705		
4.6	1	6.99	1.57	4.54	0.72	4.83	0.69	47.6	596	8.72	70	33.3	4.84	10	68.3	3.3	14.5		723		
4.71	1.06	7.14	1.68	5.05	0.86	6.18	0.88	57.8	597	6.25	61.6	34.1	5.15	11.6	95.5	2.9	12.0		712		
5.4	1.27	9.32	2.3	7.4	1.27	9.65	1.44	69.9	443	7.7	69.2	30.9	4.82	8.6	57.5	3.6	14.4		721	-10.1	
10.65	2.55	17.8	4.01	12	1.96	14.3	2.09	136	679	4.73	58.8	34.7	4.46	12.1	143.6	2.9	13.2		714		
3.47	0.82	5.4	1.2	3.6	0.59	4.35	0.64	34.9	600	6.04	62.3	32.5	4.95	9.46	99.3	3.4	12.6		708		
3.42	0.77	5.1	1.16	3.34	0.55	3.8	0.54	38.4	548	4.98	59.8	33.4	4.57	10.2	110.0	3.3	13.1		710		
7.67	1.72	12	2.7	8.21	1.29	8.6	1.27	80.9	575	4.26	69.9	36.1	5.23	11.3	135.0	3.2	13.4		721	-10.6	
1.84	0.42	2.87	0.64	2.02	0.34	2.7	0.41	18.2	652	1.96	71.9	35.3	5.92	12.9	332.7	2.7	12.1		725		
1.73	0.37	2.32	0.55	1.69	0.3	2.46	0.38	14.4	626	1.34	66.9	34.1	5.34	11.4	467.2	3.0	12.5		722	-8.4	

3.13	0.71	5.03	1.14	3.4	0.59	4.48	0.68	41.6	649	2.1	64.1	28.8	5.36	10	309.0	2.9	12.0		719	-11.2	
4.36	1	6.6	1.39	3.99	0.68	4.65	0.64	56.6	707	3	56	21.4	5.07	13.5	235.7	1.6	11.0		711	-11.3	
2.9	0.6	3.76	0.78	2.45	0.37	2.44	0.38	20.4	351	62.3	110	18.1	5.17	1.92	5.6	9.4	21.3	0.2			
8.37	1.54	9.58	1.96	6.09	0.87	5.72	0.9	54	328	38.9	91.4	34.7	4.48	4.16	8.4	8.3	20.4	0.5			Fang et al.,
6.06	1.17	7.71	1.65	5.24	0.82	5.69	0.89	47.9	247	33.5	63.4	36.1	3.46	8.4	7.4	4.3	18.3	0.4			2016
5.15	1.01	6.76	1.4	4.55	0.68	4.87	0.79	39.6	407	41.7	55.4	29.1	2.96	7.37	9.8	3.9	18.7	0.3			
4.221	0.745	2.283	0.115	0.135	0.013	0.144	0	10.2	927.769	24.047	27.321	48.558	11.778	142.471	38.6	0.3	2.3	2.17	661		
8.829	1.594	4.98	0.221	0.157	0.012	0.125	0.01	20.168	1487.55	29.907	32.683	80.615	9.116	137.005	49.7	0.6	3.6	2.24	666		Hua et al.,
5.094	0.922	2.697	0.107	0.074	0.004	0.091	0.008	9.936	808.23	17.065	28.226	54.555	8.113	150.809	47.4	0.4	3.5	2.53	661		2003
4.635	0.855	2.371	0.135	0.146	0.013	0.174	0	12.504	801.82	36.58	31.111	69.54	9.912	139.415	21.9	0.5	3.1	0.76	674		
1.39	0.3	1.3	0.09	0.08	0.01	0.07	0.01	6.92	510.8	49.7	18.2	22.5	4.38	6.84	10.3	3.3	4.2	2.23	629		
3.29	0.99	3.8	0.21	0.26	0.02	0.17	0.03	19.7	1003	23.6	30.7	56.8	5.72	103.5	42.5	0.5	5.4	0.71	666		Wu, 2017
7.53	2.04	6.26	0.27	0.28	0.02	0.21	0.03	24.3	992.6	26	17.5	41.8	3.01	46.5	35.5	0.9	5.8	0.88	625		
9.06	1.54	4.2	0.18	0.13	0.03	0.15	0.05	17.7	734	17.6	27.3	30.4	7.42	29.7	41.7	1.0	3.7	2.50	660		
7.19	1.69	6.38	0.34	0.29	0.05	0.19	0.05	18.9	647	12.7	21.7	19.8	6.93	17.1	50.9	1.2	3.1	4.00	653		
4.28	0.89	3.79	0.26	0.32	0.05	0.21	0.05	23.1	705	32.8	25.5	15.2	7.41	7.36	21.5	2.1	3.4	1.33	658		
6.15	1.11	4.14	0.34	0.51	0.06	0.45	0.08	15.8	745	24.5	27.1	56.5	6.27	42	30.4	1.3	4.3	1.24	667		
3.39	0.83	3.3	0.19	0.18	0.05	0.27	0.05	21.8	510.81	39.54	18.2	22.46	5.48	6.84	12.9	3.3	3.3	2.23	630		Zuo, 2016
3.29	0.99	3.8	0.21	0.26	0.02	0.17	0.03	13.7	902.3	27.67	30.69	56.79	6.72	53.48	32.6	1.1	4.6	0.71	667		
4.96	0.97	4.32	0.18	0.13	0.02	0.13	0.02	17.2	735.57	25.12	24.89	2.38	7.67	8.55	29.3	0.3	3.2	1.40	650		
6.43	2.04	6.26	0.27	0.28	0.02	0.21	0.04	16.7	992.62	22.57	17.49	21.79	3.01	46.46	44.0	0.5	5.8	1.43	631		
8.27	1.73	5.93	0.31	0.22	0.02	0.16	0.02	22.4	831.79	25.29	26.86	41.9	4.36	31.53	32.9	1.3	6.2	1.23	658		
7.58	1.13	3.83	0.2	0.15	0.02	0.12	0.02	20.4	962.37	32.14	66.09	39.59	7.64	28.75	29.9	1.4	8.7	1.46	720		
7.88	1.57	10.1	2.13	7.23	1.08	7.61	1.13	74.8	664	108	150	63.4	5.77	6.78	6.2	9.4	26.0	0.18	769	-8.0	Guo et al.,
7.87	1.57	9.71	2.11	7.13	1.05	7.75	1.17	69	763	76.4	157	55.3	6.56	7.2	10.0	7.7	23.9	0.59	780		2015

7.63	1.58	9.93	2.13	7.25	1.08	7.67	1.15	72.4	682	85.9	146	56.1	5.9	6.74	7.9	8.3	24.7	0.32	771		
7.54	1.54	10.1	2.13	7.5	1.15	8.29	1.24	75.3	661	86.9	153	55.7	6.2	6.95	7.6	8.0	24.7	0.41	778		
8.81	1.78	11.4	2.39	7.84	1.21	8.63	1.32	78.3	659	81	155	58.9	6.81	7.66	8.1	7.7	22.8	0.55	779		
7.74	1.52	9.39	1.94	6.29	0.96	6.84	1.02	62.2	623	97.1	164	46.2	6.41	6.32	6.4	7.3	25.6	0.35	785	-7.9	
7.19	1.42	8.34	1.73	5.86	0.85	6.21	0.97	59.6	734	87.6	165	40.6	6.16	6.16	8.4	6.6	26.8	0.03	776		
8.28	1.54	8.98	1.8	6.07	0.9	6.39	0.96	63.4	821	108	172	42.2	6.17	6.08	7.6	6.9	27.9	0.16	779	-9.9	
12.1	2.46	15.5	3.33	11.3	1.7	12.4	1.87	107	738	55.8	179	74.4	7.9	10.6	13.2	7.0	22.7	0.37	796		
9.78	1.99	12.2	2.62	8.82	1.32	9.92	1.5	87.4	680	50.5	148	66.4	6.59	14.2	13.5	4.7	22.5	0.15	779		
11	2.2	13.9	2.82	9.45	1.39	10	1.49	92	743	48.7	163	76.6	6.93	11	15.3	7.0	23.5	0.41	788		
19.7	4.23	27.8	5.46	17.8	2.77	20.3	2.95	209	1293	6.79	33.8	38.5	3.7	24.8	190.4	1.6	9.1	0.19	674	-9.0	
18.2	4.04	26.7	5.17	17.4	2.76	20.6	3.01	199	1106	6.16	42.2	27.9	5.13	20.7	179.6	1.3	8.2		681		
11.6	2.39	15.4	2.88	9.64	1.57	12	1.74	89.7	1143	8.92	37	24.9	4.42	10.4	128.1	2.4	8.4	0.02	679	-9.7	
21.9	4.55	29.6	5.6	18.2	2.71	19.9	2.76	212	1361	8.82	47.2	28.5	4.65	16.6	154.3	1.7	10.2	0.41	697		
21.5	5.03	32.4	6.13	20.7	3.52	27.5	3.96	173	1502	13.6	37.2	27.3	5.06	25.3	110.4	1.1	7.4	0.23	689		
22.7	4.99	32.4	6.23	19.9	3.03	22.9	3.26	229	1155	8.13	66.1	30.7	7.04	12.6	142.1	2.4	9.4	0.13	721		
14.1	2.97	19.1	3.57	11.8	2.03	15.8	2.24	97.7	1511	11.7	34.4	24	4.28	13.9	129.2	1.7	8.0	0.35	683		
17	3.62	23.5	4.84	15.3	2.22	14.9	2.12	163	792	20.9	76.9	43.1	6.22	15.3	37.9	2.8	12.4	0.48	736	−9.8	
22.1	4.61	30.5	6	19.5	2.88	20.6	2.93	245	781	9.42	72.4	31.4	7.04	10.5	82.9	3.0	10.3	0.40	726		
11.9	2.45	16	3.2	10.1	1.4	9.85	1.4	103	806	7.51	79.2	43.2	5.44	14.8	107.3	2.9	14.6	0.32	733		
10.7	2.3	15.2	3.13	10.1	1.43	10	1.36	100	717	8	85.3	37.3	5.12	7.58	89.6	4.9	16.7	0.59	741		
21.1	4.64	29.8	5.51	18.2	2.85	21.2	3.05	190	1059	5.48	49.1	26.6	5.53	18.8	193.3	1.4	8.9	0.04	694	-12.9	
9.3	1.29	9.9	2.1	6.05	0.87	6.22	0.92	56	458	25	134	23	4.8	3.9	18.3	5.9	27.9	0.44	776		
8	2.66	13.5	2.76	9	1.17	6.43	1.34	74	687	25	153	41	6.7	4.7	27.6	8.7	22.8	0.49	784		Jiang et al.,
14.7	3.07	20.9	4.34	12.69	2.01	12.2	1.68	122	695	10	77	36	4.7	8.9	69.0	4.0	16.4	1.04	727		2006
10.6	4.28	23.5	4.73	14.4	1.85	10	1.91	95	697	14	72	43	4.7	7.9	48.7	5.4	15.3	1.91	726		

11.2	5.54	29.3	5.99	19.9	3.03	18.3	3.81	250	962	11	121	82	11.7	9.2	88.1	8.9	10.3	0.60	759		
8.32	1.31	7.81	1.51	4.73	0.67	4.59	0.67	44.8	383	98.9	228	21.2	7.38	2.15	3.9	9.860465	30.9		809		
7.24	1.15	7.16	1.37	4.37	0.6	4.12	0.59	39.8	387	92.4	182	19.4	6.02	2.02	4.2	9.60396	30.2		786		
8.59	1.33	8.22	1.6	4.83	0.67	4.76	0.69	45.1	364	102	213	21.2	7.2	2.19	3.6	9.680365	29.6		801	-8.0	
8.14	1.26	7.61	1.52	4.58	0.67	4.32	0.65	42.3	403	99.5	214	20.3	7.32	2.11	4.1	9.620853	29.2		801	-7.8	
7.9	1.19	7.06	1.38	4.19	0.58	4.04	0.56	39.7	329	88	167	19.6	5.53	2	3.7	9.8	30.2		781	-8.2	
8.79	1.36	8.35	1.64	4.93	0.69	4.72	0.67	46.4	354	111	220	21.4	7.1	2.24	3.2	9.553571	31		806	-8.2	
7.67	1.21	7.23	1.44	4.32	0.63	4.14	0.62	40.9	348	111	192	19.6	6.43	2.05	3.1	9.560976	29.9		794	-8.2	
7.89	1.18	7.03	1.36	4.12	0.61	3.95	0.6	39.2	359	87.5	202	19	6.76	2.01	4.1	9.452736	29.9		797	-8.0	
13.7	2.92	19.9	3.75	12.5	2.2	17.1	2.45	104	789	8.03	30.8	20.9	4.62	19.7	98.3	1.060914	6.7		654	-7.3	
19	3.73	24.5	4.48	14.2	2.26	16.2	2.35	134	922	7.25	43.8	24.5	4.91	11.9	127.2	2.058824	8.9		687	-7.0	
20.4	4.33	29.2	5.61	17.7	2.89	20.6	2.98	162	1036	9.69	31.3	26.7	3.41	14.1	106.9	1.893617	9.2		666	-7.6	Chen B et al.,
11	2.28	15.2	2.86	9.45	1.63	12.4	1.85	85.3	742	11.1	30.7	24.1	3.92	17.4	66.8	1.385057	7.8		662		2014
15.9	3.17	21.7	4.15	13.3	2.13	15.7	2.33	142	830	5.33	40.9	23.5	4.68	12.8	155.7	1.835938	8.7		680		
15.6	3.15	21	3.88	12.3	1.95	14.8	2.1	126	935	6.28	27.5	25.1	3.12	14.2	148.9	1.767606	8.8		657	-7.4	
20.2	4.1	26.8	5.06	15.9	2.57	18.4	2.65	160	963	8.56	45.5	27.8	4.97	16	112.5	1.7375	9.2		692	-7.2	
12.5	2.43	16.6	3.33	10.1	1.48	10.1	1.46	101	623	9.71	61.2	33.1	4.01	6.77	64.2	4.889217	15.3		706		
17.2	3.38	22.7	4.54	14.2	2.09	14.3	2.07	135	648	10.8	85.9	33.8	5.55	8.27	60.0	4.087062	15.5		736		
13	2.51	15.7	2.78	8.87	1.47	11.1	1.63	77.2	1002	4.71	28.7	23	4.17	8.23	212.7	2.794654	6.9		664	-6.7	
22.4	4.49	28.8	5.45	16.9	2.71	19.3	2.81	161	815	6.5	32.8	23.1	4.12	10.1	125.4	2.287129	8		665	-6.0	
17.6	3.36	21	3.71	11.6	1.87	13.6	2.02	111	974	6.47	37.8	22.7	4.76	9.94	150.5	2.283702	7.9		678		
20.8	4.27	28.1	5.34	16.9	2.78	21	3.09	158	952	7.26	29.3	23.9	3.72	13.7	131.1	1.744526	7.9		662	-7.1	
19.6	3.8	24.8	4.62	14.6	2.42	18.2	2.64	149	772	7.4	34.4	27	4.24	8.8	104.3	3.068182	8.1		670	-6.8	
14.4	2.93	21.2	4.29	13.7	2.14	15.7	2.23	138	753	13.2	54.7	35.2	4.44	10.9		3.229358	12.3		699		
									774.3	37.5	110.4	66.6	9.6		20.6	0	11.5		785		Mao et al.,

									696.5	52.4	127.1	59.6	11.7		13.3	0	10.9	786		1995
14.4	2.49	14.7	3.72	11	1.84	13.4	1.81		717.5	39.9	120.2	60.6	10.1		18.0	0	11.9	781	−6. 39	
8.66	1.58	10.3	2.56	7.98	1.38	9.87	1.48		625.1	57.3	123.6	65.2	11.5		10.9	0	10.7	776	−6. 99	
9.81	1.72	11.9	2.99	9.22	1.62	11.4	1.72		571.4	40.2	113.5	66.3	9.9		14.2	0	11.5	775	−7. 33	
11.6	1.88	13.3	3.14	9.83	1.7	11.7	1.76		723.1	50.5	177.9	60.3	9.8		14.3	0	12	805	−7. 59	
41.9	7.5	41.7	9.64	27	4.74	35.3	5.07		1149.8	13.4	32.7	19.4	6.1		85.8	0	5.36	686	−7. 41	
16.6	2.71	18.9	4.64	13.5	2.34	17.3	2.36		1028.7	7.4	30.4	20.2	9.1		139.0	0	3.34	671	−6. 35	
18.6	3.07	20.8	5.27	15.2	2.65	20.1	2.97		779.2	13.3	31.7	24.2	8.3		58.6	0	3.82	674	−7. 44	
20.7	3.86	23.4	5.41	16.9	2.88	20.9	2.69		1086.3	8	25.7	21.3	4.5		135.8	0	5.71	656	−7. 27	
26.7	4.78	26.6	5.79	17.7	3.06	21.6	3.01		1007.4	8.1	39.9	24.9	7.3		124.4	0	5.47	701	−4. 25	
20.5	3.78	21.6	5.03	15.6	2.65	18.9	2.57		904.9	17.3	58.1	37.3	8.9		52.3	0	6.53	715	−7. 34	
20.7	3.58	22.3	5.11	15.6	2.68	18.7	2.77		1105.2	20.3	24.6	13.5	6.5		54.4	0	3.78	658	−7. 28	
17.6	2.96	18.6	4.31	13.4	2.25	16.1	2.33		685	46.1	36.9	<1.5	5.7		14.9	0	6.47	675	−7. 1	
4.13	0.77	4.51	1.14	3.36	0.59	4.27	0.77		682.3	59.7	35.4	<1.5	6.6		11.4	0	5.82	670	−7. 53	
									600.9	39.8	42.9	<1.5	7		15.1	0	6.13	689		
7.37	1.21	6.98	1.37	3.87	0.63	3.99	0.59	37.9	375	108	190	17.5	6.5	2.4	3.5	7.3	29.2	794		
8.15	1.31	7.46	1.57	4.22	0.67	4.17	0.66	43.7	378	98	209	19.9	6.4	2.4	3.9	8.3	32.7	803		
7.32	1.19	7.15	1.3	3.89	0.63	3.96	0.59	37.8	390	109	180	17.7	6	2.3	3.6	7.7	30.0	793		
7.73	1.39	7.85	1.54	4.59	0.71	4.49	0.66	43.3	383	88	218	20.8	6.5	2.7	4.4	7.7	33.5	810		
7.49	1.2	7.44	1.49	4.38	0.66	4.02	0.6	40.2	421	90.5	196	19.2	6.9	2.5	4.7	7.7	28.4	797		Chen et al.,
7.74	1.27	7.92	1.56	4.53	0.68	4.46	0.65	42.6	370	75.3	207	19.9	6.9	2.7	4.9	7.4	30.0	806		2016
21.6	5.13	31.4	6.35	19	3.61	28	4.14	159	1175	25.4	40	27.4	4.8	28.4	46.3	1.0	8.3	685		
19.7	4.44	28.1	5.7	17.7	3.38	26	3.91	138.5	857	17.2	35	22.8	4.1	18.7	49.8	1.2	8.5	675		
29.3	6.57	40.8	8.06	24.1	4.48	32.8	4.79	205	1100	4.7	20	15.5	2.4	14.2	234.0	1.1	8.3	640		
20.5	4.26	27.9	5.83	17.15	2.93	21.7	3.16	182.5	773	13.3	54	26.7	4.9	15.9	58.1	1.7	11.0	699		

23	4.9	30.8	6.28	18.1	3.09	23.1	3.41	191.5	995	7.9	56	28.8	5.2	15.2	126.0	1.9	10.8		704		
22.1	4.7	28.9	5.93	17.05	3.12	22.1	3.33	179	945	15.5	44	29.8	4.5	20.5	61.0	1.5	9.8		693		
20.7	4.44	28.4	5.98	17.35	3.07	21.9	3.17	183	848	10.3	40	26	3.9	15.7	82.3	1.7	10.3		678		
22.2	4.78	29.8	6.15	18.55	3.22	22.5	3.31	203	914	13.5	57	29.9	5.8	19.2	67.7	1.6	9.8		711		
38.5	8.78	55	10.8	33.2	6.18	47.8	6.99	238	1190	11	39	25.2	5.8	25.5	108.0	1.0	6.7		690		
23.3	5.11	31.8	6.2	19.5	3.31	21.6	3.16	201	886	25.6	64	41.6	5.3	18.6	34.6	2.2	12.1		724		
19.8	4.25	26.8	5.74	16.65	2.76	18.7	2.74	158	947	6	77	40.7	6	18.4	158.0	2.2	12.8		733		
13.9	2.91	19	3.91	11.4	1.92	13.3	2.01	115.5	940	6.6	61	38.3	4.8	14.55	142.0	2.6	12.7		715		
13.85	2.98	20.46			2.13	14.17	2.09	118.58	653.64	9.26	133.11	37.68	6.94	9.03	70.6	4.2	19.2	0.21	773		
11.11	2.28	14.99			1.42	9.33	1.36	84.38	520.36	13.21	106.74	32.32	5.27	5.8	39.4	5.6	20.3	0.28	756	-7.08	
14.12	2.89	18.97			1.8	11.67	1.69	107.72	631.02	23.06	135.92	32.99	6.54	5.34	27.4	6.2	20.8	0.15	777	-7.32	
5.7	1.19	7.86			0.74	4.71	0.69	41.73	475.51	10.7	106.38	29.8	5.06	3.54	44.4	8.4	21.0	0.27	757		
8.79	1.72	11.24			1.17	7.87	1.17	63.82	581.82	11.04	155.88	31.86	7.16	5.27	52.7	6.0	21.8	0.20	785		
13.63	2.78	18.4			1.79	11.63	1.68	102.24	601.02	18.11	152.25	33.89	6.99	5.3	33.2	6.4	21.8	0.32	785	-7.49	
14.81	2.72	16.61			1.4	8.71	1.23	80.27	525.06	20.14	145.81	39.79	6.62	5.38	26.1	7.4	22.0	0.21	785	-7.53	
10.93	2.17	14.06			1.36	8.91	1.29	71.41	628.3	14.57	133.98	30.11	6.45	5.72	43.1	5.3	20.8	0.06	778		
7.22	1.61	11.13	2.35	7.16	1.14	8.02	1.19	54.6	897.14	3.23	124.27	47.22	7.04	8.62	277.8	5.5	17.7	0.31	776	-7.8	Su, 2017
12.22	2.88	20.5	4.48	13.64	2.12	14.07	2.08	136.81	797.98	2.79	141.75	53.53	8.04	6.61	286.0	8.1	17.6	0.22	777		
11.46	2.58	17.74	3.81	11.75	1.96	13.53	2.03	109.21	891.67	6.28	119.15	50.99	6.98	8.91	142.0	5.7	17.1	0.13	768	-6.16	
13.3	3.09	21.83	4.74	14.29	2.25	14.86	2.18	134.26	805.56	3.37	128.92	48.32	7.52	8.08	239.0	6.0	17.1	0.03	770		
16.69	3.6	23.82	4.95	15.7	2.81	21.61	3.26	141.56	1181.23	4.81	120.63	62.37	8.54	19.17	245.6	3.3	14.1	0.13	780	-5.83	
6.01	1.56	11.65	2.63	8.9	1.67	12.6	1.99	80.66	916.77	1.18	78.72	19.26	7.36	9.82	776.9	2.0	10.7	0.26	733		
9.89	2.58	19.37	4.35	14.57	2.65	19.88	3.12	143.48	1105.82	1.91	69.07	27.01	5.96	12.43	579.0	2.2	11.6	0.06	728		
12.15	3.3	24.94	5.56	18.53	3.35	25	3.84	188.65	1370.46	2.25	73.48	32.79	6.2	14.45	609.1	2.3	11.9	0.16	729		
																				-7.33	

																				-8.1	
																				-8.23	
4.7	0.73	3.88	0.78	2.34	0.41	3.04	0.51	22.4	656	175	227	18.8	7.55	2.64	3.7	7.1	30.1	0.79	819		
8.13	1.42	8.39	1.59	4.62	0.74	4.98	0.73	47.4	400	71	160	24.6	5.35	4.82	5.6	5.1	29.9	0.40	791		
15.77	3.59	24.3	4.83	14.9	2.89	21.1	3.19	148	770	8	75.6	26.2	2.52	12.1	96.3	2.2	30.0	0.43	726		
3.46	0.53	2.94	0.58	1.79	0.35	2.57	0.44	18.9	470	129	127	19.2	4.23	4.28	3.6	4.5	30.0	0.99	786		
5.46	1.06	6.9	1.42	4.42	0.79	5.38	0.81	45.1	471	35.8	71.8	17.2	2.39	3.39	13.2	5.1	30.0	0.02	734		Chen G et al.,
4.24	0.91	6.67	1.49	4.59	0.84	5.81	0.88	48.3	359	36.4	60.1	11.8	2	2.08	9.9	5.7	30.1	0.66	716		2013, 2014
6.48	1.55	11.2	2.33	8.12	1.66	12.7	1.94	69.4	918	7.21	64.9	25.6	2.16	15.9	127.3	1.6	30.0	0.42	717		
9.2	1.5	8.69	1.57	4.67	0.74	4.81	0.67	44.7	444	48.6	173	15.5	5.77	2.02	9.1	7.7	30.0	0.45	798		
4.7	0.73	3.88	0.78	2.34	0.41	3.04	0.51	22.4	656	175	226	18.8	7.55	2.64	3.7	7.1	29.9	0.79	820		
8.13	1.42	8.39	1.59	4.62	0.74	4.98	0.73	47.4	400	71	160	24.6	5.35	4.82	5.6	5.1	29.9	0.40	792		
12.02	2.38	14.61	3.04	9.66	1.52	10.03	1.47	95.35	664.19	32.34	132.21	28.16	5.1	6.2	20.5	4.5	25.9	0.09	792		
6.74	1.17	7.51	1.53	4.5	0.78	5.75	0.85	42.41	518.9	43.51	141.1	26.15	4.64	6.82	11.9	3.8	30.4		782		
13.54	2.96	20.97	4.53	14.46	2.61	18.92	3.17	128	819.2	10	96	33.1	3.3	9.6	81.9	3.4	29.1	0.08	748		Yao et al.,
9.34	2.04	13.55	2.82	8.83	1.5	11.48	1.81	77.83	803.7	10	96	38.9	3.7	14.3	80.4	2.7	25.9	0.24	750		2013
5.54	0.98	6.13	1.3	3.87	0.66	4.4	0.69	36.21	381.5	40	7	19.3	3.6	2.7	9.5	7.1	1.9	0.33	734		
11.67	2.67	18.47	3.75	12.99	2.53	19.68	3.02	70.61	76.3	1.95	88.77	27.58	1.12	17.69	39.1	1.6	79.3		752		
4.969	0.786	4.446	0.897	2.734	0.393	2.852	0.426	23.74	283.7	182.8	150.9	15.76	4.56	2.308	1.6	6.8	4.6		778		
6.741	1.165	7.506	1.525	4.651	0.775	5.754	0.85	42.41	518.9	43.51	141.1	26.15	4.64	6.82	11.9	3.8	4.6		784		
7.33	1.24	6.76	1.3	3.32	0.48	2.6	0.32	31.62	375	49	127	20.8	5.1	1.9	7.7	10.9	5.1	0.28	761		
5.54	0.98	6.13	1.3	3.87	0.66	4.43	0.69	36.21	384.5	40	76	19.3	3.6	2.7	9.6	7.1	3.6	0.17	730		Liu et al., 2008
9.34	2.04	13.55	2.82	0.3	1.58	11.48	1.81	77.3	803.7	10	96	38.9	3.7	14.3	80.4	2.7	3.7	0.18	751		

Yuan, S., Williams-Jones, A.E., Romer, R.L., Zhao, P., Mao, J., 2019.
Protolith-Related Thermal Controls on the Decoupling of Sn and W in Sn-W Metallogenic Provinces:
Insights from the Nanling Region, China. Economic Geology, 114(5): 1005-1012.

14.4	3.55	25	5.37	16.4	2.78	19.76	2.95	121	572	26.9	88.7	24.4	8.31	16.61	21.3	1.5	10.7		767	-8.87	
11.4	2.29	15	3.24	9.61	1.49	10.04	1.5	97.4	852	11.2	132	29.5	6.03	7.84	76.1	3.8	21.9		782	-8.78	
12	2.38	15.7	3.4	10.05	1.56	10.64	1.59	106	814	11.2	159	34.7	6.99	9.23	72.7	3.8	22.7		800		
11.3	2.18	14	3	8.89	1.38	9.35	1.41	98.1	801	15.1	158	28.5	6.84	7.58	53.0	3.8	23.1		800	-8.67	
13.8	3.38	24.8	5.68	17.75	2.88	20.06	3.09	193	825	7	116	45.8	7.78	16.36	117.9	2.8	14.9		778	-8.6	
13	2.97	20.5	4.6	13.7	2.16	14.77	2.24	147	1119	20.7	132	38	7.93	12.64	54.1	3.0	16.6		772	-8.76	
11.2	2.02	12.4	2.61	7.56	1.16	7.6	1.13	74.8	833	12	211	28.5	7.46	6.71	69.4	4.2	28.3		860		
10.4	1.94	12.6	2.72	8.32	1.32	9	1.36	78.9	662	14.7	219	30.1	7.68	7.13	45.0	4.2	28.5		894	-8.76	
10.5	2.02	13	2.8	8.35	1.3	8.85	1.32	77.7	904	14.6	136	28.4	5.98	8.12	61.9	3.5	22.7		789	-7.79	
10.1	2.05	13.4	2.91	8.69	1.4	9.61	1.46	94.8	1083	23.5	145	26.5	6.88	9.29	46.1	2.9	21.1		800		Zhou et al., 2013
10.7	2.08	13.4	2.88	8.59	1.35	9.16	1.39	81.9	793	13	176	29	7.31	8.44	61.0	3.4	24.1		792		
14.3	3.19	21	4.31	11.79	1.75	11.35	1.65	140	1070	10.9	86.2	46.2	6.03	11.58	98.2	4.0	14.3		777		
9	1.78	11.5	2.48	7.39	1.17	8.12	1.22	70.5	940	10.8	120	29.43	5.52	12.2	87.0	2.4	21.7		800	-7.3	
11	2.61	18.8	4.25	13.04	2.11	14.72	2.26	139	946	6.7	105	30.3	6.77	13.12	141.2	2.3	15.5		765	-8.93	
10.8	2.33	149	3.24	9.69	1.49	9.2	1.36	102	995	4.34	97.2	36.4	5.97	10.8	229.3	3.4	16.3	0.25	753		
17.3	3.7	23.9	4.88	14.6	2.14	14.8	2.06	161	675	10.6	85	34.5	5.98	8.79	63.7	3.9	14.2		737		Zheng and Guo, 2012
18.4	3.86	24.7	5.12	15.1	2.27	15.4	2.23	189	916	5.99	98.2	43.9	6.84	12.5	152.9	3.5	14.4	0.32	753		
15.3	3.12	19.9	4.16	12	1.83	11.5	1.63	154	632	7.25	86.4	33.6	5.7	8.93	87.2	3.8	15.2	0.87	745		
10.8	1.86	10.3	1.94	5.7	0.88	5.03	0.73	54.3	323	49.6	127	22.3	5.31	3.21	6.5	6.9	23.9	0.51	781		Zhang, 2014
10.8	1.91	10.7	2.01	5.8	0.96	5.46	0.77	56.1	346	42.4	141	22	5.47	3.16	8.2	7.0	25.8	0.44	788		

9.2	1.53	8.4	1.6	4.76	0.79	4.59	0.68	47.6	342	69.3	130	15.4	5.01	2.42	4.9	6.4	25.9	0.45	780	-7	
14.8	2.53	13.5	2.49	7.11	1.1	6.08	0.85	60.4	272	83.4	211	28.3	7.47	3.69	3.3	7.7	28.2	0.37	816	-6.1	
9.3	1.43	7.6	1.42	4.25	0.63	3.69	0.59	39.6	275	88.6	199	18.1	6.99	2.41	3.1	7.5	28.5	0.83	819	-6.5	
11.4	1.86	10.3	1.98	5.75	0.97	5.41	0.77	55	293	66.7	184	24	6.5	3.25	4.4	7.4	28.3	0.32	802		
11.2	1.92	11.3	2.15	6.37	1.05	6.12	0.89	61	317	68.2	176	23.2	6.15	3.18	4.6	7.3	28.6	0.29	799		
7.2	1.3	8.1	1.59	4.49	0.69	3.73	0.53	41.7	412	16.6	102	32	5.29	5.59	24.8	5.7	19.3	0.69	756		
22.5	4.04	27.6	6.26	19.82	2.68	18.81	2.69	129.3	684.3	31.6	157.2	35.8	9.59	6.52	21.7	5.5	16.4	0.37	790	-7.1	
19	3.39	24.6	5.58	16.8	2.47	16.99	2.46	111.8	586.4	35.3	198.5	34.6	10.7	10.68	16.6	3.2	18.6	0.17	810	-7.1	
																				-7.3	
																				-6.8	
																				-6.8	
																				-7.3	
																				-7.2	
																				-6.2	
																				-6.6	
																				-5.7	
																				-6.4	
																				-6.4	
																				-5.1	
9.37	1.19	7.96	1.66	4.54	0.65	3.99	0.64	41.65	264.08	204.21	298.74	31.54	7.45	2.99	1.3	10.5	40.1	0.46	817	-6.9	
8.21	1.06	6.90	1.47	4.13	0.62	3.91	0.63	37.37	330.69	209.92	254.14	27.83	5.95	3.00	1.6	9.3	42.7	0.42	800	-6.6	
9.06	1.13	7.25	1.55	4.40	0.65	4.03	0.66	39.40	366.26	236.76	269.70	26.92	6.12	3.17	1.5	8.5	44.0	0.45	813		Zhao, et al.,
13.07	1.91	13.86	3.01	8.64	1.30	8.22	1.32	78.29	517.14	117.86	85.99	35.30	3.19	3.90	4.4	9.1	27.0	0.43	715		2012
7.31	0.96	6.26	1.37	3.99	0.59	3.78	0.62	36.05	367.72	161.68	273.08	27.28	6.31	2.77	2.3	9.8	43.3	2.96	826		
7.47	0.97	6.49	1.35	3.85	0.57	3.53	0.59	34.88	325.33	199.56	230.18	23.45	5.60	3.01	1.6	7.8	41.1	0.37	803	-7.3	

8.21	1.01	6.55	1.36	3.69	0.52	3.34	0.51	34.07	367.07	204.16	237.20	24.05	5.41	2.77	1.8	8.7	43.9	0.40	819	-7.6	
10.48	1.56	8.83	1.64	4.67	0.69	4.38	0.66	43.84	220.89	194.76	275.09	29.04	9.03	2.65	1.1	11.0	30.5	0.66	810	-6.8	
8.99	1.35	7.47	1.41	4.07	0.59	3.69	0.56	36.78	230.62	177.21	224.66	24.40	7.65	2.45	1.3	10.0	29.4	0.59	774	-6.2	
13.06	1.80	11.77	2.42	7.52	1.01	6.63	0.94	68.32	427.20	91.76	462.70	50.85	9.56	6.70	4.7	7.6	48.4	0.42	861		
11.19	1.59	10.13	2.16	6.65	0.95	6.04	0.86	63.25	421.00	152.70	372.20	47.65	8.00	5.19	2.8	9.2	46.5	0.41	837	-5.5	
10.39	1.47	8.41	1.71	4.29	0.66	4.33	0.65											0.43			
11.49	1.47	9.18	1.90	5.69	0.76	4.84	0.73	50.34	250.70	223.30	316.30	33.00	6.86	3.20	1.1	10.3	46.1	0.40	822	-5.8	
8.47	1.33	7.59	1.49	4.27	0.66	4.19	0.62	41.4	422.22	223.28	233.49	22.95	7.59	2.64		8.7	30.8		812		
8.51	1.34	7.57	1.48	4.29	0.67	4.19	0.63	41.99	387.2	230.33	289.21	23.43	8.88	2.49		9.4	32.6		827		
6.7	1.04	5.73	1.11	3.25	0.52	3.18	0.48	31.62	420.64	176.97	208.26	19.31	6.93	2.27		8.5	30.1		801		
9.55	1.51	8.48	1.66	4.83	0.75	4.72	0.75	47.23	293.34	176.4	307.07	30.56	10.03	3.42		8.9	30.6		829		
9.11	1.42	7.89	1.56	4.55	0.7	4.47	0.67	44.57	433.42	183.29	237.69	26.94	7.7	3.3		8.2	30.9		804		
14.9	2.41	13.97	2.73	7.88	1.17	7.23	1.05	76.98	328.54	168.84	311.32	45.22	10.06	4.55		9.9	30.9		818		
3.52	0.6	3.32	0.66	1.95	0.35	2.19	0.35	19.76	322.82	111.83	85.17	12.13	2.91	2.13		5.7	29.3		728		
7.85	1.24	6.97	1.36	3.91	0.62	3.8	0.57	38.67	468.29	159.16	227.94	21.05	7.38	2.25		9.4	30.9		797		
8.08	1.22	6.7	1.31	3.73	0.57	3.52	0.52	37.07	312.54	176.32	181.82	22.9	5.72	2.3		10.0	31.8		779		Deng et al.,
7.76	1.22	6.86	1.34	3.92	0.61	3.76	0.56	38.45	260.33	162.35	203.93	23.89	6.68	2.65		9.0	30.5		787		2005
9.51	1.42	7.89	1.5	4.12	0.61	3.62	0.53	42.21	262.3	220.84	266.07	15.66	8.28	1.68		9.3	32.1		812		
6.67	1.07	5.99	1.16	3.45	0.56	3.51	0.52	34.23	383.87	144.6	173.15	21.01	5.78	2.7		7.8	30.0		785		
6.64	1.19	7.41	1.55	4.97	0.87	6	0.92	49.2	654.46	21.96	166.76	27.71	7.79	5.25		5.3	21.4		789		
3.17	0.53	2.8	0.57	1.71	0.31	1.97	0.31	18.39	493.07	58.73	126.05	12.08	4.26	1.42		8.5	29.6		767		
4.94	0.87	5.02	1.02	3.17	0.56	3.64	0.57	31.48	400.71	85.03	150.15	17.95	5.46	3.02		5.9	27.5		781		
7.39	1.2	6.84	1.36	3.99	0.64	4.04	0.6	40.14	399.96	11.46	164.43	25.34	5.48	2.8		9.1	30.0		781		
8.6	1.34	7.57	1.46	4.09	0.63	3.79	0.56	41.42	274.77	227.55	215.48	23.13	6.57	2.34		9.9	32.8		794		
9.76	1.55	8.85	1.72	4.92	0.74	4.45	0.67	48.34	260.25	213.96	316.36	30.32	9.48	2.81		10.8	33.4		825		

8.76	1.38	7.91	1.55	4.45	0.67	4.19	0.62	44.49	238.53	222.58	299.13	29.36	8.76	2.79		10.5	34.1		832		
8.92	1.37	7.59	1.46	4.23	0.64	4.2	0.61	42.1	364.78	160.17	230.38	27.46	7.1	2.59	3.8	10.6	32.4	0.06	803	-7.6	
7.99	1.18	6.72	1.26	3.58	0.52	3.49	0.49	36.93	354.19	151	242.63	25.01	6.99	2.84	4.1	8.8	34.7	0.06	804	-8.3	
7.13	1.25	7.46	1.47	4.35	0.66	4.57	0.65	45.5	411.28	116.97	187.25	26.23	6.43	3.57	2.6	7.3	29.1	0.02	791	-7.7	
9.03	1.42	8.59	1.65	4.88	0.75	4.89	0.72	50	313.45	169.28	222.78	28.89	7.09	2.92	3.4	9.9	31.4	0.04	798	-7.5	
5.36	0.81	4.65	0.95	2.89	0.46	3.34	0.52	29.63	408.08	111.2	159.47	15.84	6	2.03	3.8	7.8	26.6	0.02	781		
7.71	1.23	6.88	1.33	3.94	0.61	3.97	0.57	39.46	290.17	148.76	249.39	23.65	8.19	2.26	2.0	10.5	30.5	0.06	811		
6.98	1.06	5.86	1.13	3.27	0.49	3.28	0.5	33.79	212.86	122.23	197.72	21.15	6.34	2.13	1.7	9.9	31.2	0.04	797	-7.7	
5.96	0.88	5.42	1.09	3.27	0.51	3.3	0.49	33.21	371.73	120.29	138.13	19.53	4.84	2.34	3.1	8.3	28.5	0.07	766		Fu et al.,
7.45	1.09	5.78	1.1	3.14	0.45	3.11	0.42	31.53	245.8	201.98	204.04	21.53	5.98	1.75	1.2	12.3	34.1	0.14	788		2006
13.06	1.8	11.77	2.42	7.52	1.01	6.63	0.94	68.32	427.2	91.76	462.7	50.85	9.56	6.7	4.7	7.6	48.4	0.42	861	-8.6	
11.49	1.47	9.18	1.9	5.69	0.76	4.84	0.73	50.34	250.7	223.3	316.3	33	6.86	3.2	1.1	10.3	46.1	0.40	822		
5.91	0.89	5.12	0.96	2.71	0.4	2.65	0.35	28.48	278.7	112.89	148.55	22.49	4.65	3.2	2.5	7.0	31.9	0.13	769	-5.6	
6.22	1.09	6.69	1.39	4.42	0.72	5.34	0.79	45.81	549.01	19.18	147.54	27.88	6.12	3.39	28.6	8.2	24.1	0.05	781		
6.8	1.18	7.53	1.57	5.11	0.85	5.92	0.91	51.03	551.84	21.48	153.02	30.06	6.52	4.09	25.7	7.3	23.5	0.00	788		
5.28	0.76	4.85	0.99	3.21	0.46	3.41	0.5	29.05	493.96	72.85	168.8	20.6	5.92	2.4	6.8	8.6	28.5	0.07	786		
4.96	0.88	5.9	1.15	3.71	0.58	4.37	0.57	35.16	427.49	57.79	179.81	23.28	7.68	3.44	7.4	6.8	23.4	0.13	799		
5.49	0.8	4.53	0.93	2.69	0.44	2.91	0.46	24.6	416	61	151	23.7	6.6	2.7	6.8	8.8	22.9	0.22	785		
7.17	1.24	7.37	1.57	4.88	0.87	6.15	0.95	47.48	506.6	19	221	30.2	8.8	0.9	26.7	33.6	25.1	0.21	818		
7.14	1.22	7.31	1.5	4.43	0.8	5.4	0.8	39.11	504.8	33	155	30.2	5.7	6	15.3	5.0	27.2	0.13	789		
6.8	1.16	7.2	1.47	4.42	0.77	5.3	0.81	42.76	515.3	54	150	28.1	6.9	5.2	9.5	5.4	21.7	0.11	776		Bai et al.,
8.57	1.42	7.95	1.69	4.91	0.88	6	0.86	45.34	383.1	113	194	28.4	7.8	4.6	3.4	6.2	24.9	0.22	792		2005
6.75	1.06	5.68	1.14	3.04	0.47	2.82	0.41	29.6	359.6	124	187	22.2	6.3	2.5	2.9	8.9	29.7	0.19	821		
8.98	1.49	8.52	1.68	4.68	0.79	5.3	0.83	46.35	424.4	96	172	24.7	6.5	3.2	4.4	7.7	26.5	0.32	790		
9.35	1.46	8.22	1.66	4.48	0.69	4.42	0.65	42.28	273.9	200	262	28.7	9.8	3.5	1.4	8.2	26.7	0.41	808	-6.98	

7.36	1.16	6.5	1.29	3.46	0.55	3.34	0.48	33.91	307.6	161	216	24.9	7.1	2.3	1.9	10.8	30.4	0.20	795		
9.01	1.44	8.02	1.54	4.18	0.65	3.84	0.55	39.24	278.7	168	237	24.9	8.1	2.1	1.7	11.9	29.3	0.32	802	-7.57	
7.56	1.24	6.85	1.36	3.79	0.59	3.79	0.54	36.29	317.1	145	180	23	7.1	2.8	2.2	8.2	25.4	0.20	787		
11.16	1.8	10.89	2.03	5.5	0.81	4.83	0.73	51	255.5	146	243	27.7	8.6	2.9	1.8	9.6	28.3	0.17	803	-7.41	
8.6	1.36	7.77	1.5	4.07	0.65	4.06	0.59	39.14	252	211	288	29.9	9.4	2.7	1.2	11.1	30.6	0.24	813	-6.93	
8.7	1.33	7.62	1.48	4.02	0.63	3.94	0.57	37.02	239.6	232	228	24.1	8.3	1.7	1.0	14.2	27.5	0.31	792		
7.38	1.13	6.45	1.42	3.75	0.61	3.96	0.6	39.43	319.33	196.91	240.9	26.51	7.29	2.75		9.6	33.0		812		
8.68	1.37	8.59	1.9	5.19	0.78	5.06	0.71	55.85	130.1	273.46	265.03	24.49	7.73	2.37		10.3	34.3		804		
9.69	1.32	6.93	1.46	3.85	0.58	3.77	0.55	41.75	283.99	225.82	269.52	25.93	7.95	2.58		10.1	33.9		812		
6.8	0.94	4.96	1.12	3.14	0.47	3.15	0.48	32.45	317.04	146.88	256.99	18.55	7.86	2.02		9.2	32.7		823		
6.67	0.97	5.65	1.25	3.33	0.53	3.41	0.5	36.36	372.26	159.59	294.11	21.19	8.25	2.29		9.3	35.6		836		
8.02	1.14	6.72	1.4	3.9	0.56	3.84	0.53	40.06	341.5	230.7	279.75	28.85	8.03	2.84		10.2	34.8		814		
7.74	1.06	5.53	1.18	3.58	0.57	3.65	0.56	34.6	405.64	144.45	199.53	23.96	6.95	3.32		7.2	28.7		799		
10.36	1.53	8.26	1.69	4.54	0.67	4.27	0.62	48.38	318.73	271.01	265.41	34.85	7.21	3.02		11.5	36.8		807		
7.58	1.17	6.56	1.36	3.74	0.58	3.81	0.54	40.19	301.01	157.89	328.3	26.22	9.42	2.49		10.5	34.9		839		Li et al.,
7.16	1.09	6.16	1.22	3.27	0.53	3.35	0.49	35.77	279.41	181.2	284.61	24.03	8.09	2.34		10.3	35.2		823		2010
7.17	1.04	5.89	1.18	3.41	0.51	3.33	0.5	35.3	340.63	165.81	216.41	22.79	6.29	2.49		9.2	34.4		802		
7.56	1.27	8.24	1.82	5.37	0.86	6.09	0.91	53.34	461.12	42.35	126.6	24.91	5.69	4.24		5.9	22.2		768		
7.48	1.25	7.95	1.75	5.14	0.88	5.93	0.82	48.84	478.19	51.79	117.52	23.8	5.42	4.22		5.6	21.7		782		
4.47	0.76	4.86	1.07	3.32	0.51	3.49	0.52	34.34	474.96	49.87	95.06	18.01	4.32	2.41		7.5	22.0		745		
7.34	1.21	7.41	1.54	4.48	0.7	4.61	0.68	46.84	470.01	103.44	125.21	27.94	4.4	3.46		8.1	28.5		766		
7.02	1.19	6.83	1.53	4.42	0.67	4.5	0.61	44.21	372.19	117.56	160.83	24.95	5.68	3.35		7.4	28.3		785		
4.7	0.7	4.07	0.95	2.97	0.49	3.75	0.61	31.04	446.58	78.1	203.8	21.64	8.23	2.77		7.8	24.8		812		
8.19	1.72	12.03	2.59	8.18	1.65	12.42	1.8	40.54	1078.07	38.79	92.27	34.11	7.08	14.03		2.4	13.0				

Zircon saturation temperature (Tzr) were calculated using the method of Watson and Harrison, 1983.

$T_{Zr} = 12{,}900/[2.95 + 0.85M + \ln(496{,}000/\mathrm{Zr})]$; $M = (\mathrm{Na} + \mathrm{K} + 2\mathrm{Ca})/(\mathrm{Al} \cdot \mathrm{Si})$.

Table DR2 Zircon Lu-Hf isotopic data of the representative Late Jurassic (160-150 Ma) W-Sn-related granite in the Nanling region, South China

	Spot	$^{176}Yb/^{177}Hf$	$^{176}Lu/^{177}Hf$	$^{176}Hf/^{177}Hf$	$\varepsilon_{Hf}(t)$	T_{DM2} (Ma)	Reference
	XHS-4@1		0.001074	0.282345	-11.7	1950	
	XHS-4@2		0.000914	0.282405	-9.6	1817	
	XHS-4@3		0.002677	0.282399	-10.0	1842	
	XHS-4@4		0.001147	0.282374	-10.7	1888	
	XHS-4@5		0.001436	0.282373	-10.8	1938	
	XHS-4@6		0.001161	0.282362	-11.2	1850	
	XHS-4@7		0.000974	0.282400	-9.8	1915	
	XHS-4@8		0.000982	0.282395	-10.0	1828	
	XHS-4@9		0.001834	0.282429	-8.7	1841	
	XHS-4@10		0.001038	0.282405	-9.6	1767	
	XHS-4@11		0.001145	0.282387	-10.3	1818	
	XHS-4@12		0.002485	0.282393	-10.2	1860	
	XHS-4@13		0.002686	0.282349	-11.7	1854	
	XHS-4@14		0.003719	0.282470	-7.6	1952	
	XHS-4@15		0.002645	0.282342	-12.0	1689	
	XHS-4@16		0.001200	0.282360	-11.2	1964	
	XHS-4@17		0.001082	0.282423	-9.0	1920	
	XHS-4@18		0.003316	0.282458	-8.1	1774	
	XHS-4@19		0.002722	0.282547	-4.8	1717	
	XHS-4@20		0.001254	0.282340	-11.9	1510	
Xihuashan W deposit	XHS-4@21		0.001360	0.282407	-9.6	1965	Guo et al.,. 2012
	XHS-4@22		0.001083	0.282284	-14.0	1817	
	XHS-4@23		0.001388	0.282362	-11.2	2091	
	XHS-4@24		0.003337	0.282393	-10.4	1919	
	XHS-4@25		0.001208	0.282438	-8.5	1993	
	XHS-4@26		0.001353	0.282363	-11.1	2006	
	XHS-4@27		0.001840	0.282413	-9.4	1913	
	XHS-4@28		0.001581	0.282413	-9.4	1804	
	XHS-4@29		0.000887	0.282365	-11.0	1804	
	XHS-4@30		0.000911	0.282348	-11.7	1908	
	XHS-4@31		0.002117	0.282362	-11.3	1946	
	XHS-4@32		0.002377	0.282419	-9.3	1921	
	XHS-4@33		0.001603	0.282357	-11.4	1796	
	XHS-22@1		0.002630	0.282410	-9.5	1813	
	XHS-22@2		0.001673	0.282329	-12.2	1988	
	XHS-22@3		0.001783	0.282310	-13.1	2037	
	XHS-22@4		0.002153	0.282384	-10.5	1871	
	XHS-22@5		0.003066	0.282397	-10.0	1846	
	XHS-22@6		0.003878	0.282514	-6.0	1589	
	XHS-22@7		0.002671	0.282407	-9.5	1819	

XHS-22@9	0.003142	0.282326	-12.2	1997
XHS-22@11	0.002496	0.282383	-10.2	1869
XHS-22@12	0.001948	0.282391	-9.8	1845
XHS-22@13	0.003121	0.282391	-9.9	1852
XHS-22@14	0.003895	0.282459	-7.8	1709
XHS-22@16	0.003512	0.282411	-9.4	1814
XHS-22@17	0.002346	0.282386	-9.8	1854
XHS-22@18	0.002360	0.282363	-10.9	1912
XHS-22@19	0.002351	0.282429	-8.8	1769
XHS-22@20	0.002257	0.282360	-11.2	1922
XHS-15@1	0.002716	0.282339	-12.0	1974
XHS-15@2	0.002026	0.282345	-11.7	1954
XHS-15@3	0.001479	0.282425	-8.9	1775
XHS-15@4	0.000952	0.282398	-9.9	1834
XHS-15@5	0.001481	0.282364	-11.0	1909
XHS-15@6	0.001900	0.282388	-10.3	1862
XHS-15@7	0.001135	0.282404	-9.7	1821
XHS-15@8	0.002149	0.282405	-9.7	1824
XHS-15@9	0.001800	0.282382	-10.5	1873
XHS-15@10	0.003114	0.282443	-8.4	1744
XHS-15@11	0.001429	0.282439	-8.4	1742
XHS-15@12	0.000808	0.282369	-11.0	1900
XHS-15@13	0.001449	0.282429	-8.8	1768
XHS-15@14	0.002067	0.282431	-8.9	1769
XHS-15@15	0.001103	0.282408	-9.5	1811
XHS-15@16	0.003159	0.282396	-10.2	1852
XHS-15@17	0.002431	0.282363	-11.2	1918
XHS-15@18	0.001964	0.282397	-9.9	1839
XHS-15@19	0.001120	0.282365	-10.9	1906
XHS-15@20	0.002603	0.282460	-7.7	1700
XHS-15@21	0.000946	0.282362	-11.1	1915
XHS-15@22	0.002382	0.282324	-12.8	2012
XHS-15@23	0.001724	0.282397	-10.0	1841
XHS-15@24	0.003243	0.282417	-9.4	1806
XHS-15@25	0.001578	0.282395	-9.9	1840
XHS-15@26	0.002969	0.282455	-8.1	1720
XHS-15@27	0.002964	0.282300	-13.5	2063
XHS-15@28	0.001868	0.282286	-13.9	2089
XHS-15@29	0.001536	0.282320	-12.5	2008
XHS-37@1	0.001242	0.282334	-12.1	1975
XHS-37@2	0.001945	0.282365	-11.1	1913
XHS-37@3	0.002244	0.282295	-13.6	2070
XHS-37@4	0.001009	0.282422	-9.0	1781
XHS-37@5	0.001677	0.282380	-10.5	1877

XHS-37@6		0.001255	0.282400	-9.7	1827	
XHS-37@7		0.001126	0.282371	-11.0	1901	
XHS-37@8		0.002117	0.282408	-9.8	1822	
XHS-37@9		0.001654	0.282354	-11.5	1935	
XHS-37@10		0.001021	0.282361	-11.2	1917	
XHS-37@11		0.001333	0.282352	-11.6	1940	
XHS-37@12		0.001205	0.282402	-9.8	1829	
XHS-37@13		0.000939	0.282372	-10.8	1893	
XHS-37@14		0.001895	0.282390	-10.3	1859	
XHS-37@15		0.001081	0.282379	-10.5	1875	
XHS-37@16		0.002001	0.282470	-7.4	1678	
XHS-37@17		0.001443	0.282425	-9.0	1776	
XHS-37@18		0.001925	0.282391	-10.2	1855	
XHS-37@19		0.002531	0.282445	-8.4	1737	
XHS-37@20		0.001328	0.282384	-10.4	1867	
XHS-37@21		0.001281	0.282346	-11.7	1951	
XHS-37@22		0.000939	0.282391	-10.1	1849	
XHS-37@23		0.001850	0.282386	-10.4	1865	
XHS-37@24		0.002540	0.282442	-8.5	1746	
XHS-37@25		0.001294	0.282349	-11.6	1945	
XHS-37@26		0.001151	0.282289	-13.7	2078	
XHS-37@27		0.001141	0.282400	-9.8	1831	
XHS-37@28		0.001948	0.282411	-9.5	1810	
XHS-37@29		0.002124	0.282476	-7.2	1667	
XHS-37@30		0.000947	0.282365	-11.0	1907	
XHS-37@31		0.001428	0.282341	-11.9	1964	
XHS-37@32		0.001266	0.282410	-9.5	1809	
XHS-37@33		0.001318	0.282360	-11.2	1920	
XHS-37@34		0.001453	0.282442	-8.4	1738	
XHS-37@35		0.002797	0.282361	-11.3	1927	
XHS-19@1	0.029240	0.001020	0.282296	-13.5		
XHS-19@2	0.012240	0.000450	0.282298	-13.4		
XHS-19@3	0.064760	0.002090	0.282310	-13.1		
XHS-19@4	0.031470	0.001080	0.282346	-11.7		
XHS-19@5	0.032420	0.001210	0.282274	-14.3		
XHS-19@6	0.024090	0.000850	0.282323	-12.5		
XHS-19@7	0.023770	0.000840	0.282271	-14.3		Yang et al., 2018
XHS-19@9	0.024630	0.000870	0.282345	-11.7		
XHS-19@10	0.054150	0.001870	0.282352	-11.6		
XHS-19@11	0.030110	0.001000	0.282257	-14.9		
XHS-19@13	0.030340	0.001060	0.282333	-12.2		
XHS-19@14	0.036880	0.001370	0.282340	-12.0		
XHS-19@16	0.040930	0.001550	0.282306	-13.2		
XHS-19@17	0.034980	0.001180	0.282287	-13.8		

	XHS-19@18	0.030310	0.001060	0.282306	-13.1		
	XHS-19@19	0.024420	0.000900	0.282344	-11.8		
	XHS-19@20	0.028680	0.001070	0.282349	-11.6		
	XHS-9@8	0.134650	0.004380	0.282339	-12.3		
	XHS-9@10	0.056690	0.001970	0.282323	-12.6		
	XHS-9@15	0.133490	0.004450	0.282320	-13.0		
	XHS-9@17	0.071940	0.002740	0.282331	-12.4		
	XHS-9@18	0.078130	0.002860	0.282343	-12.0		
	XHS-9@19	0.041430	0.001510	0.282356	-11.4		
	XHS-9@20	0.217450	0.007760	0.282351	-12.2		
	XHS-10@4	0.029760	0.001030	0.282353	-11.5		
	XHS-10@5	0.127690	0.004430	0.282347	-12.0		
	XHS-10@6	0.027770	0.001050	0.282335	-12.1		
	XHS-10@10	0.101210	0.003690	0.282358	-11.6		
	XHS-10@18	0.075790	0.002830	0.282341	-12.1		
	XHS-10@19	0.131340	0.004740	0.282355	-11.8		
Qianlishan Sn-W deposit	SZY-23-01	0.020000	0.000500	0.282429	-9.0	1768	Guo et al., 2015
	SZY-23-02	0.020000	0.000800	0.282471	-7.3	1671	
	SZY-23-03	0.020000	0.000700	0.282415	-9.3	1797	
	SZY-23-04	0.020000	0.000700	0.282437	-8.6	1748	
	SZY-23-05	0.020000	0.000800	0.282366	-11.1	1908	
	SZY-23-06	0.020000	0.000600	0.282447	-8.1	1722	
	SZY-23-07	0.030000	0.001200	0.282410	-9.6	1812	
	SZY-23-08	0.020000	0.000800	0.282469	-7.5	1677	
	SZY-23-09	0.020000	0.000500	0.282423	-9.1	1779	
	SZY-23-10	0.040000	0.001000	0.282473	-7.3	1668	
	SZY-23-11	0.040000	0.001000	0.282497	-6.6	1618	
	SZY-23-12	0.030000	0.000700	0.282401	-9.8	1828	
	SZY-23-14	0.050000	0.001200	0.282421	-9.1	1784	
	SZY-23-15	0.050000	0.001500	0.282434	-8.7	1758	
	SZY-28-01	0.020000	0.000500	0.282454	-7.8	1705	
	SZY-28-02	0.030000	0.001000	0.282405	-9.8	1823	
	SZY-28-03	0.020000	0.000500	0.282434	-8.6	1753	
	SZY-28-04	0.030000	0.000800	0.282411	-9.5	1808	
	SZY-28-05	0.020000	0.000700	0.282406	-9.6	1816	
	SZY-28-06	0.020000	0.000600	0.282405	-9.7	1820	
	SZY-28-08	0.030000	0.001000	0.282395	-10.1	1844	
	SZY-28-09	0.030000	0.000800	0.282448	-8.1	1721	
	SZY-28-10	0.030000	0.000900	0.282455	-7.9	1707	
	SZY-28-11	0.020000	0.000700	0.282459	-7.7	1694	
	SZY-28-12	0.030000	0.000900	0.282395	-10.0	1839	
	SZY-28-15	0.030000	0.000800	0.282419	-9.2	1787	
	SZY-28-16	0.020000	0.000700	0.282480	-6.9	1648	

SZY-14-01	0.030000	0.001000	0.282404	-9.8	1824
SZY-14-02	0.030000	0.001000	0.282412	-9.5	1804
SZY-14-04	0.020000	0.000700	0.282409	-9.5	1808
SZY-14-05	0.020000	0.000700	0.282430	-8.7	1761
SZY-14-06	0.020000	0.000800	0.282452	-8.1	1718
SZY-14-07	0.020000	0.000700	0.282417	-9.2	1791
SZY-14-08	0.020000	0.000700	0.282470	-9.4	1673
SZY-14-09	0.030000	0.000900	0.282412	-9.4	1804
SZY-14-10	0.020000	0.000700	0.282412	-9.5	1803
SZY-14-11	0.020000	0.000700	0.282459	-7.9	1701
SZY-14-12	0.030000	0.000900	0.282464	-7.6	1689
SZY-14-13	0.020000	0.000700	0.282440	-8.5	1741
SZY-14-14	0.020000	0.000700	0.282433	-8.8	1759
SZY-14-15	0.030000	0.001000	0.282441	-8.5	1741
SZY-30-01	0.030000	0.000800	0.282480	-7.2	1655
SZY-30-02	0.030000	0.001000	0.282426	-8.9	1770
SZY-30-03	0.030000	0.000800	0.282420	-9.1	1785
SZY-30-04	0.020000	0.000600	0.282511	-5.8	1578
SZY-30-05	0.020000	0.000700	0.282440	-8.4	1739
SZY-30-06	0.020000	0.000800	0.282490	-6.7	1630
SZY-30-07	0.030000	0.001200	0.282487	-6.8	1638
SZY-30-08	0.020000	0.000900	0.282460	-7.8	1697
SZY-30-09	0.030000	0.001000	0.282435	-8.7	1755
SZY-30-10	0.020000	0.000500	0.282441	-8.4	1738
SZY-30-11	0.020000	0.000700	0.282455	-8.0	1708
SZY-30-12	0.030000	0.000800	0.282382	-10.5	1871
SZY-30-13	0.030000	0.000800	0.282394	-10.3	1849
SZY-30-14	0.020000	0.000800	0.282412	-9.3	1799
SZY-30-15	0.030000	0.000800	0.282476	-7.2	1660
SZY-21-01	0.020000	0.000600	0.282487	-6.8	1636
SZY-21-02	0.040000	0.001200	0.282462	-7.8	1697
SZY-21-03	0.030000	0.001000	0.282480	-7.1	1653
SZY-21-04	0.020000	0.000600	0.282500	-6.4	1608
SZY-21-05	0.030000	0.000900	0.282492	-6.6	1626
SZY-21-06	0.020000	0.000700	0.282496	-6.5	1617
SZY-21-07	0.020000	0.000800	0.282509	-6.0	1586
SZY-21-08	0.020000	0.000700	0.282483	-7.0	1646
SZY-21-09	0.030000	0.000900	0.282479	-7.1	1654
SZY-21-10	0.020000	0.000700	0.282495	-6.5	1617
SZY-21-11	0.030000	0.000900	0.282521	-5.7	1562
SZY-21-12	0.030000	0.000900	0.282528	-5.4	1545
SZY-21-13	0.020000	0.000700	0.282449	-8.2	1722
SZY-21-14	0.030000	0.000800	0.282514	-5.7	1572

	SZY-21-15	0.020000	0.000800	0.282521	-5.6	1560	
	SZY-22-01	0.040000	0.001200	0.282397	-10.1	1843	
	SZY-22-02	0.040000	0.001200	0.282465	-7.7	1690	
	SZY-22-03	0.120000	0.003600	0.282433	-8.9	1771	
	SZY-22-04	0.020000	0.000800	0.282452	-8.1	1715	
	SZY-22-05	0.030000	0.000900	0.282428	-8.9	1769	
	SZY-22-06	0.030000	0.001000	0.282523	-5.5	1556	
	SZY-22-07	0.050000	0.001500	0.282511	-6.0	1586	
	SZY-22-08	0.090000	0.002600	0.282496	-6.7	1627	
	SZY-22-09	0.030000	0.000900	0.282535	-5.1	1530	
	SZY-22-10	0.040000	0.001300	0.282442	-8.5	1741	
	SZY-22-11	0.030000	0.000900	0.282492	-6.7	1629	
	SZY-22-12	0.040000	0.001200	0.282510	-6.1	1588	
	SZY-22-13	0.040000	0.001200	0.282473	-7.4	1670	
	SZY-22-14	0.040000	0.001400	0.282462	-7.9	1698	
	SZY-22-15	0.020000	0.000700	0.282479	-7.0	1650	
	SZY-22-16	0.020000	0.000800	0.282494	-6.7	1624	
	SZY-22-17	0.030000	0.000900	0.282376	-10.7	1886	
	SZY-22-18	0.030000	0.001100	0.282480	-7.1	1653	
	SZY35-2	0.038120	0.000700	0.282480	-7.2	1663	
	SZY35-3	0.033880	0.000730	0.282520	-5.7	1569	
	SZY35-4	0.045060	0.000960	0.282390	-10.2	1856	
	SZY35-5	0.031720	0.000680	0.282520	-5.7	1569	
	SZY35-6	0.036990	0.000770	0.282360	-11.1	1913	
	SZY35-7	0.043540	0.000940	0.282480	-6.9	1645	
	SZY35-8	0.057020	0.001230	0.282390	-10.3	1860	
	SZY35-8-2	0.036510	0.000780	0.282450	-8.1	1720	
	SZY35-9	0.046920	0.001000	0.282370	-11.0	1907	
	SZY35-10	0.057890	0.001230	0.282310	-13.0	2032	
	SZY35-11	0.078520	0.001630	0.282400	-10.0	1843	
	SZY35-12	0.036330	0.000780	0.282500	-6.2	1600	
	SZY35-13	0.037810	0.000800	0.282550	-4.4	1487	Chen et al., 2016
	SZY35-14	0.041620	0.000890	0.282420	-9.4	1800	
	SZY35-15	0.033290	0.000720	0.282520	-5.6	1563	
	SZY35-16	0.032060	0.000700	0.282530	-5.2	1538	
	SZY35-17	0.032550	0.000700	0.282520	-5.8	1573	
	SZY35-18	0.038370	0.000820	0.282460	-7.8	1703	
	SZY35-19	0.028900	0.000620	0.282530	-5.1	1530	
	SZY35-20	0.038690	0.000830	0.282390	-10.4	1865	
	SZY35-21	0.040550	0.000880	0.282320	-12.7	2014	
	SZY35-22	0.030670	0.000670	0.282390	-10.2	1855	
	SZY35-23	0.049180	0.001120	0.282380	-10.6	1877	
	SZY35-24	0.031360	0.000680	0.282460	-7.6	1692	

	SZY35-25	0.041700	0.000890	0.282490	-6.7	1631	
	SZY35-26	0.042750	0.000920	0.282350	-11.5	1935	
	HN013-001	0.018368	0.000644	0.282473	-7.3	1670	
	HN013-002	0.020115	0.000700	0.282607	-2.4	1360	
	HN013-003	0.020384	0.000708	0.282545	-4.8	1510	
	HN013-004	0.022336	0.000780	0.282513	-5.9	1580	
	HN013-007	0.042322	0.001450	0.282550	-4.8	1500	
	HN013-009	0.014609	0.000511	0.282552	-4.4	1490	
	HN013-010	0.014888	0.000512	0.282490	-6.7	1630	
	HN013-011	0.017140	0.000604	0.282523	-5.5	1550	
	HN013-012	0.015413	0.000537	0.282597	-3.0	1390	
	HN013-014	0.028944	0.000975	0.282464	-7.7	1690	
	HN013-014	0.019317	0.000688	0.282560	-4.3	1470	
	HN013-015	0.017218	0.000620	0.282436	-8.7	1750	
	HN013-016	0.010919	0.000395	0.282420	-9.1	1780	Liu, 2011
	HN013-017	0.010919	0.002258	0.282606	-3.0	1380	
	HN013-018	0.016808	0.000572	0.282614	-2.3	1350	
	HN013-020	0.017387	0.000610	0.282512	-5.9	1580	
	HN013-021	0.017322	0.000586	0.282573	-3.9	1450	
	HN013-022	0.018468	0.000645	0.282380	-10.4	1870	
	HN013-024	0.018564	0.000628	0.282514	-5.9	1580	
	HN013-25	0.013669	0.000479	0.282435	-8.6	1750	
	HN013-27	0.017548	0.000616	0.282403	-9.6	1820	
	HN013-27	0.014685	0.000511	0.282394	-10.2	1840	
	HN013-28	0.028234	0.001006	0.282519	-5.7	1570	
	HN013-29	0.019170	0.000683	0.282430	-8.7	1760	
	HN013-30	0.060576	0.002031	0.282707	0.6	1160	
	HN013-31	0.021138	0.000719	0.282613	-2.4	1360	
	QLS-76.1	0.029067	0.001064	0.282523	-5.4	1553	
	QLS-76.3	0.021437	0.000818	0.282478	-7.0	1652	
	QLS-76.5	0.033760	0.001301	0.282412	-9.4	1803	
	QLS-76.6	0.020239	0.000782	0.282351	-11.5	1937	
	QLS-76.7	0.031034	0.001142	0.282510	-5.9	1582	
	QLS-76.8	0.015941	0.000627	0.282398	-9.8	1830	
	QLS-76.9	0.014308	0.000554	0.282383	-10.3	1864	
	QLS-76.10	0.009115	0.000359	0.282516	-5.6	1564	Chen B et al., 2014
	QLS-76.11	0.029620	0.001090	0.282352	-11.5	1935	
	QLS-76.12	0.016495	0.000629	0.282509	-5.9	1582	
	QLS-76.14	0.020786	0.000791	0.282377	-10.5	1877	
	QLS-76.15	0.034032	0.001284	0.282251	-15.1	2163	
	QLS-76.16	0.025095	0.000899	0.282442	-8.3	1734	
	QLS-76.17	0.027012	0.001007	0.282280	-14.0	2097	
	QLS-76.20	0.024330	0.000904	0.282452	-7.9	1710	

	QLS-76.21	0.020635	0.000783	0.282531	-5.1	1532	
	QLS-29.1	0.099826	0.003492	0.282543	-5.1	1523	
	QLS-29.2	0.031502	0.001153	0.282450	-8.1	1720	
	QLS-29.3	0.128115	0.004401	0.282565	-4.4	1483	
	QLS-29.5	0.063225	0.002206	0.282520	-5.8	1570	
	QLS-29.6	0.155639	0.005156	0.282513	-6.3	1604	
	QLS-29.7	0.055027	0.001772	0.282516	-5.9	1576	
	QLS-29.8	0.092594	0.003026	0.282502	-6.5	1615	
	QLS-29.9	0.029013	0.001067	0.282490	-6.7	1629	
	QLS-29.10	0.085015	0.002804	0.282499	-6.6	1621	
	QLS-29.11	0.284608	0.008845	0.282616	-3.0	1396	
	QLS-29.12	0.111278	0.003678	0.282549	-4.9	1513	
	QLS-29.13	0.162841	0.006120	0.282512	-6.4	1613	
	QLS-29.14	0.474624	0.014592	0.282722	0.1	1195	
	QLS-29.15	0.299959	0.009029	0.282641	-2.2	1341	
	QLS-29.16	0.139684	0.004646	0.282428	-9.3	1791	
	QLS-29.17	0.163528	0.005150	0.282494	-7.0	1645	
	QLS-29.18	0.072337	0.002755	0.282442	-8.6	1747	
	QLS-29.19	0.097144	0.003319	0.282515	-6.0	1588	
	QLS-29.20	0.084606	0.002961	0.282542	-5.0	1525	
	ZK14B04-02-1	0.025492	0.000657	0.282452	-8.1	1371	
	ZK14B04-02-5	0.047723	0.001229	0.282436	-8.6	1401	
	ZK14B04-02-6	0.031403	0.000874	0.282462	-7.7	1354	
	ZK14B04-02-7	0.027740	0.000752	0.282461	-7.7	1354	
	ZK14B04-02-8	0.029599	0.000830	0.282444	-8.3	1385	
	ZK14B04-02-9	0.048912	0.001259	0.282438	-8.5	1397	
	ZK14B04-02-10	0.030425	0.000846	0.282370	-10.9	1514	Zhou et al., 2015
	ZK14B04-02-11	0.032385	0.000864	0.282471	-7.4	1338	
	ZK14B04-02-12	0.054171	0.001463	0.282448	-8.3	1382	
	ZK14B04-02-13	0.035361	0.000895	0.282444	-8.4	1385	
	ZK14B04-02-14	0.052787	0.001385	0.282400	-10.0	1464	
Xitian Sn deposit	ZK14B04-02-15	0.027140	0.000791	0.282368	-11.0	1516	
	ZK14B04-02-17	0.022403	0.000604	0.282460	-7.8	1357	
	XT60-02	0.282495	0.002112	0.060348	-6.6	1620	
	XT60-18	0.282501	0.001203	0.033668	-6.3	1600	
	XT60-22	0.282543	0.003616	0.103302	-5.1	1520	
	XT60-24	0.282454	0.000830	0.023782	-8.0	1700	
	XT60-25	0.282474	0.001262	0.036938	-7.3	1660	
	XT60-26	0.282506	0.001071	0.032947	-6.2	1590	Yao et al., 2013
	XT60-27	0.282485	0.001188	0.034087	-6.9	1640	
	XT60-28	0.282478	0.001283	0.037870	-7.2	1650	
	XT60-34	0.282517	0.001700	0.046509	-5.8	1570	
	XT60-36	0.282443	0.001108	0.031579	-8.4	1730	

	XT60-37	0.282514	0.002855	0.081250	-6.0	1580	
	XT60-38	0.282517	0.005776	0.163173	-6.2	1590	
	XT60-39	0.282557	0.006665	0.192480	-4.9	1510	
	XT60-40	0.282491	0.004421	0.127374	-7.0	1640	
	XT60-41	0.282489	0.003780	0.102548	-7.0	1650	
	XT60-42	0.282483	0.004566	0.131216	-7.3	1660	
	XT60-43	0.282514	0.001581	0.045160	-5.9	1570	
	XT32-02	0.038427	0.000896	0.282421	-9.0	1780	
	XT32-03	0.035846	0.000850	0.282427	-7.0	1654	
	XT32-06	0.027815	0.000674	0.282464	-7.4	1681	
	XT32-07	0.031956	0.000764	0.282462	-7.5	1687	
	XT32-08	0.039126	0.000900	0.282426	-8.8	1769	
	XT32-09	0.032823	0.000787	0.282465	-7.4	1681	
	XT32-10	0.034470	0.000815	0.282459	-7.6	1695	
	XT32-11	0.026931	0.000646	0.282512	-5.8	1575	
	XT32-12	0.033279	0.000811	0.282500	-6.1	1601	
	XT32-13	0.036039	0.000851	0.282443	-8.2	1731	
	XT32-15	0.028992	0.000716	0.282350	-11.5	1938	
	XT32-17	0.029300	0.000719	0.282364	-11.0	1906	
	XT32-20	0.027212	0.000674	0.282461	-7.6	1691	
	XT33-01	0.027964	0.000688	0.282461	-7.6	1691	
	XT33-03	0.030158	0.000737	0.282433	-8.6	1755	
	XT33-04	0.026585	0.000656	0.282455	-7.8	1704	
	XT33-05	0.029558	0.000732	0.282395	-10.0	1838	
	XT33-06	0.029229	0.000719	0.282369	-10.8	1896	Su et al., 2015
	XT33-08	0.029952	0.000738	0.282398	-9.8	1831	
	XT33-09	0.025779	0.000643	0.282428	-8.7	1763	
	XT33-10	0.035472	0.000856	0.282404	-9.6	1819	
	XT33-11	0.056731	0.001371	0.282446	-8.2	1729	
	XT33-12	0.039074	0.000947	0.282328	-12.3	1990	
	XT33-13	0.035025	0.000863	0.282393	-10.0	1844	
	XT33-14	0.027932	0.000683	0.282454	-7.8	1704	
	XT33-15	0.035865	0.000843	0.282457	-7.8	1703	
	XT33-16	0.026741	0.000667	0.282473	-7.2	1665	
	XT33-17	0.036707	0.000884	0.282401	-9.7	1826	
	XT33-18	0.028791	0.000721	0.282422	-9.0	1780	
	XT33-19	0.036133	0.000884	0.282464	-7.5	1684	
	XT33-20	0.028723	0.000711	0.282442	-8.3	1733	
	XT35-02	0.044438	0.001100	0.282412	-9.3	1803	
	XT35-04	0.039967	0.001057	0.282388	-10.2	1855	
	XT35-05	0.044349	0.000961	0.282411	-9.3	1803	
	XT35-10	0.060071	0.001392	0.282414	-12.8	2022	
	XT35-11	0.031774	0.000779	0.282442	-8.2	1733	

	XT35-12	0.032884	0.000810	0.282402	-9.6	1822	
	XT35-13	0.024966	0.000624	0.282438	-8.4	1740	
	XT35-14	0.072006	0.001793	0.282385	-10.4	1867	
	XT35-15	0.030543	0.000753	0.282447	-8.1	1722	
	XT35-16	0.034625	0.000853	0.282393	-10.0	1842	
	XT35-18	0.027519	0.000693	0.282496	-6.3	1611	
	XT35-19	0.020081	0.000515	0.282457	-7.7	1697	
	XT35-20	0.028099	0.000706	0.282421	-9.0	1779	
Furong Sn deposit	HN016-1-01	0.010561	0.000400	0.282611	-2.2	1351	Liu, 2011
	HN016-1-03	0.027834	0.000991	0.282620	-1.9	1332	
	HN016-1-04	0.016332	0.000603	0.282462	-7.4	1682	
	HN016-1-05	0.019285	0.000686	0.282384	-10.4	1861	
	HN016-1-06	0.016853	0.000631	0.282503	-5.9	1558	
	HN016-1-07	0.026116	0.009240	0.282423	-8.8	1769	
	HN016-1-08	0.016883	0.000623	0.282447	-7.5	1705	
	HN016-1-11	0.030475	0.001123	0.282426	-8.8	1768	
	HN016-1-12	0.021670	0.000804	0.282601	-2.5	1373	
	HN016-1-13	0.015957	0.000587	0.282579	-3.1	1417	
	HN016-1-14	0.022143	0.000824	0.282419	-8.9	1777	
	HN016-1-15	0.022554	0.000846	0.282391	-10.2	1848	
	HN016-1-16	0.152600	0.000561	0.282387	-9.8	1842	
	HN016-1-17	0.016401	0.000601	0.282490	-6.4	1618	
	HN016-1-18	0.014634	0.000542	0.282480	-6.9	1646	
	HN016-1-19	0.014824	0.000566	0.282484	-6.3	1625	
	HN016-1-20	0.014597	0.000528	0.282299	-13.2	2042	
	HN016-1-21	0.016564	0.000603	0.282449	-7.8	1710	
	HN016-1-22	0.018789	0.000658	0.282440	-8.0	1725	
	HN016-1-23	0.020916	0.000742	0.282491	-6.3	1617	
	HN016-1-24	0.015622	0.000579	0.282507	-5.8	1580	
	HN016-1-25	0.047311	0.001662	0.282542	-4.8	1513	
	HN016-1-26	0.014572	0.000542	0.282454	-7.8	1701	
	HN016-1-27	0.042435	0.001494	0.252483	-7.1	1651	
	HN016-1-28	0.016301	0.000598	0.282554	-4.1	1475	
	HN016-1-29	0.014983	0.000553	0.282534	-4.8	1519	
	HN016-1-30	0.015933	0.000586	0.282494	-6.3	1611	
	HN016-1-31	0.038232	0.001374	0.282519	-5.4	1559	
	HN016-1-32	0.071075	0.002707	0.282425	-9.2	1786	
	HN016-1-32	0.056636	0.002093	0.282544	-4.9	1516	
					-4.7	1330	Shan et al., 2014
					-3.4	1270	
					-4.8	1340	
					-6.7	1450	
Hehuaping Sn deposit	WXL-16-2	0.056376	0.002033	0.282378	-10.7	1875	Zheng and Guo, 2012
	WXL-16-4	0.032758	0.001244	0.282439	-8.5	1736	

	WXL-16-7	0.140164	0.005044	0.282433	-9.1	1774	
	WXL-16-8	0.084101	0.002961	0.282488	-6.9	1638	
	WXL-16-9	0.025353	0.001013	0.282418	-9.2	1783	
	WXL-16-10	0.066319	0.002233	0.282480	-7.1	1651	
	WXL-16-11	0.038059	0.001248	0.282411	-9.5	1799	
	WXL-16-15	0.087039	0.002768	0.282533	-5.4	1538	
	WXL-16-18	0.014363	0.000591	0.282433	-8.7	1746	
	WXL-16-19	0.052882	0.001833	0.282458	-7.9	1697	
	HHPD42	0.021733	0.000538	0.282554	-4.3	1480	
	HHPD42	0.053642	0.001387	0.282573	-3.7	1440	
	HHPD42	0.036157	0.000977	0.282438	-8.5	1740	
	HHPD42	0.054865	0.001650	0.282556	-4.4	1480	
	HHPD42	0.023077	0.000479	0.282460	-7.6	1690	
	HHPD42	0.039746	0.000874	0.282530	-5.2	1530	
	HHPD42	0.052750	0.001402	0.282476	-7.2	1660	
	HHPD42	0.046966	0.001249	0.282546	-4.7	1500	
	HHPD42	0.060853	0.001431	0.282590	-3.1	1400	
	HHPD42	0.041848	0.001063	0.282577	-3.6	1430	
	HHPD42	0.035583	0.000823	0.282528	-5.3	1540	
	HHPD42	0.139680	0.003765	0.282520	-5.8	1570	
	HHPD42	0.076295	0.002172	0.282510	-6.0	1590	
	HHPD42	0.026679	0.000734	0.282494	-6.5	1610	
	HHPD42	0.053343	0.001187	0.282703	-0.9	1150	
	HHPD42	0.079947	0.002407	0.282495	-6.6	1620	
	HHPD42	0.122678	0.002798	0.282601	-2.9	1390	
	HHPD42	0.112687	0.003176	0.282550	-4.8	1500	Zhang, 2014
	HHPD42	0.114617	0.002597	0.282586	-3.4	1420	
	HHPD42	0.176605	0.004796	0.282553	-4.8	1510	
	HHPD42	0.095725	0.002313	0.282530	-5.3	1540	
	HHPD42	0.136189	0.003941	0.282553	-4.7	1500	
	HHPD42	0.070564	0.002242	0.282509	-6.1	1590	
	6302-38	0.024857	0.000889	0.282407	-9.6	1810	
	6302-38	0.096506	0.003295	0.282539	-5.2	1530	
	6302-38	0.075415	0.002435	0.282422	-9.2	1780	
	6302-38	0.098066	0.003377	0.282483	-7.2	1660	
	6302-38 06	0.047048	0.001631	0.282508	-6.1	1590	
	6302-38 08	0.075875	0.002575	0.282448	-8.3	1730	
	6302-38 09	0.024065	0.000836	0.282505	-6.1	1590	
	6302-38 13	0.088940	0.002968	0.282532	-5.4	1540	
	6302-38 14	0.041995	0.001602	0.282881	-7.1	750	
	6302-38 15	0.018257	0.000661	0.282506	-6.1	1580	
	6302-38 18	0.040874	0.001425	0.282451	-8.1	1710	
	6302-38 20	0.087443	0.002988	0.282539	-5.2	1530	

6302-38 21	0.051792	0.001813	0.282513	-5.9	1580
6302-38 23	0.225678	0.007387	0.282508	-6.7	1620
6302-38 25	0.093270	0.003147	0.282512	-6.1	1590
6302-38 28	0.070967	0.002545	0.282496	-6.6	1620
6302-38 29	0.156718	0.005330	0.282521	-6.0	1580
6302-38 30	0.107783	0.003734	0.282567	-4.2	1470

Reference

Bai, D.Y., Chen, J.C., Ma, T.Q., Wang, and X,H., 2005, Geochemical Characteristics and Tectonic Setting of Qitianling A-type Granitic Pluton in Southeast Hunan: Acta Petrologica et Mineralogica, v. 24, p.255-272 (in Chinese with English abstract)

Chen, B., Ma, X.H., and Wang, Z.Q., 2014, Origin of the fluorine-rich highly differentiated granites from the Qianlishan composite plutons (South China) and implications for polymetallic mineralization: Journal of Asian Earth Sciences, v. 93, p. 301-314.

Chen, D., Shao, Y.J., Liu, W., Ma A.J., and Liu YR.. 2013, Petrological and geochemical characteristics of Xitian pluton in Hunan province: Geology and Mineral Resources of South China, v. 31, p.11-25 (in Chinese with English abstract)

Chen, D., Chen, YM., Ma, AJ., Liu, W., Liu, YR., and Ni, Y.J., 2014, Magma mixing in the Xitian pluton of Hunan Province: Evidence from petrography, geochemistry and zircon U-Pb age: Geology in China, v. 41, p. 61-78 (in Chinese with English abstract).

Chen, Y.X., Li, H., Sun, W.D., Ireland, T., Tian, XF., Hu, Y.B., Yang, W.B., Chen, C., and Xu, D.R., 2016, Generation of Late Mesozoic Qianlishan A2-type granite in Nanling Range, South China: Implications for Shizhuyuan W-Sn mineralization and tectonic evolution: Lithos, v. 266-267, p. 435-452.

Deng, X.G., Li, X.H., Liu, Y.M., Huang, G.F., and Hou, M.S., 2005, Geochemical characteristics of Qitianling granites and their implications for mineralization: Acta Petrologica et Mineralogica, v. 24, p. 93-102 (in Chinese with English abstract)

Dong, S.H., Bi, X.W., Hu, R.H., and Chen, Y.W., 2014, Petrogenesis of the Yaogangxian granites and implications for W mineralization, Hunan Province. Acta Petrologica Sinica: v. 30, p. 2749-2764 (in Chinese with English abstract)

Fang, G.C., Cheng, Y.C., Chen, Z.H., Zeng, Z.L., Liu, C.H., Tong, Q.Q., Sun, J., and Zhu, G.H., 2016, Petrology and geochemistry of granite in the Pangushan tungsten deposit, south Jiangxi Province: Geology in China, v. 43, p. 1558-1568 (in Chinese with English abstract).

Fu, J.M., Xie, C.F., Peng, S.B., Yang, X.J., and Mei, Y.P., 2006, Geochemistry and Crust-Mantle Magmatic Mixing of the Qitianling Granites and Their Dark Microgranular Enclaves in Hunan Province: Acta Geoscientica Sinica, v. 27, p. 557-569 (in Chinese with English abstract).

Guo, C.L., Chen, Y.C., Zeng, Z.L., and Lou, FS., 2012, Petrogenesis of the Xihuashan granites in southeastern China: Constraints from geochemistry and in-situ analyses of zircon U-Pb-Hf-O isotopes: Lithos, v. 148, p. 209-227.

Guo, C.L., Wang, R.C., Yuan, S.D., Wu, S.H., and Yin, B., 2015, Geochronological and geochemical constraints on the petrogenesis and geodynamic setting of the Qianlishan granitic pluton, Southeast China: Mineralogy and Petrology, v. 109, p. 253-282.

He, Z.Y., Xu, X.S., Zou, H.B., Wang, X.D., and Yu, Y., 2010, Geochronology, petrogenesis and metallogeny of Piaotang granitoids in the tungsten deposit region of South China: Geochemical Journal, v. 44, p. 299-313.

Hua, R.M., Zhang, W.L., Chen, P.R., and Wang, R.C., 2003, Comparison in the characteristics, origin and related metallogeny granites in Dajishan and Piaotang, southern Jiangxi, China: Geological Journal of China Universities, v.9, p. 609-619 (in Chinese with English abstract)

Ishihara, S., 1981, The granitoid series and mineralization: Economic Geology, 75th Anniversary Volume, p. 458-484.

Jiang, Y.H., Jiang, S.Y., Zhao, K.D., and Ling, H.F., 2006, Petrogenesis of Late Jurassic Qianlishan granites and mafic dykes, Southeast China: implications for a back–arc extension setting: Geological Magazine, v. 143, p.457–474.

Li, G.L., 2011, The evolution of Yanshanian granite and tungsten mineralization in southern Jiangxi Province and adjacent region: A Disseration submitted to China University of Geosciences for doctor degree (in Chinese with English abstract).

Li, X.M., Hu, R.Z., Bi, X.W., and Peng, J.T., 2010, Geochemistry and tin metallogenic potential for Qitianling granite mass in southern Hunan: Journal of jilin University, v. 40, p. 81-108 (in Chinese with English abstract).

Liu, G.Q., Wu, S.H., Du, A.D., Fu, J.M., Yang, X.J., Tang, Z.H., and Wei, J.Q., 2008, Metallogenic ages of the Xitian tungsten-tin deposit, eastern Hunan province: Geotectonica et Metallogenia, v. 32, p. 63-71 (in Chinese with English abstract).

Liu, Y., 2011, Crust-mantle interaction of Yanshanian granitic magma in Qitianling and Daoxian area southern Hunan: Dissertation submitted to Chinese Academy of Geological Sciences for Doctoral Degree (in Chinese with English abstract).

Mao, J.W., and Li, H.Y., 1995, Evolution of the Qianlishan granite stock and its relation to the Shizhuyuan polymetallic tungsten deposit: International Geology Review, v. 37, p. 63-80.

Mole, D.R., Fiorentini, M.L., Thebaud, N., Cassidy, K.F., McCuaig, T.C., Kirkland, C.L., Romano, N., Belousova, E.A., Barnes, S.J., and Mill, J., 2014, Archean komatiite volcanism controlled by the evolution of early continents: PNAS v. 111, p. 10083-10088.

Shan, Q., Zeng, Q.S., Li, J.K., Lu, H.Z., Hou, M.Z., Yu, X.Y., and Wu, C.J., 2014, Diagenetic and metallogenic sources of Furong tin deposit, Qitianling: Constraints from Lu-Hf and He-Ar isotope for fluid inclusions: Acta Geologica Sinica, v. 88, p. 704-715(in Chinese with English abstract).

Su, H.Z., Guo, C.L., Wu, S.C., Hou, K.J., and Zhang, Y., 2015, Magma-hydrothermal fluid activity duration and material sources in the Xitian Indosian-Yanshanian complex: Acta Geologica Sinica, v. 89, p. 1853-1872 (in Chinese with English abstract).

Su, H.Z., 2017, The petrogenesis studies of the Mesozoic Xiangyuan tungsten-tin deposit and related granites in Hunan Province: A Dissertation submitted to China University of Geosciences for master degree (in Chinese with English abstract).

Watson, E.B., and Harrison, T. M., 1983, Zircon saturation revisited: temperature and composition effects in a variety of crustal magma types: Earth and Planetary Science Letters, v.64, p. 295-304.

Wu, M.Q., 2017, Mineralogy, geochemistry, and metallogeny of the Yichun and the Dajishan deposits: A Dissertation submitted to China University of Geosciences for doctoral degree (in Chinese with English abstract).

Yao, Y., Chen, J., Lu, J.J., and Zhang, R.Q., 2013, Geochronology, Hf isotopic compositions and geochemical characteristics of Xitian A-type granite and its geological significance: Mineral Deposits, v. 32, p. 467-488 (in Chinese with English abstract).

Yang, J.H., Peng, J.T., Zhao, J.M., Fu, Y.Z., Cheng, Y., and Hong, Y.L., 2012, Petrogenesis of the Xihuashan Granite in Southern Jiangxi Province, South China: Constraints from Zircon U-Pb

Geochronology, Geochemistry and Nd Isotopes: Acta Geologica Sinica (English Edition), v. 86, p. 131-152

Yang, J.H., Kang, L.F., Peng, J.T., Zhong, H., Gao, J.F., and Liu, L., 2018, In-situ elemental and isotopic compositions of apatite and zircon from the Shuikoushan and Xihuashan granitic plutons: Implication for Jurassic granitoid-related Cu-Pb-Zn and W mineralization in the Nanling Range, South China, Ore Geology Reviews, v. 93, p.382-403.

Zhang, R.Q., 2014, Petrogenesis and metallogeny of the W- and Sn-bearing granites in southern Hunan province: Case study from Wangxianling and Xintianling: A Dissertation submitted to Nanjing University for doctor degree (in Chinese with English abstract).

Zhao, K.D., Jiang, S.Y., Yang, S.Y., Dai, B.Z., and Lu, J.J., 2012, Mineral chemistry, trace elements and Sr–Nd–Hf isotope geochemistry and petrogenesis of Cailing and Furong granites and mafic enclaves from the Qitianling batholith in the Shi-Hang zone, South China: Gondwana Research, v. 22, p. 310-324.

Zheng, J.H., and Guo, C.L., 2012, Geochronology, geochemistry and zircon Hf isotopes of the Wangxianling granitic intrusion in South Hunan Province and its geological significance: Acta Petrologica Sinica, v. 28, p. 75-90 (in Chinese with English abstract)

Zhou, Y., Liang, X.Q., Liang, X.R., Wu, S.C,. Jiang, Y., Wen, S.N., and Cai, Y.F., 2013, Geochronology and Geochemical Characteristics of the Xitian Tungsten-Tin-Bearing A-type Granites, Hunan Province, China: Geotectonica et Metallogenia, v. 37, p. 511-529 (in Chinese with English abstract).

Zhou, Y., Liang, X.Q., Wu, S.C., Cai, Y.F., Liang, X.R., Shao, T.B., Wang, C., Fu, J.G., and Jiang, Y., 2015, Isotopic geochemistry, zircon U－Pb ages and Hf isotopes of A-type granites from the Xitian W－Sn deposit, SE China: Constraints on petrogenesis and tectonic significance: Journal of Asian Earth Sciences, v. 105, p. 122-139.

Zuo, M.L., 2016, The research of differences of the rare-metal granites mineralization between Yichun Yashan and Quannan Dajishan in Jiangxi Province: A Dissertation submitted to China University of Geosciences for doctoral degree (in Chinese with English abstract).

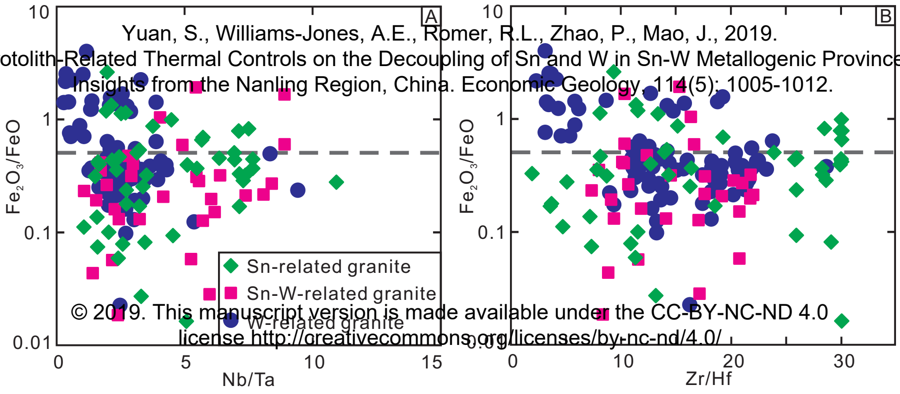
A
B
10
1
0.1
0.01
Fe_2O_3/FeO
0
5
10
15
Nb/Ta
20
30
Zr/Hf
Sn-related granite
Sn-W-related granite
W-related granite

Yuan, S., Williams-Jones, A.E., Romer, R.L, Zhao, P., Mao, J., 2019.
Protolith-Related Thermal Controls on the Decoupling of Sn and W in Sn-W Metallogenic Provinces:
Insights from the Nanling Region, China. Economic Geology, 114(5): 1005-1012.

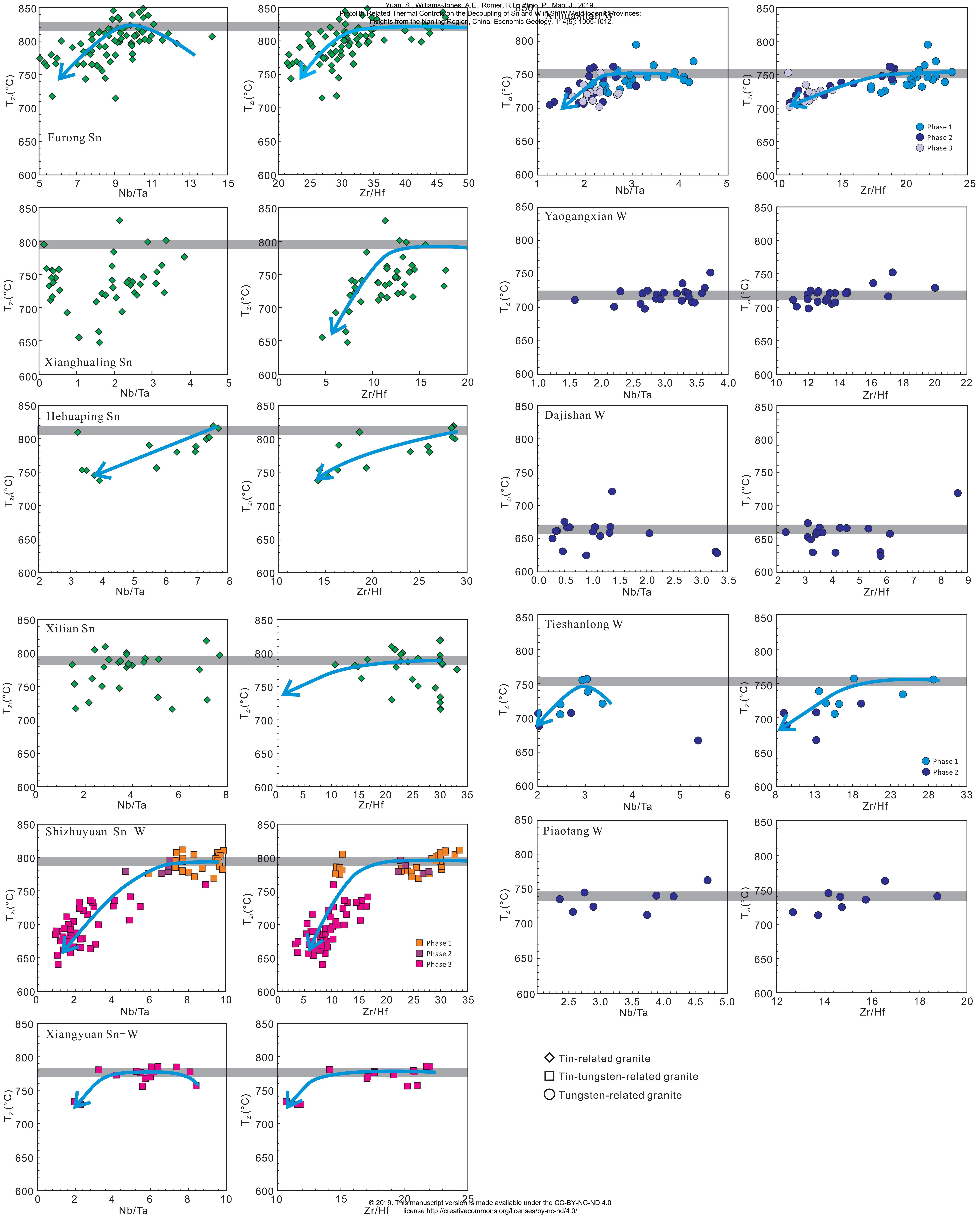

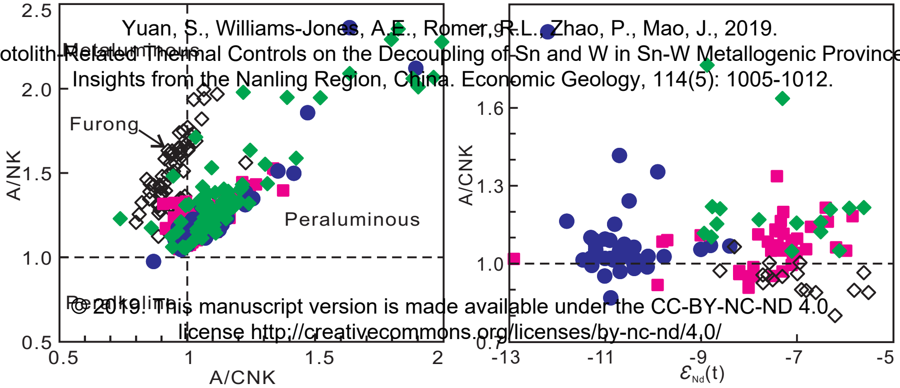
2.5
Metaluminous
2.0
Furong
A/NK
1.5
Peraluminous
1.0
Peralkaline
0.5
1
1.5
2
A/CNK
1.6
A/CNK
1.3
1.0
0.7
-13
-11
-9
-7
-5
$\varepsilon_{Nd}(t)$